Uniwersytet Rolniczy im. Hugona Kołłątaja w Krakowie
Wydział Biotechnologii i Ogrodnictwa

mgr inż. Tomasz Oleszkiewicz

Tkanka kalusowa jako układ modelowy do badania biosyntezy i akumulacji karotenoidów u marchwi uprawnej (*Daucus carota* L. subsp. *sativus*)

Praca doktorska

Praca wykonana pod kierunkiem
Prof. dr hab. inż. Rafała Barańskiego
Wydział Biotechnologii i Ogrodnictwa
Katedra Biologii Roślin i Biotechnologii

Kraków, listopad 2021

Składam serdeczne podziękowania

prof. dr hab. inż. Rafałowi Barańskiemu
za wszelką pomoc oraz cenne uwagi udzielone w trakcie realizacji badań
oraz pisania publikacji i pracy doktorskiej

Współautorom publikacji
za owocną współpracę i cenny wkład w dokonane osiągnięcia naukowe

Współpracownikom z Katedry Biologii Roślin i Biotechnologii
za miłą współpracę oraz pomoc w trakcie realizacji badań

oraz Rodzicom i Przyjaciołom za wsparcie w trakcie realizacji doktoratu

Spis treści

1. Wykaz publikacji wchodzących w skład rozprawy doktorskiej

Publikacja 1 (P1):

Oleszkiewicz T., Klimek-Chodacka M., Milewska-Hendel A., Zubko M., Stróż D., Kurczyńska E., Boba A., Szopa J., Baranski R. Unique chromoplast organization and carotenoid gene expression in carotenoid-rich carrot callus.

Planta **2018**, 248, 1455–1471

https://doi.org/10.1007/s00425-018-2988-5

IF_{2018}: 3,060

Publikacja 2 (P2):

Oleszkiewicz T., Kruczek M., Baranski R. Repression of carotenoid accumulation by nitrogen and NH_4^+ supply in carrot callus cells *in vitro*.

Plants **2021**, 10, 1813

https://doi.org/10.3390/plants10091813

IF_{2020}: 3,935

Publikacja 3 (P3):

Oleszkiewicz T., Klimek-Chodacka M., Kruczek M., Godel-Jędrychowska K., Sala K., Milewska-Hendel A., Zubko M., Kurczyńska E., Qi Y., Baranski R. Inhibition of carotenoid biosynthesis by CRISPR/Cas9 triggers cell wall remodelling in carrot.

International Journal of Molecular Sciences **2021**, 22, 6516

https://doi.org/10.3390/ijms22126516

IF_{2020}: 5,923

Sumaryczny IF: 12,918

Praca doktorska została wykonana w ramach badań realizowanych w projektach finansowanych przez Narodowe Centrum Nauki:

Determinanty biosyntezy karotenoidów u marchwi: podejście modelowe

Nr grantu: 2013/09/B/NZ9/02379

Projekt w ramach konkursu OPUS 5 realizowanego w latach 2014 – 2017

Kierownik projektu: prof. dr hab. Rafał Barański

Wpływ dostępności różnych form azotu na ekspresję genów związanych z akumulacją karotenoidów u marchwi

Nr grantu: 2018/31/N/NZ9/02368

Projekt w ramach konkursu PRELUDIUM 16 realizowanego w latach 2019 – 2021

Kierownik projektu: mgr inż. Tomasz Oleszkiewicz

W trakcie realizacji pracy doktorskiej otrzymałem 12 miesięczne stypendium doktoranckie Narodowego Centrum Nauki w konkursie ETIUDA 7 (2019/32/T/NZ9/00463), w ramach którego zaplanowane zostało odbycie sześciomiesięcznego stażu zagranicznego.

2. Wykaz używanych skrótów

2,4-D – kwas 2,4-dichlorofenoksyoctowy

B5 – pożywka mineralna wg Gamborga (Gamborg i in. 1968)

Cas9 – białko związane z CRISPR (ang. CRISPR associated protein)

CRISPR – zgrupowane, regularnie oddzielone krótkie powtórzenia palindromiczne (ang. Clustered Regularly Interspaced Short Palindromic Repeats)

MS – pożywka mineralna wg Murashige i Skoog (Murashige i Skoog 1962)

P1, P2, P3 – publikacje 1 – 3 wchodzące w skład rozprawy doktorskiej

PSY – syntaza fitoenu (ang. phytoene synthase)

psy1-g1g2 – wektor plazmidowy CRISPR/Cas9 zawierający dwa naprowadzające RNA (gRNA1 i gRNA2) komplementarne do genu *PSY1*

psy2-g1g2 – wektor plazmidowy CRISPR/Cas9 zawierający dwa naprowadzające RNA (gRNA1 i gRNA2) komplementarne do genu *PSY2*

sm – sucha masa

3. Streszczenie

W ramach pracy doktorskiej uzyskano w kulturach *in vitro* unikalny, nietransgeniczny pomarańczowy kalus marchwi linii DH1 charakteryzujący się zdolnością do akumulacji karotenoidów w podobnej ilości jaka występuje w pomarańczowych korzeniach marchwi. Scharakteryzowano otrzymany kalus pod względem zawartości tych związków, ekspresji genów i ultrastruktury komórek porównując go z kalusem ubogim w karotenoidy, z którego został on uzyskany oraz z korzeniem marchwi, wykorzystanym do indukcji kalusa. Wykazano różnice w ekspresji genów związanych z biosyntezą karotenoidów pomiędzy badanymi kalusami, w szczególności paralogów syntazy fitoenu (*PSY1* i *PSY2*), ε-cyklazy likopenu (*LCYE*) i hydroksylazy karotenu (*BCH2*). W komórkach pomarańczowego kalusa zaobserwowano plastydy różnego rodzaju i w różnych stadiach rozwoju, w tym amylochromoplasty. Otrzymany pomarańczowy kalus został wykorzystany jako model do badania biosyntezy i akumulacji karotenoidów. Zbadano wpływ składu pożywki mineralnej na akumulację karotenoidów w kalusie. Wykazano, że istotny wpływ miał tylko skład soli azotowych. Zwiększenie zawartości azotu lub zmniejszenie stosunku jonów azotanowych do amonowych spowodowało ograniczenie akumulacji karotenoidów. Zaobserwowano również powstawanie struktur proembriogennych i zarodków somatycznych niezależnie od akumulacji karotenoidów, jednak nie były one zdolne do dalszego rozwoju. Otrzymany pomarańczowy kalus został wykorzystany także do badań nad rolą paralogów *PSY* u marchwi. Wykorzystując technikę edycji genomów CRISPR/Cas9 otrzymano linie kalusowe z mutacjami w regionach dwóch paralogów: *PSY1* oraz *PSY2*. Powstałe mutacje w genie *PSY2* spowodowały całkowite zahamowanie akumulacji karotenoidów, podczas gdy edycja genu *PSY1* nie miała efektu na ilość zgromadzonych karotenoidów. Zbadano ekspresję obu paralogów w uzyskanych mutantach i zaobserwowano, że edycja badanych genów spowodowała obniżenie poziomów ich ekspresji. Dodatkowo, w przypadku genu *PSY2*, jego modyfikacja spowodowała również zmniejszenie ekspresji drugiego paraloga *PSY1*. Całkowite zatrzymanie biosyntezy karotenoidów w mutantach *PSY2* miało wpływ na ultrastrukturę plastydów oraz na skład ściany komórkowej, powodując zmniejszenie zawartości metylestryfikowanych pektyn oraz białek arabinogalaktanowych. Tym samym wykazano przebudowę ściany komórkowej zaindukowaną zmianą w szlaku biosyntezy karotenoidów. Pomarańczowy kalus marchwi okazał się dobrym modelem do badania procesów związanych z biosyntezą i akumulacją karotenoidów, rozwojem plastydów oraz jako źródło kryształów karotenoidowych.

Słowa kluczowe: CRISPR/Cas9, azot, ekspresja genów, syntaza fitoenu

4. Summary

Callus tissue as a model for studying biosynthesis and accumulation of carotenoids in carrot (*Daucus carota* L. subsp. *sativus*)

In this dissertation, a unique, non-transgenic orange carrot callus from a DH1 line was obtained in *in vitro* culture, characterized by its ability to accumulate carotenoids in similar amounts as found in orange carrot roots. The obtained callus was characterized in terms of the content of this compounds, gene expression and cell ultrastructure by comparison with a carotenoid poor callus and a carrot root, which was used for a callus induction. Differences between analyzed calli were shown in a carotenoid biosynthesis genes expression, especially in expression of two phytoene synthase paralogs (*PSY1* and *PSY2*), lycopene ε-cyclase (*LCYE*) and carotene hydroxylase (*BCH2*). Plastids of various types and stages of development, including amylochromoplasts, were observed in orange callus cells. The orange callus was used as a model to study carotenoid biosynthesis and accumulation. The effect of mineral medium composition on carotenoid accumulation in callus was investigated. Only nitrogen salts composition was shown to have a significant effect. Increase of total nitrogen or decrease of nitrate to ammonium ratio resulted in a decrease of accumulated carotenoids. Formation of proembryogenic structures and somatic embryos were observed regardless of carotenoid accumulation, however they were not able to further develop. Obtained orange callus was also used to study roles of *PSY* paralogs in carrot. Using a CRISPR/Cas9 genome editing technique callus lines with mutations in two paralogs: *PSY1* and *PSY2* were acquired. The mutations in *PSY2* caused a complete inhibition of carotenoid accumulation, while editing *PSY1* gene did not affect carotenoid accumulation. The expression of both paralogs in acquired mutants was examined and it was observed that editing of the studied genes resulted in a decrease of expression levels. Additionally, in the case of *PSY2* its modification also resulted in decrease of the second paralog expression. Complete carotenoid biosynthesis inhibition in *PSY2* mutants affected the ultrastructure of plastids and a cell wall composition, resulting in a decrease of methylesteryfied pectins and arabinogalactan proteins content. Thus, it was demonstrated cell wall remodeling induced by changes in carotenoid biosynthesis pathway. Orange carrot callus proved to be a good model to study carotenoid biosynthesis and accumulation related processes, plastids development and as a source of carotenoid crystals.

Keywords: CRISPR/Cas9, nitrogen, gene expression, phytoene synthase

5. Wstęp

Marchew uprawna (*Daucus carota* L. *subsp. sativus* Hoffm.) jest rośliną dwuletnią należącą do rodziny selerowatych (Apiaceae). Wytwarza ona w pierwszym roku rozetę liściową i korzeń spichrzowy, a dopiero w drugim roku pęd kwiatostanowy. Korzenie spichrzowe marchwi mają zdolność do akumulowania barwników, takich jak karotenoidy czy antocyjany i w zależności od tego jakie i w jakich ilościach są gromadzone, to korzenie mogą mieć barwę pomarańczową, żółtą, czerwoną, fioletową lub białą. Najpopularniejsze odmiany marchwi mają korzenie spichrzowe o charakterystycznej pomarańczowej barwie, dzięki zgromadzonym w dużych ilościach karotenoidów, głównie β-karotenu i α-karotenu, będących prowitaminą A. Karotenoidy posiadają wiele właściwości prozdrowotnych. Dzięki właściwościom antyoksydacyjnym działają ochronne na układ sercowo-naczyniowy, są stosowane w profilaktyce przeciw powstawaniu nowotworów oraz w leczeniu chorób wzroku (Eggersdorfer i Wyss 2018). Duża zawartość karotenoidów gromadzonych w korzeniach powoduje, że marchew jest jednym z ważniejszych ich źródeł w diecie człowieka (Simon 1990). Sprawia to, że marchew jest warzywem o dużym znaczeniu gospodarczym i jednym z najbardziej znanych warzyw korzeniowych. W 2019 roku produkcja marchwi na świecie przekroczyła 44,76 mln ton (razem z produkcją rzepy wg FAO; FAOstat 2019). W Polsce w 2020 roku wyprodukowano 678 tys. ton marchwi, tym samym zajmując trzecie miejsce wśród producentów marchwi w Unii Europejskiej (Eurostat 2020).

Karotenoidy to obszerna grupa barwników powszechnie występujących w przyrodzie. Nie tylko nadają one roślinom charakterystyczne żółte, pomarańczowe i czerwone barwy ale także pełnią funkcje niezbędne dla wzrostu i rozwoju roślin. Stanowią ważny element fotosystemu, działając ochronnie przed uszkodzeniami fotoksydacyjnymi i zwiększając zakres długości fal światła widzialnego, z których energia jest przekazywana do chlorofilu. Karotenoidy są również prekursorami fitohormonów, takich jak kwas abscysynowy czy strigolaktony, które biorą udział w odpowiedzi na stres, w regulacji wzrostu i rozwoju rośliny, rozwoju nasion czy rozpoznawaniu przez grzyby mikoryzowe (Rosas-Saavedra i Stange 2016, Chen i in. 2020, Faizan i in. 2020). W ostatnich latach pojawiły się również doniesienia o związku biosyntezy karotenoidów oraz strigolaktonów z biosyntezą elementów ściany komórkowej i wpływie na jej strukturę (Diretto i in. 2020, Quin i in. 2020, Wang i in. 2021, Ramirez i in. 2018).

Karotenoidy są to 40-węglowe tetraterpeny zbudowane z ośmiu pięciowęglowych jednostek izoprenowych. Karotenoidy mogą ulegać różnym modyfikacjom np. cyklizacji,

uwodornianiu/odwodornianiu, przyłączaniu grup tlenowych, zmianie długości łańcucha polienowego, zmianie położenia wiązań podwójnych czy reakcjom przegrupowania. Dzielone są na dwie grupy: karoteny, będące węglowodorami, oraz ksantofile, będące tlenowymi pochodnymi karotenów (Rodriguez-Amaya 2016). Procesy związane z biosyntezą karotenoidów są aktualnie dobrze opisane. Prekursorami karotenoidów są 5-węglowe izoprenoidy – difosforan izopentenylu (IPP) oraz difosforan dimetyloallilu (DMAPP), które tworzą difosforan geranylogeranylu (GGPP). IPP oraz DMAPP mogą powstawać na drodze cytoplazmatycznego szlaku mewalonowego (MVA) lub plastydowego niemewalonowego szlaku fosforanu metylerytritolu (MEP), przy czym szlak MEP jest głównym źródłem tych prekursorów u roślin. Pierwszym i kluczowym etapem biosyntezy karotenoidów jest utworzenie fitoenu poprzez kondensację dwóch cząsteczek GGPP, za co odpowiedzialny jest enzym syntaza fitoenu (PSY). W kolejnym etapie, po serii reakcji desaturacji i izomeryzacji, fitoen jest przekształcany do likopenu. Liniowa cząsteczka likopenu jest następnie poddawana cyklizacji na jego końcach. U roślin występują dwa enzymy odpowiedzialne za cyklizację likopenu, β-cyklaza likopenu (LCYB) oraz ε-cyklaza likopenu (LCYE), które tworzą odpowiednio pierścień β- lub ε-jononu. Cyklizacja prowadzi do powstania β-karotenu (z dwoma pierścieniami typu β) lub α-karotenu (z jednym pierścieniem β i jednym ε). Dalsze hydroksylacje i epoksydacje powodują powstanie zróżnicowanych ksantofili z obu karotenów. Ostatecznie, w wyniku działania dioksygenazy 9-cis-epoksykarotenoidowej (NCED) z ksantofili może powstawać kwas abscysynowy (ABA) (Rosas-Saavedra i Stange 2016). Karotenoidy u roślin powstają i są następnie gromadzone w plastydach. Mogą występować zarówno w etioplastach, amyloplastach, chloroplastach i chromoplastach. Spośród nich chromoplasty są plastydami odpowiedzialnymi za żółte, pomarańczowe i czerwone barwy różnych organów roślin jak np. kwiatów, owoców czy korzeni. Chromoplasty można podzielić ze względu na ich strukturę na: globularne, błoniaste, cylindryczne i krystaliczne. Chromoplasty mogą powstawać z chloroplastów (np. w dojrzewających owocach) lub z proplastydów czy amyloplastów w tkankach fotosyntetycznie nieaktywnych np. w korzeniach (Sun i in. 2018). Amyloplasty były obserwowane w młodych korzeniach marchwi i zanikały wraz z rozwojem tego organu. W dojrzałych pomarańczowych korzeniach już nie obserwowano obecności amyloplastów, jednak w białych korzeniach były one obecne. Dlatego przypuszcza się, że chromoplasty w korzeniach marchwi powstają z amyloplastów (Kim i in. 2010). U marchwi chromoplasty zawierają karotenoidy głównie w formie krystalicznej (Schweiggert i in. 2012). Kryształy karotenoidowe marchwi składają się głównie z β-karotenu, ale mogą również zawierać α-karoten (Rygula i in. 2018)

Szlak biosyntezy i metabolizmu karotenoidów u marchwi jest analogiczny jak u innych gatunków roślin i tym samym dobrze poznany. W ostatnich latach badania skupiają się na dokładniejszym poznaniu i zrozumieniu mechanizmów związanych z jego regulacją (Simpson i in. 2016). Obecnie wiadomo, że czynniki rozwojowe i środowiskowe, takie jak np. światło, oddziałują na akumulację karotenoidów w komórkach marchwi (Rodriguez-Concepcion i Stange 2013, Perrin i in. 2017). Ekspresja genów w szlaku karotenoidowym jest regulowana przez ekspresję innych genów. Wykazano, że wyciszenie genu desaturazy ζ-karotenu 1 (*ZDS1*) powoduje zmniejszenie ekspresji drugiego paraloga *ZDS2* oraz *PSY2*, jednak wyciszenie *ZDS2* nie wpływa na ekspresję *ZDS1* oraz *PSY2* (Florez-Ortiz i in. 2020). Również ekspresja β-cyklazy likopenu 1 (*LCYB1*), poza oddziaływaniem na akumulację karotenoidów, wpływa na ekspresję innych genów ze szlaku biosyntezy karotenoidów (Moreno i in. 2013). W szlaku biosyntezy karotenoidów u marchwi istnieją paralogi niektórych genów, np. *PSY*, *ZDS* czy *LCYB* i ich ekspresja jest różna w liściach oraz korzeniach w trakcie rozwoju rośliny (Rodriguez-Concepcion i Stange 2013, Simpson i in. 2016). Dla genu *PSY* u marchwi znane są dwa funkcjonalne paralogi: *PSY1* oraz *PSY2* (Maass i in. 2009, Iorizzo i in. 2016). Poziom ekspresji obu tych genów pozytywnie koreluje z zawartością akumulowanych karotenoidów, jednak ich ekspresja jest różna w liściach i korzeniach. Ekspresja genu *PSY1* zwiększa się pod wpływem światła w liściach, co wskazuje na jego znaczenie w tkankach fotosyntetycznie aktywnych. Ekspresja *PSY2* nie jest regulowana przez światło w korzeniach, natomiast jest ograniczana w liściach (Fuentes i in. 2012, Bowman i in. 2014, Wang i in. 2014). Ekspresja genu *PSY2* jest również tkankowo specyficzna i jego ekspresja jest różna między ksylemem i floemem w korzeniach marchwi (Perrin i in. 2017). *PSY2* ulega również ekspresji pod wpływem stresu solnego poprzez szlak sygnalny ABA (Simpson i in. 2018). U marchwi występują również dwa paralogi genu *ZDS* i ich znaczenie oraz funkcje zostało niedawno zbadane. Wykazano że *ZDS1* jest niezbędny do rozwoju marchwi i jego wyciszenie powoduje ograniczenie akumulacji karotenoidów, natomiast wyciszenie *ZDS2* nie ma wpływu na akumulację karotenoidów (Florez-Ortiz i in. 2020).

Wpływ na akumulację karotenoidów mają również geny znajdujące się poza szlakiem ich biosyntezy, z którym są pośrednio powiązane. Wraz z opracowaniem genomu marchwi zidentyfikowano gen *Y* (DCAR_032551), co do którego istnieje przypuszczenie, że ma związek z represją fotomorfogenezy i wpływa na karotenogenezę w korzeniach marchwi (Iorizzo i in. 2016). Kolejnym genem wpływającym na regulację biosyntezy karotenoidów

jest gen *Or*, początkowo zidentyfikowany w kalafiorze z pomarańczową różą i mający ważną rolę w rozwoju chromoplastów (Li i in. 2016, Ellison i in. 2018).

Badania nad wpływem nawożenia, w tym dostępności związków azotowych, na zawartość karotenoidów w korzeniach marchwi nie dostarczyły do tej pory jednoznacznych wyników. Główną przyczyną niepowodzenia najprawdopodobniej był wpływ zmiennych innych czynników środowiskowych oraz wykorzystanie różnych odmian w badaniach. Porównanie wyników badań jest także problematyczne, z uwagi na stosowanie w nich różnych rodzajów nawozów, a tym samym źródła związków azotowych (Evers 1989, Boskovic-Rakocevic i in. 2012, Smoleń i Sady 2009, Gajewski i Węglarz 2010). Problem ten można częściowo wyeliminować poprzez użycie kultur *in vitro*, które pozwalają na prowadzenie badań w ściśle kontrolowanych warunkach. Uzyskanie prawidłowo wykształconych korzeni spichrzowych marchwi w warunkach *in vitro* jest niemożliwe, dlatego alternatywą dla celów badawczych pozostaje wykorzystanie kultur komórkowych i analiza zmian zachodzących na poziomie komórkowym i tkankowym.

Odkąd ponad 80 lat temu wykazano możliwość uzyskania kultur kalusa w warunkach *in vitro* to znajduje on zastosowanie w wielu badaniach. Kalus u roślin jest to struktura złożona z najczęściej luźno połączony niezróżnicowanych komórek, które następnie mogą ulegać różnicowaniu i tworzyć organy np. pędy czy korzenie lub zarodki somatyczne. Kalus powstaje w wyniku uszkodzenia tkanki, na skutek działania patogenu (np. *Agrobacterium tumefaciens*) czy poprzez wpływ egzogennych regulatorów wzrostu. Dlatego tworzenie kalusa może być łatwo zaindukowane w odpowiednich warunkach laboratoryjnych (Ikeuchi i in. 2013). Dzięki temu, że kalus może być łatwo namnażany i nieprzerwanie utrzymywany w warunkach *in vitro* to może być stałym źródłem dużych ilości materiału do doświadczeń. W kulturach roślin *in vitro* występuje zmienność somaklonalna. Może być to zarówno korzystne zjawisko jako źródło zmienności genetycznej dla ważnych cech u roślin uprawnych np. odporności na patogeny, jak również negatywne np. skutkujące utratą pożądanych cech lub zdolności do regeneracji (Brar i Jain 1998). Kultury kalusowe, poza wykorzystaniem jako model do badań, mają zastosowanie również jako materiał do namnażania roślin, tworzenia roślin o ulepszonych cechach czy produkcji różnych metabolitów o właściwościach prozdrowotnych (Efferth 2019). Marchew była jednym z pierwszych gatunków, u których otrzymano kultury kalusowe i zawiesinowe oraz zaobserwowano możliwość regeneracji roślin z komórek somatycznych (Su i in. 2021). Najczęściej powstający kalus marchwi akumuluje bardzo małe ilości karotenoidów (Baranska i in. 2006, Baranski i in. 2006), co powoduje, że dotychczas kalus u marchwi miał małe zastosowanie w badaniach nad

metabolizmem karotenoidów. Ponad 50 lat temu z czerwonego korzenia marchwi odmiany Kintoki uzyskano linie kalusowe oraz zawiesiny komórkowe zdolne do akumulacji karotenoidów, β-karotenu (kalus GD-1) lub likopenu (kalus GD-2, GD-3). Wykorzystane zostały one do badań nad dynamiką biosyntezy karotenoidów czy wpływu różnych czynników (np. stężenia 2,4-D lub fosforanów w pożywce) na biosyntezę karotenoidów (Sugano i in. 1971, Shimizu i in. 1979, Nishi i Kurosaki 1993). W ostatnich latach również inny zespół uzyskał żółte i pomarańczowe kalusy, które posłużyły do indukcji mutacji w genie *PDS* i regeneracji roślin z zahamowaną akumulacją karotenoidów (Xu i in. 2019). U innych gatunków otrzymano transgeniczny kalus zdolny do akumulacji karotenoidów, który np. u Arabidopsis został wykorzystany do badania biosyntezy, regulacji i akumulacja karotenoidów (Kim i in. 2013, Schaub i in. 2018).

Zastosowanie technik edycji genomów pozwala na dokonywanie precyzyjnych zmian w genomie. Umożliwia to zarówno badanie funkcji genów poprzez ich inaktywację lub aktywację, ale także do wprowadzania nowych cech użytkowych. W celu edycji genomów wykorzystuje się sekwencyjno-specyficzne nukleazy, które powodują przerwanie podwójnej nici DNA w rozpoznawanym przez nie miejscu. Powstałe uszkodzenia DNA są najczęściej naprawiane poprzez niehomologiczne łączenie końców. W trakcie naprawy powstałych uszkodzeń DNA mogą powstawać mutacje, najczęściej krótkie insercje lub delecje. Mogą one skutkować zmianą ramki odczytu i tym samym prowadzić do utraty funkcji genu, w obrębie którego powstały. Wcześniej do precyzyjnej edycji genomów wykorzystywane były technologie z wykorzystaniem np. meganukleaz czy palców cynkowych (ZFN). Rozpoznają one sekwencje poprzez interakcje białka z DNA, przez co ich zastosowanie jest ograniczone ze względu na trudności w dostosowywaniu ich do rozpoznawania miejsc, w których mają być indukowane mutacje (Songstad i in. 2017). Ważnym dokonaniem było opracowanie metod edycji genomu w oparciu o system Clustered Regularly Interspaced Short Palindromic Repeats (CRISPR) i CRISPR-associated proteins (Cas). CRISPR jest to rodzina sekwencji DNA występująca w genomach bakterii, złożona z palindromicznych powtórzeń oddzielanymi krótkimi sekwencjami DNA wirusów. CRISPR stanowi źródło krótkich sekwencji RNA, które łącząc się z kompleksem białek Cas, z których przynajmniej jedno jest endonukleazą DNA, służą do naprowadzania endonukleazy na sekwencje DNA wirusów. CRISPR jest więc systemem obronnym bakterii przed wirusowym DNA. Ten system został zaadoptowany w celu edycji genomów. Obecnie najczęściej stosowany system CRISPR/Cas do edycji genomu opiera się na wykorzystaniu pojedynczej endonukleazy Cas9 oraz jednoniciowego RNA (guide RNA, gRNA)

naprowadzającego Cas9 na komplementarną sekwencję w docelowym miejscu w genomie organizmu biorcy (El-Mounadi 2020). Wdrożenie tej metody uznawane jest za przełomowe dla postępu w badaniach biologicznych, o czym świadczy przyznanie w 2020 roku Nagrody Nobla dla Emmanuelle Charpentier i Jennifer A. Doudna za ich wkład w opracowanie metody edycji CRISPR/Cas9. W ciągu zaledwie kilku lat, metoda ta została wykorzystana u wielu gatunków roślin, głównie w celu zaindukowania utraty funkcjonalności genu (El-Mounadi 2020). Pomimo możliwości jakie oferują techniki precyzyjnych edycji genomów, to pozostają wątpliwości dotyczące regulacji prawnych w stosunku do organizmów uzyskanych z wykorzystaniem technik edycji genomów, tj. czy powinny być uznawane jako organizmy genetycznie modyfikowane (GMO), i co aktualnie ogranicza ich zastosowanie w różnych państwach, w tym w Unii Europejskiej (Zhang i in. 2020).

Dla marchwi opracowane i stosowane są różne metody transformacji genetycznej, zarówno wektorowe jak i bezwektorowe, które są wykorzystywane głównie w badaniach podstawowych. Spośród nich najczęściej wykorzystywana jest transformacja z zastosowaniem *Agrobacterium tumefaciens*. Do transformacji mogą być wykorzystywane zarówno całe siewki, ich fragmenty, eksplantaty korzeniowe, kalus, zawiesiny komórkowe czy protoplasty (Baranski i Lukasiewicz 2019). Dzięki dużej ilości opracowanych skutecznych metod transformacji marchwi, edycja genomu u marchwi z wykorzystaniem CRISPR/Cas9 jest znacznie ułatwiona. W trakcie realizacji pracy doktorskiej, w innym modelowym kalusie akumulującym antocyjany skuteczne wyłączono gen 3-hydroksylazy flawononowej (*F3H*) metodą CRISPR/Cas9 powodując zatrzymanie biosyntezy antocyjanów w komórkach (Klimek-Chodacka i in. 2018). Równocześnie inne geny z szlaku biosyntezy karotenoidów były celem edycji z wykorzystaniem jasnego kalusa marchwi (Klimek-Chodacka i in. 2019). Technika CRISPR/Cas9 została także wykorzystana do indukcji mutacji w genach *PDS* i *MYB113-like* prowadząc do uzyskania roślin odpowiednio albinotycznych lub pozbawionych fioletowego zabarwienia (Xu i in. 2019).

6. Cel, hipotezy i zadania badawcze

Badania nad mechanizmami biosyntezy i akumulacji karotenoidów u marchwi są trudne i czasochłonne z powodu jej długiego, dwuletniego cyklu rozwojowego. Rośliny regenerowane w warunkach *in vitro* nie wytwarzają prawidłowo rozwiniętego korzenia, co powoduje, że analizy związane z metabolizmem karotenoidów mogą być realizowane dopiero w kolejnym pokoleniu otrzymanym w warunkach *ex vitro*. Ponadto, analizy związane z akumulacją karotenoidów w korzeniach są utrudnione z uwagi na badania w organie podziemnym. Dlatego celem pracy doktorskiej było opracowanie modelowego systemu i jego wykorzystanie do badania funkcji genów związanych z biosyntezą i akumulacją karotenoidów oraz powiązanymi procesami w komórkach marchwi.

W pracy doktorskiej postawiono następujące hipotezy badawcze:

1. Zróżnicowana zawartość karotenoidów w kalusie marchwi jest związana z różnym poziomem ekspresji genów szlaku biosyntezy tych związków oraz różnicami na poziomie ultrastruktury komórek.
2. Skład chemiczny pożywki mineralnej wykorzystywanej w kulturach *in vitro* marchwi wpływa na akumulację karotenoidów w kalusie.
3. System CRISPR/Cas9 jest skuteczny do ukierunkowanego indukowania mutacji w genach szlaku biosyntezy karotenoidów skutkujących zmianą w akumulacji karotenoidów w komórkach kalusa marchwi.
4. Paralogi syntazy fitoenu (*PSY*) odgrywają różną rolę w procesie biosyntezy karotenoidów w komórkach kalusa marchwi.

W celu weryfikacji hipotez wyznaczono i zrealizowano następujące zadania badawcze, których wyniki zostały opisane w publikacjach (**P1**, **P2** i **P3**) stanowiących niniejszą rozprawę doktorską:

1. Uzyskanie kalusa akumulującego karotenoidy w zbliżonej ilości jak w pomarańczowych korzeniach spichrzowych marchwi (**P1**).
2. Charakterystyka kalusa pod względem, zawartości karotenoidów, ekspresji genów związanych z biosyntezą karotenoidów oraz ultrastruktury komórek (**P1**).
3. Analiza wpływu składu pożywki mineralnej na rozwój kalusa marchwi *in vitro* oraz na zawartość akumulowanych karotenoidów (**P2**).
4. Otrzymanie mutantów funkcjonalnych dwóch paralogów syntazy fitoenu, przy wykorzystaniu narzędzi opartych o elementy systemu CRISPR/Cas9 (**P3**).
5. Określenie roli paralogów syntazy fitoenu w akumulacji karotenoidów w komórkach marchwi i poznanie konsekwencji zahamowania biosyntezy karotenoidów na biogenezę plastydów i strukturę komórki (**P3**).

7. Materiały i metody

Materiałem wykorzystywanym we wszystkich pracach był kalus marchwi uprawnej (*Daucus carota* L. *subsp. sativus* Hoffm.) charakteryzujący się zdolnością do akumulacji karotenoidów. Do indukcji kalusa zostały wykorzystane pomarańczowe korzenie spichrzowe, typu Nantejskiego linii podwojonego haploida DH1, wykorzystanej w projekcie sekwencjonowania genomu marchwi (Iorizzo i in. 2016). Nasiona linii DH1 zostały otrzymane od prof. Philippa Simona z Uniwersytetu w Wisconsin (USA). Indukcja oraz kultury kalusa były prowadzone w warunkach *in vitro* na zmodyfikowanej pożywce B5 o składzie mineralnym makro- i mikroelementów oraz witamin wg Gamborga (Gamborg i in. 1968) i zawierającej 30 g l^{-1} sacharozy, 1 mg l^{-1} 2,4-D, 0,0215 mg l^{-1} kinetyny i 2,7 g l^{-1} phytagelu, którą oznaczono w rozprawie i załączonych publikacjach symbolem BI. Kultury były prowadzone na szalkach Petriego umieszczonych w 26 °C w ciemności. Pasaże eksplantatów, a następnie kalusa na świeżą pożywkę były wykonywane co cztery tygodnie.
W doświadczeniach związanych z badaniem wpływu składu pożywki na rozwój kalusa i zawartość karotenoidów stosowano pożywkę BI, zmodyfikowaną pożywkę MS opartą o skład wg Murashige i Skoog (1962), tj. pożywkę oznaczoną w rozprawie i załączonych publikacjach symbolem R oraz pożywki oparte o skład BI i R, w których dokonano modyfikacji składu i zawartości poszczególnych związków.

W zrealizowanych badaniach wykorzystano następujące techniki badawcze:

- Oznaczanie karotenoidów:
    - metoda ultra sprawnej chromatografii cieczowej (UPLC): ekstrakcja była wykonana w metanolu, acetonie i eterze naftowym. Analizy wykonano na chromatografie z kolumną BEH C18 (1.7 μm) (**P1**);
    - metoda spektrofotometryczna, w ekstraktach w acetonie, pomiar absorbancji przy długości fali 450 nm (**P2**);
    - metoda wysokosprawnej chromatografii cieczowej (HPLC), w ekstraktach mieszaniną etanol:*n*-heksan (1:1, *v*;*v*). Analizy wykonano na chromatografie z kolumną C18 RP (5 μm) (**P2** i **P3**).
- Oznaczenie zawartości kwasu abscysynowego metodą spektrofotometryczną z wykorzystaniem komercyjnego zestawu do immunodetekcji (**P1**).
- Barwienie immunohistochemicznie, z wykorzystaniem przeciwciał do pektyn (JIM5 i JIM7), arabinogalaktanoprotein (LM2 i JIM13) oraz ekstensyn (JIM20) (**P3**).
- Obserwacje z wykorzystaniem:

  - mikroskopu świetlnego (**P1**, **P2** i **P3**);
  - mikroskopu polaryzacyjnego (**P1**);
  - mikroskopu elektronowego (**P1** i **P3**).
- Analiza ekspresji genów związanych z biosyntezą i metabolizmem karotenoidów metodą RT-qPCR (**P1** i **P3**).
- Techniki molekularne, w tym klonowanie Golden Gate i Gateway, w celu stworzenia konstruktów CRISPR/Cas9 oraz metoda elektroporacji do wprowadzenia wektorów plazmidowych do szczepu LBA4404 *A. tumefaciens* (**P3**).
- Transformacje kalusa poprzez inokulację grudek kalusa z *A. tumefaciens* oraz selekcje transformantów na pożywce selekcyjnej (**P3**).
- Techniki do analiz molekularnych otrzymanych kalusów po transformacji: łańcuchowa reakcja polimerazy (PCR), elektroforeza w żelu agarozowym, trawienia produktów PCR enzymami restrykcyjnymi (specyficznymi do sekwencji genów lub niespecyficznym enzymem T7E1), klonowanie z wykorzystaniem plazmidu pGEM-T, sekwencjonowanie Sangera oraz analizy bioinformatyczne (**P3**).

Szczegółowe opisy wszystkich wykorzystanych metod badawczych znajdują się w każdej z publikacji wchodzących w skład rozprawy doktorskiej. Oznaczenia metodą UPLC zostały zrealizowane we współpracy z zespołem z Uniwersytetu Wrocławskiego. Analizy histologiczne, immunohistochemiczne oraz ultrastruktury zostały wykonane w ramach współpracy przez zespół z Uniwersytetu Śląskiego w Katowicach.

8. Omówienie wyników przeprowadzonych badań

8.1. Otrzymanie i charakterystyka modelowego kalusa o pomarańczowej barwie

Publikacja P1:

Oleszkiewicz T., Klimek-Chodacka M., Milewska-Hendel A., Zubko M., Stróż D., Kurczyńska E., Boba A., Szopa J., Baranski R. 2018. Unique chromoplast organization and carotenoid gene expression in carotenoid-rich carrot callus. *Planta* 248, 1455-1471. https://doi.org/10.1007/s00425-018-2988-5

W publikacji P1 przedstawiono wyniki realizacji pierwszego celu pracy czyli otrzymanie kalusa marchwi zdolnego do akumulacji karotenoidów oraz jego charakterystykę. Na powierzchni eksplantatów korzeniowych wyłożonych na pożywkę do indukcji kalusa rozwijał się jasno żółty kalus, który po oddzieleniu od eksplantatów i dalszym namnażaniu utworzył jasno żółtą linię kalusową (Ryc. 1a). Jasno żółty kalus charakteryzował się intensywnym wzrostem i luźną strukturą. Złożony był z luźno połączonych komórek zawierających dużą wakuolę. Rzadko, w niektórych komórkach zauważalne były pojedyncze pomarańczowe kryształy karotenoidowe. W trakcie kolejnych pasaży na powierzchni jasno żółtego kalusa powstawały punktowo, intensywnie pomarańczowe fragmenty tkanki, które po oddzieleniu i osobnym namnożeniu dały początek pomarańczowej linii kalusowej (Ryc. 1b). Pomarańczowy kalus charakteryzował się grudkowatą strukturą, złożoną z mniejszych komórek tworzących zwarte agregaty. Komórki pomarańczowego kalusa posiadały gęstą cytoplazmę oraz dużą ilość pomarańczowych kryształów karotenoidowych obserwowanych w prawie każdej komórce.

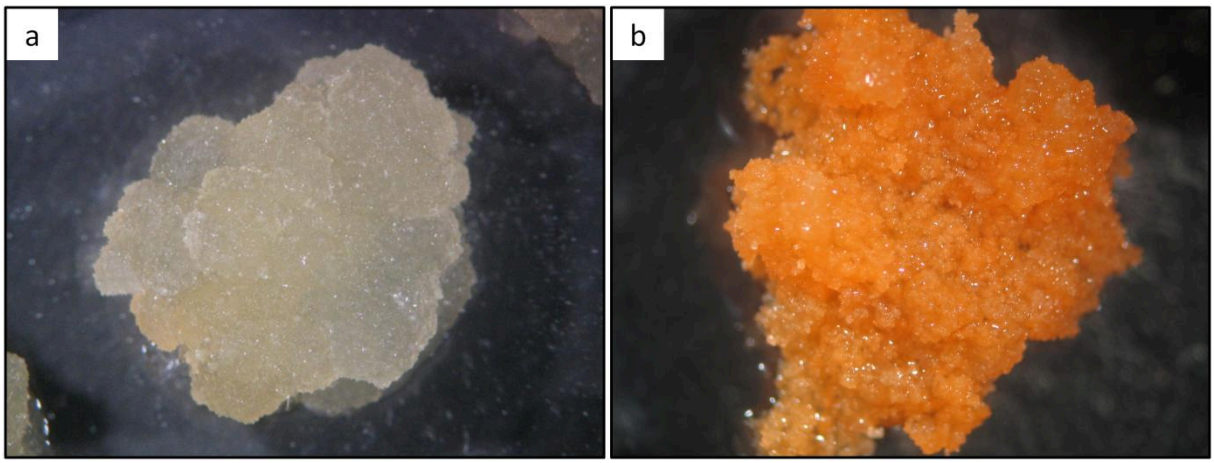

Ryc. 1. Otrzymana jasno żółta linia kalusowa DH1 (**a**) oraz wyselekcjonowana pomarańczowa linia kalusowa DH1 (**b**)

Analiza UPLC karotenoidów potwierdziła, że zaobserwowana pomarańczowa barwa kalusa była spowodowana akumulacją dużych ilości karotenoidów. Wykazała również znaczne różnice w ich zawartości pomiędzy otrzymanymi liniami kalusowymi. Jasny kalus zawierał niewielką ilość karotenoidów (231 μg g^{-1} sm). Było to 8,5 razy mniej niż zawartość karotenoidów w korzeniach wykorzystanych jako eksplantaty do indukcji kalusa (1985 μg g^{-1} sm). Pomarańczowy kalus zawierał 2150 μg g^{-1} sm karotenoidów, czyli zbliżoną ilość do zawartości karotenoidów w korzeniach marchwi. Dominującym karotenoidem znajdującym się we wszystkich badanych kalusach był β-karoten (95% sumy karotenoidów w jasnym kalusie, 94% w pomarańczowym kalusie i 90% w korzeniach). Pomarańczowy kalus różnił się pod względem składu karotenoidów od jasnego kalusa. Posiadał 9,3 razy więcej karotenoidów, w tym: 9,1x więcej β-karotenu, 48,8x więcej α-karotenu, 4,3x więcej luteiny, 1,6x więcej pozostałych ksantofili, 3,7x więcej fitoenu oraz 3,4x więcej kwasu abscysynowego.

Obie otrzymane linie kalusowe porównano między sobą, a także z korzeniem marchwi użytym do indukcji kalusa, pod względem ekspresji 33 genów związanych z biosyntezą karotenoidów. Ekspresja genów związanych z biosyntezą prekursorów karotenoidów w pomarańczowym kalusie była na podobnym poziomie co w korzeniach marchwi. Spośród pięciu paralogów syntazy difosforanu geranylogeranylu odpowiedzialnego za biosyntezę prekursora karotenoidów trzy (*GGPS1.5*, *GGPS1.1* i *GGPS1.8*) miały większą ekspresję w pomarańczowym kalusie i korzeniach niż w jasnym kalusie. Ich zwiększona ekspresja prawdopodobnie powodowała również zwiększoną biosyntezę difosforanu geranylogeranylu, substratu dla PSY. W pomarańczowym kalusie 12 genów z szlaku biosyntezy karotenoidów miało taką samą ekspresję co w jasnym kalusie. W pomarańczowym kalusie była 4,0-krotnie zwiększona ekspresja *PSY2* i 4,6-krotnie obniżona ekspresja *PSY1* niż w jasnym kalusie. Ekspresja *PSY2* w pomarańczowym kalusie była prawie 4 razy mniejsza niż w korzeniu, zawierającym podobną ilość karotenoidów. Dlatego zwiększona ekspresja *PSY2* tylko częściowo tłumaczy zwiększoną akumulację karotenoidów. W pomarańczowym kalusie ekspresja genu ε-cyklazy likopenu (*LCYE*) była również 7-krotnie większa niż w jasnym kalusie i 3-krotnie większa niż w korzeniu. Nie miało to jednak przełożenia na zawartość α-karotenu i luteiny, których było mniej w pomarańczowym kalusie niż w korzeniu. Gen *BCH2* odpowiedzialny za hydroksylację karotenów miał 155 razy mniejszą ekspresję w pomarańczowym kalusie w porównaniu do korzenia i 12 razy mniejszą niż w jasnym kalusie. Wskazuje to, że zwiększona akumulacja β-karotenu w pomarańczowym kalusie była również spowodowana zahamowaną hydroksylacją β-karotenu, prowadzącą zwykle

do powstawania związków szlaku ksantofilowego, a które występowały w tym kalusie w znikomej ilości. Zbadano również ekspresję genu *Y* (DCAR_032551). W pomarańczowym kalusie jego ekspresja była 49-krotnie mniejsza niż w korzeniu, ale 5-krotnie większa niż w jasnym kalusie. Duża różnica w ekspresji genu *Y* między pomarańczowym kalusem i korzeniem, wskazuje na brak związku jego ekspresji z akumulacją karotenoidów w tym kalusie.

W publikacji P1 przedstawione zostały również wyniki obserwacji mikroskopowych obu kalusów. Wykazano znaczne różnice w ultrastrukturze komórek jasnego i pomarańczowego kalusa, w szczególności zmiany widoczne były w plastydach. W jasnym kalusie głównymi obserwowanymi plastydami były proplastydy, w mniejszym stopniu amyloplasty i rzadko chromoplasty. W pomarańczowym kalusie dominowały chromoplasty, a ogólna liczba plastydów była dwa razy większa niż w jasnym kalusie. W obrębie jednej komórki pomarańczowego kalusa można było zaobserwować różne typy chromoplastów. Najczęstszymi były chromoplasty krystaliczne tworzące kształty podobne do igieł lub wstążek. Zaobserwowano również chromoplasty globularne, cylindryczne oraz błoniaste. Tym samym wykazano po raz pierwszy, że komórki marchwi są zdolne do tworzenia chromoplastów błoniastych. Jednoczesne występowanie chromoplastów i amylochromoplastów wskazuje, że biosynteza i akumulacja karotenoidów zachodzi w chromoplastach o różnej ultrastrukturze. Obecność amylochromoplastów w pomarańczowym kalusie wskazuje na pośrednie stadia rozwoju chromoplastów, które były obserwowane u innych gatunków, ale dotychczas nie zaobserwowano ich u marchwi (Horner i in. 2007). Zauważona obecność dużych agregatów fitoferrytyny w niektórych chromoplastach wskazuje na ich starzenie się, co nie było wcześniej zaobserwowane w komórkach marchwi. Duża liczba różnych chromoplastów w komórkach pomarańczowego kalusa sprawia, że otrzymany kalus można uznać za dogodny obiekt do badań nad rozwojem i różnicowaniem plastydów.

8.2. Wpływ składu pożywki mineralnej na akumulację karotenoidów w kalusie marchwi

Publikacja P2:

Oleszkiewicz T., Kruczek M., Baranski R. 2021. Repression of carotenoid accumulation by nitrogen and NH_4^+ supply in carrot callus cells in vitro. *Plants* 10, 1813, https://doi.org/10.3390/plants10091813

W trakcie realizacji badań zaobserwowano, że pomarańczowy kalus rosnący na pożywce R do regeneracji roślin (Ryc. 2b) ma znacznie jaśniejszą barwę niż rosnący na pożywce BI do indukcji kalusa (Ryc. 2a). Obie pożywki różnią się w składzie makroelementów, mikroelementów, zawartości związków organicznych, obecnością regulatorów wzrostu i ilością sacharozy. Dlatego przeprowadzono serię doświadczeń by zbadać wpływ składu pożywek na akumulację karotenoidów w kalusie. Poza pożywkami BI i R zbadano 10 wariantów pożywek z zamienionymi grupami składników między pożywkami, sześć wariantów pożywek ze zmodyfikowanym składem makroelementów oraz dziewięć pożywek ze zmienioną zawartością soli azotowych.

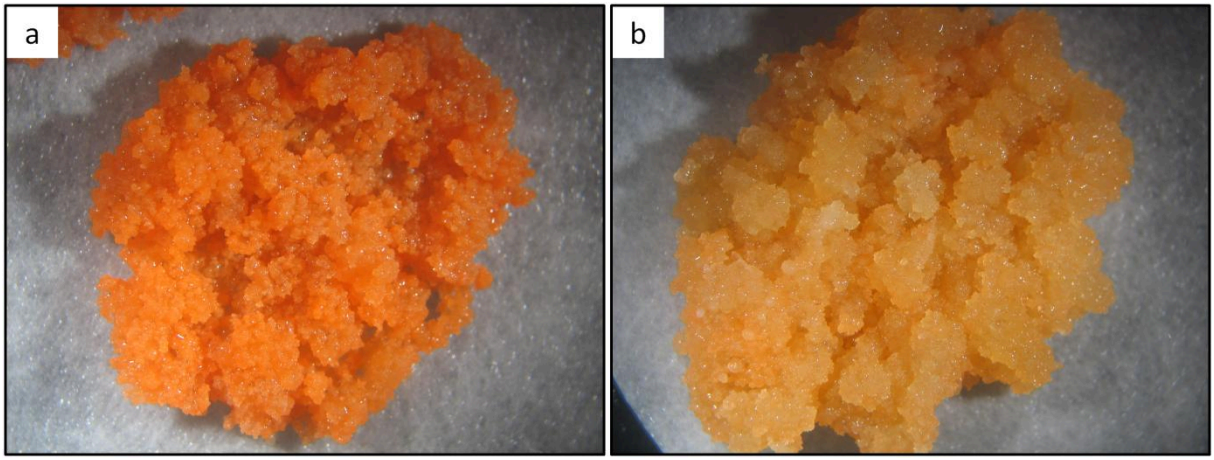

Ryc. 2. Pomarańczowy kalus marchwi na pożywce BI (**a**) oraz R (**b**).

W zrealizowanych badaniach nie zaobserwowano różnic między intensywnością wzrostu pomarańczowego kalusa na pożywkach BI i R, oraz pod wpływem modyfikacji ich składu. Słabszy wzrost kalusa zaobserwowano tylko na pożywkach z ilością N wg składu B5 (26,76 mM), ale ze zmniejszonym stosunkiem NO_3:NH_4 poniżej 1,91. Przy stosunku NO_3:NH_4 równym 1 wzrost kalusa został całkowicie zahamowany. Pozwoliło to na wskazanie granicznego stosunku zawartości jonów NO_3:NH_4 w pożywce, poniżej którego występuje negatywny wpływ pożywki na wzrost kalusa. Zarówno kalus rosnący na pożywce kontrolnej jak i kalus z ograniczoną akumulacją karotenoidów charakteryzowały się zwartą i grudkowatą

strukturą, stworzoną z niewielkich kulistych komórek, charakterystyczną dla pomarańczowego kalusa. Niezależnie od pożywki kalus miejscami tworzył luźniejsze, mniej zwarte struktury. Kalus rosnący na pożywkach pozbawionych 2,4-D i kinetyny tworzył struktury proembriogenne oraz zarodki we wczesnych stadiach rozwoju. Nie zaobserwowano związku między składem mineralnym i tym samym zawartością karotenoidów, a somatyczną embriogenezą w pomarańczowym kalusie. Jednak dalszy rozwój powstających zarodków był zahamowany i albo brązowiały i zamierały albo na ich powierzchni ponownie rozwijał się kalus.

Analiza HPLC wykazała podobną zawartość karotenoidów (2264 µg g^{-1} sm) w pomarańczowym kalusie rosnącym na pożywce kontrolnej (BI) do wartości uzyskanej z analiz ULPC (2150 µg g^{-1} sm) podczas dokonywania charakterystyki kalusa przedstawionej w publikacji P1. Kalus rosnący na pożywce R zawierał 5,3 razy mniej karotenów (425 µg g^{-1} sm) niż kalus rosnący na pożywce kontrolnej. Ilość karotenoidów oznaczona metodą spektrofotometryczną była mniejsza (1169 µg g^{-1} sm) niż oznaczona metodą HPLC w tych samych próbkach. Pozostawała jednak silna liniowa zależność pomiędzy wynikami otrzymanymi obydwoma metodami (R^2 = 0,96; p < 0,001), co skłoniło do wykorzystania w dalszych badaniach wyłącznie prostszej metody spektrofotometrycznej.

Spośród badanych grup składników pożywki tylko skład makroelementów miał wpływ na zawartość karotenoidów w pomarańczowym kalusie. Kalus rosnący na pożywce BI, mającej po modyfikacji makroelementy według MS zawierał 531 µg g^{-1} sm karotenoidów, podobnie jak kalus rosnący na pożywce R (404 µg g^{-1} sm). Zamienienie składu makroelementów w pożywce R na skład według B5 spowodowało wzrost zawartości karotenoidów w kalusie. Modyfikacja składu makroelementów pożywki BI poprzez zamienienie soli azotowych na skład według pożywki R, spowodowała ograniczenie akumulacji karotenoidów w kalusie rosnącym na tej pożywce o prawie 40%, podobnie jak na pożywce R. Modyfikacje składu soli dostarczających P, K, Ca, lub Mg w pożywce BI na skład według pożywki R nie spowodowały zmian w morfologii, kolorze czy składzie karotenoidów w kalusie. Pozostałe badane modyfikacje pożywek BI i R (zamiana mikroelementów, witamin, regulatorów wzrostu i ilości sacharozy) nie miały wpływu na akumulację karotenoidów. Ponieważ wyniki wskazały, że spośród wszystkich składników pożywki tylko N wpływa na zawartość karotenoidów, w dalszej kolejności badano wpływ ilości tego pierwiastka i formy związków w jakich był dostarczany. Zwiększenie zawartości N w pożywce w zakresie od 27 mM do 80 mM spowodowało ograniczenie akumulacji karotenoidów w kalusie z 1252 µg g^{-1} sm do 411 µg g^{-1} sm karotenoidów. Obserwowane

zmiany w akumulacji karotenoidów pod wpływem zwiększenia ilości N były widoczne zarówno na pożywkach ze stałym stosunkiem NO_3:NH_4 wynoszącym 12,19 oraz na pożywkach, w których stosunek NO_3:NH_4 był zwiększany do 38,5 (dla obu zestawów pożywek $p < 0,001$). Malejąca zawartość karotenoidów w kalusie wraz ze wzrostem ilości N dobrze opisuje dopasowana krzywa regresji ($R^2 = 0,82$ dla stałego NO_3:NH_4 i $R^2 = 0,95$ dla rosnącego NO_3:NH_4). Obniżanie stosunku NO_3:NH_4 w pożywce, przy zachowaniu stałej ilości N, wynoszącej 26,76 mM, również powodowało znaczne ograniczanie akumulacji karotenoidów w kalusie ($p < 0,001$). Przy stosunku NO_3:NH_4 wynoszącym tyle samo co w pożywce R (1,91) ilość karotenoidów była 3x mniejsza niż w kalusie na pożywce kontrolnej. Dalsze obniżenie NO_3:NH_4 do 1 spowodowało ponad 10-cio krotne zmniejszenie akumulacji karotenoidów do 115 $\mu g\ g^{-1}$ sm. Podobnie jak zwiększanie ilości N, zmiany w stosunku zawartości NO_3:NH_4 w pożywce dobrze opisywała dopasowana krzywa regresji ($R^2 = 0,97$). Otrzymane wyniki wskazują, że jedynie modyfikacje składu soli azotowych w pożywce, zwiększające całkowitą ilość N lub zmniejszające stosunek NO_3:NH_4, powodują ograniczenie akumulacji karotenoidów w uzyskanym modelowym pomarańczowym kalusie. Zaobserwowany wpływ zwiększonej ilości azotu lub zmienionej jego formy na akumulację karotenoidów w komórkach marchwi może być ograniczony do modelu w warunkach *in vitro*, dlatego potrzebna byłaby weryfikacja zaobserwowanych zależności w roślinach. Pomimo tego, otrzymane wyniki dostarczają dodatkowej wiedzy o wpływie substancji mineralnych na produkcję metabolitów wtórnych w kulturach *in vitro*, która może być przydatna w dalszych badaniach lub przy optymalizacji warunków kultury do produkcji metabolitów.

8.3. Rola paralogów syntazy fitoenu w pomarańczowym kalusie marchwi

Publikacja P3:

Oleszkiewicz T., Klimek-Chodacka M., Kruczek M., Godel-Jędrychowska K., Sala K., Milewska-Hendel A., Zubko M., Kurczyńska E., Qi Y., Baranski R. 2021. Inhibition of carotenoid biosynthesis by CRISPR/Cas9 triggers cell wall remodelling in carrot. *International Journal of Molecular Sciences* 22, 6516. https://doi.org/10.3390/ijms22126516

Do zaindukowania mutacji paralogów syntazy fitoenu wykorzystano system CRISPR/Cas9. W tym celu stworzono dwa wektory plazmidowe zawierające w T-DNA gen selekcyjny *aph* (oporność na higromycynę), gen *Cas9* oraz dwa guideRNA komplementarne do genu *PSY1* (wektor psy1-g1g2) lub *PSY2* (wektor psy2-g1g2). Po transformacji z wykorzystaniem *A. tumefaciens* na powierzchni kalusa rosnącego na pożywce selekcyjnej tworzyły się nowe, pojedyncze grudki kalusowe. Rozwijające się nowe grudki kalusowe w większości były pomarańczowe, niektóre z nich miały jaśniejszą barwę i wyłącznie na kalusach po transformacji psy2-g1g2 obserwowane było powstawanie całkowicie białych grudek kalusa. Po selekcji, na podstawie analiz molekularnych oraz intensywności wzrostu kalusów wybrano 5 linii kalusowych zawierających mutacje w genie *PSY1*, 5 linii zawierających mutacje w genie *PSY2* oraz linię kalusową zawierającą wprowadzony konstrukt psy2-g1g2, ale bez mutacji w rejonie genu *PSY2*. Wszystkie otrzymane linie kalusowe zawierające mutacje w genie *PSY1* miały pomarańczową barwę, od intensywnie pomarańczowej do jasno pomarańczowej, podobnie do kontroli (Ryc. 3a). Natomiast wszystkie zidentyfikowane linie z mutacjami w genie *PSY2* były całkiem białe (Ryc. 3b) lub z miejscami blado żółtymi.

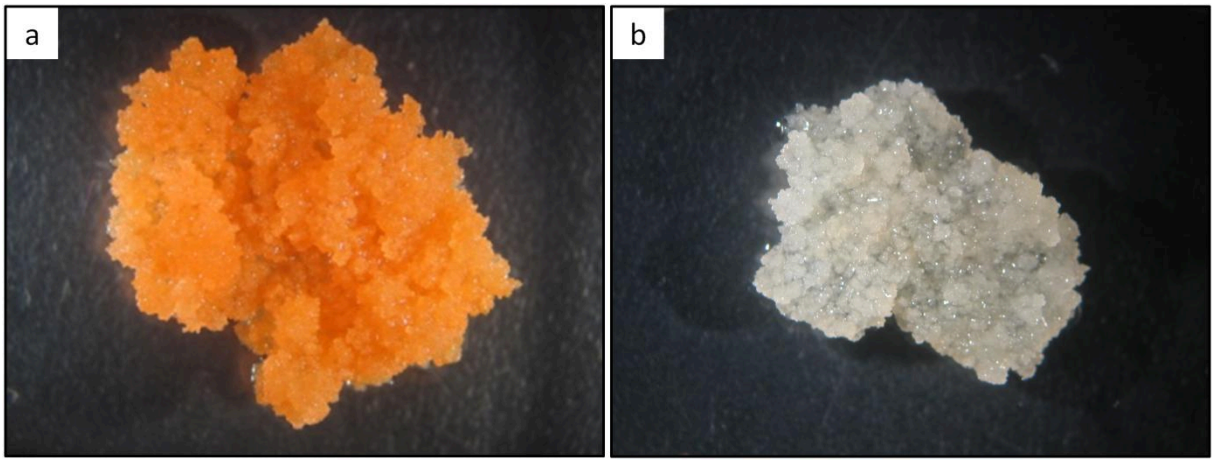

Ryc. 3. Nietransformowany pomarańczowy kalus (**a**) oraz transformowany z zaindukowaną mutacją funkcjonalną genu *PSY2* (**b**).

Sekwencjonowanie produktów PCR potwierdziło obecność mutacji w badanych liniach kalusowych w regionach genów *PSY*. Tylko w jednej linii kalusowej psy1-g1g2 znaleziono mutacje w regionie pierwszego gRNA i była to insercja pojedynczego nukleotydu (T). We wszystkich liniach psy1-g1g2 wykryto mutacje w regionie drugiego gRNA. Były to pojedyncze insercje (A), substytucje C/A i G/A lub delecje od 1 do 20 nukleotydów. W ramach pojedynczych linii kalusowych obserwowano od 1 do 5 różnych mutacji. Analiza translacji zmienionych sekwencji genu *PSY1* wykazała, że wszystkie mutacje poza substytucjami oraz jedną cichą mutacją powodują zmianę sekwencji aminokwasowej i powstawanie krótszego, niefunkcjonalnego białka. W liniach psy2-g1g2 większością mutacji były insercje pojedynczych nukleotydów (A, T lub G) lub delecje (krótkie od 1 do 4 nukleotydów i dłuższe od 27 do 82 nukleotydów). Obecne były również substytucje C/A i C/T. W jednej linii psy2-g1g2 cały fragment (286 nukleotydów) między oboma guideRNA uległ delecji, jednocześnie w tej samej linii była duplikacja tego fragmentu. Przeprowadzona analiza bioinformatyczna wskazała, że powstałe zmiany w sekwencji genu *PSY2* w większości powodowały również znaczne zmiany w sekwencji aminokwasowej i tym samym powstawanie niefunkcjonalnego białka.

Analizy HPLC potwierdziły, że obserwowane różnice w barwie kalusów są spowodowane różną zawartością karotenoidów i wykazały różnice w zawartości karotenoidów w otrzymanych liniach kalusowych zawierających mutacje genów *PSY*. Wykorzystany w tym doświadczeniu kontrolny, nietransgeniczny kalus zawierał 1599 µg g^{-1} sm karotenoidów, głównie β-karotenu i α-karotenu. Linie kalusowe z mutacjami *PSY1* znacznie różniły się w zawartości karotenoidów i ich ilość była od 131 do 2493 µg g^{-1} sm. W dwóch liniach z mutacjami *PSY2* były bardzo małe ilości karotenoidów (16 µg g^{-1} sm i 28 µg g^{-1} sm). W pozostałych trzech liniach *PSY2* ilość karotenoidów była ledwo mierzalna i wynosiła 0,5 – 4,0 µg g^{-1} sm.

Analiza qPCR wykazała zmiany w ekspresji genów *PSY*. W mutantach *PSY1* ekspresja genu *PSY1* zmniejszyła się do poziomu 0,29 względem kontroli (p = 0,002), a ekspresja *PSY2* nie uległa zmianie i wyniosła 0,77 względem kontroli (p = 0,117). We wszystkich mutantach *PSY2* ekspresja *PSY2* była obniżona (p = 0,003) do 0,29 względem kontroli. Jednocześnie ekspresja *PSY1* również była obniżona (p = 0,002) do 0,37 względnej ekspresji. W mutantach *PSY1* nie było korelacji między poziomami ekspresji obu genów (r = -0,265; p = 0,612), jednak w przypadku mutantów *PSY2* ekspresja obu genów korelowała z sobą (r = 0,97; p = 0,001). Ekspresja *PSY1* nie korelowała z zawartością karotenoidów (r = 0,05; p = 0,923) w mutantach *PSY1*, jednak w przypadków mutantów *PSY2* zaobserwowano korelację między

ekspresją *PSY1* a zawartością karotenoidów (r = 0,97; p = 0,001). Istniała korelacja między ekspresją *PSY2* a zawartością karotenoidów niezależnie od zaindukowanych mutacji (dla mutantów *PSY1*: r = 0,94, p = 0,006; dla mutantów *PSY2*: r = 0,93, p = 0,006).

Przeprowadzona analiza ultrastruktury komórek zawierających mutacje *PSY2* wykazała zmiany w ich plastydach. W mutantach *PSY2* dominującymi plastydami były amyloplasty wypełnione całkowicie skrobią. W niektórych plastydach można było zaobserwować obecność plastoglobul oraz błon wewnętrznych. Poza plastydami, mutant *PSY2* nie różnił się na poziomie ultrastruktury od kalusa nietransgenicznego. Zwizualizowane zostały również zmiany w składzie ściany komórkowej u mutantów *PSY2*. W komórkach pozbawionych karotenoidów było mniej zmetylestryfikowanych pektyn oraz mniej białek arabinogalaktanowych w porównaniu do kalusa nietransgenicznego.

Analiza mutantów *PSY1* i *PSY2* wykazały, że biosynteza karotenoidów w kalusie marchwi jest zależna od obecności funkcjonalnego PSY2, podczas gdy PSY1 odgrywa raczej rolę pomocniczą. Wykazano, że powstałe mutacje powodują obniżenie ekspresji genu, w którym zostały zaindukowane. Również, obniżenie poziomu ekspresji *PSY1* w mutantach *PSY2* wskazuje na skoordynowaną regulację ekspresji obu paralogów, co może być tłumaczone wsteczną regulacją spowodowaną brakiem metabolitów ze szlaku biosyntezy karotenoidów. Obserwowane różne stadia rozwoju chromoplastów u mutantów świadczą o przemianie amyloplastów w amylochromoplasty, a następnie w chromoplasty, co pozostawało do tej pory niepotwierdzone. Zaobserwowane różnice w występowaniu estryfikowanych pektyn i AGP u mutantów *PSY2* w porównaniu do pomarańczowego kalusa świadczą o związku między występowaniem tych związków i metabolizmem karotenoidów. Po raz pierwszy przedstawiona została wizualizacja zmian składu ściany komórkowej wywołanych zmianą w szlaku biosyntezy karotenoidów. Ponieważ otrzymane mutanty różnią się pod względem genetycznym od nietransgenicznego pomarańczowego kalusa jedynie zmianą funkcjonalną w genie *PSY2* prowadzącą do zahamowania akumulacji karotenoidów, to otrzymane linie kalusowe stanowią unikalny materiał nie tylko do badań nad biogenezą plastydów, ale także wpływu karotenoidów na inne procesy komórkowe.

9. Podsumowanie i wnioski

W trakcie realizacji pracy doktorskiej otrzymano unikalny, nietransgeniczny kalus marchwi linii podwojonego haploida DH1 akumulujący karotenoidy w ilości porównywalnej do tej, jaka występuje w pomarańczowym korzeniu spichrzowym marchwi. Uznano, że może stanowić on dogodny model do badania wpływu różnych czynników na biosyntezę i akumulację karotenoidów. Przy jego pomocy wykazano istotny wpływ dostępności różnych form azotu na akumulację karotenoidów w komórkach kalusa marchwi. Skutecznie zaindukowano ukierunkowane mutacje dwóch genów, *PSY1* oraz *PSY2*, w intensywnie pomarańczowym kalusie z wykorzystaniem techniki CRISPR/Cas9, doprowadzając do zahamowania biosyntezy karotenoidów w kalusach mutantów *PSY2*. Zrealizowane badania dostarczają nowej wiedzy o charakterystyce tkanek kalusowych bogatych w karotenoidy, wpływu dostępności substancji odżywczych na akumulację karotenoidów w komórkach marchwi oraz wiedzy o roli paralogów genu syntazy fitoenu w komórkach kalusa marchwi.

Na podstawie zrealizowanych badań wyciągnięto następujące wnioski:

1. Poprzez selekcję wariantów somaklonalnych ubogiego w karotenoidy kalusa marchwi możliwe jest otrzymanie kalusa akumulującego podobne ilości karotenoidów co korzeń marchwi, z którego został wyprowadzony jasny kalus.
2. Kalusy o różnej zawartości karotenoidów różnią się istotnie pod względem ekspresji genów związanych z biosyntezą karotenoidów, w szczególności paralogów syntazy fitoenu (*PSY1* i *PSY2*), ε-cyklazy likopenu (*LCYE*) i hydroksylazy karotenu (*BCH2*).
3. Skład soli azotowych w pożywce istotnie wpływa na akumulację karotenoidów w komórkach kalusach marchwi *in vitro*. Zwiększenie zawartości azotu lub zmniejszenie stosunku jonów azotanowych do amonowych powoduje ograniczenie akumulacji karotenoidów.
4. Powstawanie struktur proembriogennych i zarodków somatycznych w kalusie marchwi nie zależy od ilości akumulowanych karotenoidów w komórkach kalusa. Powstałe zarodki z pomarańczowego kalusa nie są zdolne do dalszego rozwoju.
5. Indukcja mutacji w genie *PSY2* skutkujących powstawaniem niefunkcjonalnego białka powoduje całkowite zahamowanie akumulacji karotenoidów, co wskazuje że *PSY2* jest kluczowym genem dla biosyntezy karotenoidów w kalusie marchwi. Indukcja mutacji w genie *PSY1* nie powoduje zahamowania akumulacji karotenoidów, co wskazuje że rola *PSY1* w kalusie marchwi jest tylko pomocnicza dla biosyntezy karotenoidów.

6. Ekspresja *PSY1* ulega zmniejszeniu po indukcji mutacji w genie *PSY2* i zahamowaniu biosyntezy karotenoidów, co wskazuje na wsteczną regulację spowodowaną brakiem metabolitów ze szlaku biosyntezy karotenoidów.
7. W komórkach pomarańczowego kalusa występują jednocześnie różnego rodzaju plastydy i w różnych stadiach rozwoju, co umożliwia obserwacje tworzenia chromoplastów. Obecność amylochromoplastów w pomarańczowym kalusie dostarcza dowodów na pośrednie stadia rozwoju chromoplastów, które nie były wcześniej zaobserwowane u marchwi.
8. Całkowite zahamowanie akumulacji karotenoidów w komórkach kalusa marchwi powoduje zmiany w składzie ściany komórkowej, zmniejszenie zawartości metylestryfikowanych pektyn oraz białek arabinogalaktanowych, co wskazuje na związek między metabolizmem karotenoidów i składem ściany komórkowej.
9. Technologia CRISPR/Cas9 jest skuteczna do indukcji ukierunkowanych mutacji w komórkach pomarańczowego kalusa marchwi w celu modyfikacji procesów związanych z biosyntezą karotenoidów.
10. Kalus marchwi bogaty w karotenoidy jest dobrym modelem do badania procesów związanych z biosyntezą i akumulacją karotenoidów, rozwojem plastydów, a także jako źródło kryształów karotenoidowych do badań nad ich strukturą.

Uzupełnienie

Otrzymany modelowy kalus o wysokiej zawartości karotenoidów okazał się przydatny do badań, które wykraczają poza zakres niniejszej rozprawy, i które prowadziłem we współpracy z naukowcami z Uniwersytetu Jagiellońskiego i Polskiej Akademii Nauk. Otrzymany pomarańczowy kalus wykorzystano do zbadania właściwości fizykochemicznych kryształów karotenoidowych i mapowania ich lokalizacji w komórkach. Zastosowane zostało obrazowanie z wykorzystaniem spektroskopii ramanowskiej, mikroskopii sił atomowych (AFM) oraz mikroskopii skaningowej bliskiego pola (SNOM) do zbadania składu chemicznego i różnic strukturalnych kryształów karotenoidowych bez konieczności ich izolacji, tj. bezpośrednio w komórkach kalusa. Wyniki opublikowano w *Spectrochimica Acta - Part A: Molecular and Biomolecular Spectroscopy* (**IF_{2018} = 2,653**; Rygula i in. 2018). Została także opracowana metoda izolacji kryształów karotenoidowych z kalusa marchwi i wykonywania z nich preparatów do pomiarów metodą spektroskopii ramanowskiej, która została opublikowana jako rozdział w monografii wydawnictwa Springer z serii "*Methods in molecular biology*" (Oleszkiewicz i in. 2020). Pozyskane kryształy karotenoidowe zostały wykorzystane także do dokonania obserwacji wzmocnienia chiralności cząsteczek karotenoidowych. Wykazano, że kryształy karotenoidowe, stworzone głównie z niechiralnego β-karotenu, wykazują chiralność dzięki obecności w swojej strukturze niewielkich ilości chiralnych cząsteczek (α-karotenu lub luteiny). Wyniki te zostały opublikowane w prestiżowym czasopiśmie *Angewandte Chemie International Edition* (**IF_{2019} = 12,102**; Dudek i in. 2019).

Publikacje zawierające wyniki badań zrealizowanych z wykorzystaniem otrzymanego pomarańczowego kalusa i niewchodzące w skład rozprawy doktorskiej:

- Dudek, M.; Machalska, E.; **Oleszkiewicz**, **T**.; Grzebelus, E.; Baranski, R.; Szcześniak, P.; Mlynarski, J.; Zajac, G.; Kaczor, A.; Baranska, M. Chiral Amplification in Nature: Studying Cell-Extracted Chiral Carotenoid Microcrystals via the Resonance Raman Optical Activity of Model Systems. *Angew. Chem. Int. Ed.* **2019**, 58, 8383–8388
- Rygula, A.; **Oleszkiewicz**, **T**.; Grzebelus, E.; Pacia, M.Z.; Baranska, M.; Baranski, R. Raman, AFM and SNOM high resolution imaging of carotene crystals in a model carrot cell system. *Spectrochim. Acta A* **2018**, 197, 47–55
- **Oleszkiewicz**, **T**.; Pacia, M.Z.; Grzebelus, E.; Baranski, R. **2020**. Light Microscopy and Raman Imaging of Carotenoids in Plant Cells In Situ and in Released Carotene Crystals. W: Rodríguez-Concepción, M. i Welsch, R. (red.), *Plant and food carotenoids : methods and protocols. Methods in molecular biology* (Clifton, N.J.). Springer Science+Business Media, 2083: 245–260

10. Literatura

1. Baranska, M.; Baranski, R.; Schulz, H.; Nothnagel, T. Tissue-specific accumulation of carotenoids in carrot roots. *Planta* **2006**, 224, 1028–1037
2. Baranski, R.; Klocke, E.; Schumann, G. Green fluorescent protein as an efficient selection marker for *Agrobacterium rhizogenes* mediated carrot transformation. *Plant Cell Rep.* **2006**, 25, 190–197
3. Baranski, R.; Lukasiewicz, A. **2019**. Genetic engineering of carrot. In *Carrot Genome*; Simon P., Iorizzo M., Grzebelus D., Baranski R. Eds.; Springer International Publishing: Cham, Switzerland; pp. 149–186
4. Boskovic-Rakocevic, L.; Pavlovic, R.; Zdravkovic, J.; Zdravkovic, M.; Pavlovic, N.; Djuric, M. Effect of nitrogen fertilization on carrot quality. *Afr. J. Agric. Res.* **2012**, 7, 2884–2900
5. Bowman, M.J.; Willis, D.K.; Simon, P.W. Transcript abundance of phytoene synthase 1 and phytoene synthase 2 is associated with natural variation of storage root carotenoid pigmentation in carrot. *J. Am. Soc. Hortic. Sci.* **2014**, 139, 63–68
6. Brar, D.S.; Jain S.M. **1998**. Somaclonal variation: Mechanism and applications in crop improvement. In: *Somaclonal Variation and Induced Mutations in Crop Improvement. Current Plant Science and Biotechnology in Agriculture, vol 32*; Jain S.M., Brar D.S., Ahloowalia B.S. Eds.; Springer, Dordrecht; pp. 15–37
7. Chen, K.; Li, G.-J.; Bressan, R.A.; Song, C.-P.; Zhu, J.-K.; Zhao, Y. Abscisic acid dynamics, signaling, and functions in plants. *J. Integr. Plant Biol.* **2020**, 62, 25–54
8. Diretto, G.; Frusciante, S.; Fabbri, C.; Schauer, N.; Busta, L.; Wang, Z.; Matas, A.J.; Fiore, A.; Rose, J.K.C.; Fernie, A.R.; et al. Manipulation of β-carotene levels in tomato fruits results in increased ABA content and extended shelf life. *Plant Biotechnol. J.* **2020**, 18, 1185–1199
9. Eggersdorfer, M.; Wyss, A. Carotenoids in human nutrition and health. *Arch. Biochem. Biophys.* **2018**, 652, 18–28
10. El-Mounadi, K.; Morales-Floriano, M.L.; Garcia-Ruiz H. Principles, applications, and biosafety of plant genome editing using CRISPR-Cas9. *Front. Plant Sci.* **2020**, 11, 56
11. Ellison, S.L.; Luby, C.H.; Corak, K.E.; Coe, K.M.; Senalik, D.; Iorizzo, M.; Goldman, I.L.; Simon, P.W.; Dawson, J.C. Carotenoid presence in associated with the *Or* gene in domesticated carrot. *Genetics* **2018**, 210, 1497–1508
12. Efferth, T. Biotechnology applications of plant callus cultures. *Engineering* **2019**, 5, 50–59
13. Eurostat 2020. *https://ec.europa.eu/eurostat/statistics-explained/index.php/Agricultural_production_-_crops*, **20.09.2021**
14. Evers, A.-M. Effects of different fertilization practices on the carotene content of carrot. *Agric. Food Sci.* **1989**, 61, 7–14
15. Faizan, M.; Faraz, A.; Sami, F.; Siddiqui, H.; Yusuf, M.; Gruszka, D.; Hayat, S. Role of strigolactones: Signalling and crosstalk with other phytohormones. *Open Life Sci.* **2020**, 15, 217–228
16. FAOstat 2019. *http://www.fao.org/faostat/*, **20.09.2021**
17. Flores-Ortiz, C.; Alvarez, M.L.; Undurraga, A.; Arias, D.; Durán, F.; Wegener, G.; Stange, C. Differential role of the two ζ-carotene desaturase paralogs in carrot (*Daucus carota*): *ZDS1* is a functional gene essential for plant development and carotenoid synthesis. *Plant Sci.* **2020**, 291, 110327
18. Fuentes, P.; Pizarro, L.; Moreno, J.C.; Handford, M.; Rodriguez-Concepcion, M.; Stange, C. Light-dependent changes in plastid differentiation influence carotenoid gene expression and accumulation in carrot roots. *Plant Mol. Biol.* **2012**, 79, 47–59.

19. Gajewski, M.; W˛eglarz, Z.; Sereda, A.; Bajer, M.; Kuczkowska, A.; Majewski, M. Carotenoid accumulation by carrot storage roots in relation to nitrogen fertilization Level. *Not. Bot. Horti Agrobot. Cluj-Napoca* **2010**, 38, 71–75
20. Gamborg, O.L.; Miller, R.A.; Ojima, K. 1968. Nutrient requirements of suspension cultures of soybean root cells. *Exp. Cell. Res.* **1968**, 50, 151–158
21. Horrner, H.T.; Healy, R.A.; Ren, G.; Fritz, D.; Klyne, A.; Seames, C.; Thornburg, R.W. Amyloplast to chromoplast conversion in developing ornamental tobacco floral nectaries provides sugar for nectar and antioxidants for protection. *Am. J Bot.* **2007**, 94, 12–24
22. Iorizzo, M.; Ellison, S.; Senalik, D.; Zeng, P.; Satapoomin, P.; Huang, J.; Bowman, M.; Iovene, M.; Sanseverino, W.; Cavagnaro, P.; i in. A high-quality carrot genome assembly provides new insights into carotenoid accumulation and asterid genome evolution. *Nat. Genet.* **2016**, 48, 657–666
23. Ikeuchi, M.; Sugimoto, K.; Iwase, A. Plant callus: Mechanisms of induction and repression. *Plant Cell* **2013**, 25, 3159–3173
24. Kim, J.E.; Rensing, K.H.; Douglas, C.J.; Cheng, K.M. Chromoplasts ultrastructure and estimated carotene content in root secondary phloem of different carrot varieties. *Planta* **2010**, 231, 549–558
25. Kim, S.; Kim, Y.; Ahn, Y.; Ahn, M.; Jeong, J.; Lee, H.; Kwak, S. Downregulation of the lycopene ε-cyclase gene increases carotenoid synthesis via the β-branch-specific pathway and enhances salt stress tolerance in sweet potato transgenic calli. *Physiol. Plant.* **2013**, 147, 432–442
26. Klimek-Chodacka, M.; Oleszkiewicz, T.; Lowder, L.G.; Qi, Y.; Baranski, R. Efficient CRISPR/Cas9-based genome editing in carrot cells. *Plant Cell Rep.* **2018**, 37, 575–586
27. Klimek-Chodacka, M.; Oleszkiewicz, T.; Qi, Y.; Baranski, R. Carrot genome editing using CRISPR-based systems. *Acta Hortic.* **2019**, 1264, 53–66
28. Li, L.; Yuan, H.; Zeng, Y.; Xu, Q. **2016**. Plastids and carotenoid accumulation. In: *Carotenoids in nature*. Subcellular Biochemistry, vol 79. Stange C. Eds.; Springer
29. Moreno, J.C.; Pizarro, L.; Fuentes, P.; Handford, M.; Cifuentes, V.; Stange, C. Levels of lycopene beta-cyclase 1 modulate carotenoid gene expression and accumulation in *Daucus carota*, *PLoS One* **2013**, 8, e58144
30. Maass, D.; Arango, J.; Wust, F.; Beyer, P.; Welsch, R. Carotenoid crystal formation in Arabidopsis and carrot roots caused by increased phytoene synthase protein levels. *PLoS ONE* **2009**, 4, e6373
31. Murashige, T.; Skoog, F. A revised medium for rapid growth and bio assays with tobacco tissue cultures. *Phys. Plant.* **1962**, 15, 474–497
32. Nishi, A.; Kurosaki, F. **1993**. *Daucus carota* L. (Carrot): In vitro production of carotenoids and phytoalexins. In *Medicinal and Aromatic Plants V. Biotechnology in Agriculture and Forestry*; Bajaj, Y.P.S., Ed.; Springer: Berlin/Heidelberg, Germany,; pp. 178–191
33. Perrin, F.; Hartmann, L.; Dubois-Laurent, C.; Welsch, R.; Huet, S.; Hamama, L.; Briard, M.; Peltier, D.; Gagné, S.; Geoffriau, E. Carotenoid gene expression explains the difference of carotenoid accumulation in carrot root tissues. *Planta* **2017**, 245, 737–747
34. Qin, Y.; Woo, H.-J.; Shin, K.-S.; Lim, M.-H.; Lee, S.-K. Comparative transcriptome profiling of different tissues from betacarotene-enhanced transgenic soybean and its non-transgenic counterpart. *Plant Cell Tiss. Organ. Cult.* **2020**, 140, 341–356
35. Ramirez, V.; Xiong, G.; Mashiguchi, K.; Yamaguchi, S.; Pauly, M. Growth-and stress-related defects associated with wall hypoacetylation are strigolactone-dependent. *Plant Direct* **2018**, 2, 1–11
36. Rodriguez-Amaya, D.B. **2016**. Structures and analysis of carotenoid molecules. In *Carotenoids in Nature: Biosynthesis, Regulation and Function*; Stange, C., Ed.; Springer International Publishing: Cham, Switzerland; pp. 71–108

37. Rodriguez-Concepcion, M.; Stange, C. Biosynthesis of carotenoids in carrot: An underground story comes to light. *Arch. Biochem. Biophys.* **2013**, 539, 110–116
38. Rosas-Saavedra, C.; Stange, C. **2016**. Biosynthesis of carotenoids in plants: Enzymes and color. In *Carotenoids in Nature: Biosynthesis, Regulation and Function*; Stange, C., Ed.; Springer International Publishing: Cham, Switzerland; pp. 35–69
39. Rygula, A.; Oleszkiewicz, T.; Grzebelus, E.; Baranska, M.; Baranski, R. Raman, AFM and SNOM high resolution imaging of carotene crystals in a model carrot cell system. *Spectrochim. Acta A* **2018**, 197, 47–55
40. Schaub, P.; Rodriguez-Franco, M.; Cazzonelli, C.I.; Alvarez, D.; Wust, F.; Welsch, R. Establishment of an Arabidopsis callus system to study the interrelations of biosynthesis, degradation and accumulation of carotenoids. *PLoS One* **2018**, 13, e0192158
41. Schweiggert, R.; Mezger, D.; Schimpf, F.; Steingass, C.; Carle, R. Influence of chromoplast morphology on carotenoid bioaccessibility of carrot, mango, papaya, and tomato. *Food Chem.* **2012**, 135, 2736–2742
42. Shimizu, K.; Kikuchi, T.; Sugano, N.; Nishi, A. Carotenoid and steroid syntheses by carrot cells in suspension culture. *Physiol. Plant.* **1979**, 46, 127–132
43. Simon, P.W. Carrots and other horticultural crops as a source of provitamin A carotenes. *HortScience* **1990**, 25, 1495–1499
44. Simpson K.; Cerda A.; Stange C. **2016**. Carotenoid biosynthesis in *Daucus carota*. In: *Carotenoids in nature. Subcellular Biochemistry*, vol 79. Stange C. Eds.; Springer
45. Simpson, K.; Fuentes, P.; Quiroz-Iturra, L.F.; Flores-Ortiz, C.; Contreras, R.; Handford, M.; Stange, C. Unraveling the induction of phytoene synthase 2 expression by salt stress and abscisic acid in *Daucus carota*. *J. Exp. Bot.* **2018**, 69, 4113–4126
46. Sugano, N.; Miya, S.; Nishi, A. Carotenoid synthesis in a suspension culture of carrot cells. *Plant Cell Physiol.* **1971**, 12, 525–531
47. Smoleń, S.; Sady, W. The effect of various nitrogen fertilization and foliar nutrition regimes on the concentrations of sugars, carotenoids and phenolic compounds in carrot (*Daucus carota* L.). *Sci. Hortic.* **2009**, 120, 315–324
48. Songstad, D.D.; Petolino, J.F.; Voytas, D.G.; Reichert, N.A. Genome editing of plants. *Crit. Rev. Plant Sci.* **2017**, 36, 1–23
49. Su, Y.H.; Tang, L.P.; Zhao, X.Y.; Zhang, X.S. Plant cell totipotency: Insights into cellular reprogramming. *J. Integr. Plant Biol.* **2021**, 63: 228–240
50. Sun, T.; Yuan, H.; Cao, H.; Yazdani, M.; Tadmor, Y.; Li, L. Carotenoid metabolism in plants: The role of plastids. *Molecular Plant* **2018**, 11, 58–74
51. Wang, H.; Ou, C.-G.; Zhuang, F.-Y.; Ma, Z.-G. The dual role of phytoene synthase genes in carotenogenesis in carrot roots and leaves. *Mol. Breed.* **2014**, 34, 2065–2079
52. Wang, Z.; Zhang, L.; Dong, C.; Guo, J.; Jin, L.; Wei, P.; Li, F.; Zhang, X.; Wang, R. Characterization and functional analysis of phytoene synthase gene family in tobacco. *BMC Plant Biol.* **2021**, 21, 32
53. Xu, Z.-S.; Feng, K.; Xiong, A.-S. CRISPR/Cas9-Mediated Multiply Targeted Mutagenesis in Orange and Purple Carrot Plants. *Mol. Biotechnol.* **2019**, 61, 191–199
54. Zhang, Y.; Pribil, M.; Palmgren, M.; Gao, C. A CRISRP way for accelerating improvement of food crops. *Nat. Food* **2020**, 1, 200–205

11. Publikacje stanowiące rozprawę doktorską

Publikacja 1: Unique chromoplast organization and carotenoid gene expression in carotenoid-rich carrot callus

Oleszkiewicz T., Klimek-Chodacka M., Milewska-Hendel A., Zubko M., Stróż D., Kurczyńska E., Boba A., Szopa J., Baranski R. Unique chromoplast organization and carotenoid gene expression in carotenoid-rich carrot callus.

Planta **2018**, 248, 1455–1471

https://doi.org/10.1007/s00425-018-2988-5

IF_{2018}: 3,060

Materiały uzupełniające dostępne online

Supplementary material 1: Carrot genes with references to NCBI, and primers used for quantitative expression analysis

https://static-content.springer.com/esm/art:10.1007/s00425-018-2988-5/MediaObjects/425_2018_2988_MOESM1_ESM.xlsx

Supplementary material 2: Gene expression levels in dark orange (d-o) callus and roots calculated as fold difference relative to pale yellow (p-y) callus

https://static-content.springer.com/esm/art:10.1007/s00425-018-2988-5/MediaObjects/425_2018_2988_MOESM2_ESM.xlsx

Planta (2018) 248:1455–1471
https://doi.org/10.1007/s00425-018-2988-5

ORIGINAL ARTICLE

Unique chromoplast organisation and carotenoid gene expression in carotenoid-rich carrot callus

Tomasz Oleszkiewicz[1] · Magdalena Klimek-Chodacka[1] · Anna Milewska-Hendel[2] · Maciej Zubko[3] · Danuta Stróż[3] · Ewa Kurczyńska[2] · Aleksandra Boba[4] · Jan Szopa[4,5] · Rafal Baranski[1]

Received: 5 June 2018 / Accepted: 15 August 2018 / Published online: 21 August 2018

Abstract

Main conclusion **The new model orange callus line, similar to carrot root, was rich in carotenoids due to altered expression of some carotenogenesis-associated genes and possessed unique diversity of chromoplast ultrastructure.**

Callus induced from carrot root segments cultured in vitro is usually pale yellow (p-y) and poor in carotenoids. A unique, non-engineered callus line of dark orange (d-o) colour was developed in this work. The content of carotenoid pigments in d-o callus was at the same level as in an orange carrot storage root and nine-fold higher than in p-y callus. Carotenoids accumulated mainly in abundant crystalline chromoplasts that are also common in carrot root but not in p-y callus. Using transmission electron microscopy, other types of chromoplasts were also found in d-o callus, including membranous chromoplasts rarely identified in plants and not observed in carrot root until now. At the transcriptional level, most carotenogenesis-associated genes were upregulated in d-o callus in comparison to p-y callus, but their expression was downregulated or unchanged when compared to root tissue. Two pathway steps were critical and could explain the massive carotenoid accumulation in this tissue. The geranylgeranyl diphosphate synthase gene involved in the biosynthesis of carotenoid precursors was highly expressed, while the β-carotene hydroxylase gene involved in β-carotene conversion to downstream xanthophylls was highly repressed. Additionally, paralogues of these genes and phytoene synthase were differentially expressed, indicating their tissue-specific roles in carotenoid biosynthesis and metabolism. The established system may serve as a novel model for elucidating plastid biogenesis that coincides with carotenogenesis.

Keywords Callus tissue in vitro · Carotenoid biosynthesis pathway · Chromoplast biogenesis · Chromoplast ultrastructure · Transcript level · Ultra performance liquid chromatography (UPLC)

Abbreviations

d-o	Dark orange
p-y	Pale yellow
PSY	Phytoene synthase

Introduction

Carotenoids are essential in plant development and growth as they are common components of cell photosystems, but in some species they are also sequestered in photosynthetically inactive tissues (Sun et al. 2018). Their presence in human and animal diet is critical as some of them are provitamin A precursors while others are important in age-related

Electronic supplementary material The online version of this article (https://doi.org/10.1007/s00425-018-2988-5) contains supplementary material, which is available to authorized users.

✉ Rafal Baranski
rafal.baranski@urk.edu.pl

[1] Institute of Plant Biology and Biotechnology, Faculty of Biotechnology and Horticulture, University of Agriculture in Krakow, AL. 29 Listopada 54, 31-425 Kraków, Poland

[2] Department of Cell Biology, Faculty of Biology and Environmental Protection, University of Silesia in Katowice, Jagiellońska 28, 40-032 Katowice, Poland

[3] Institute of Materials Science, University of Silesia in Katowice, 75 Pułku Piechoty 1a, 41-500 Chorzow, Poland

[4] Department of Genetic Biochemistry, Faculty of Biotechnology, University of Wroclaw, Przybyszewskiego 63/77, 51-148 Wrocław, Poland

[5] Department of Genetics, Plant Breeding and Seed Production, Wroclaw University of Environmental and Life Sciences, Pl. Grunwaldzki 24A, 50-363 Wrocław, Poland

dysfunctions such as macular degeneration, and have also antioxidant properties (Milani et al. 2017). The high significance of these compounds boosted research using model plants, and stimulated programmes aimed at the enhancement of crop plants by altering carotenoid content and composition (Giuliano 2017).

Accumulation of carotenoids in plants is determined by the rate of biosynthesis and subsequent degradation carried out in plastids (Cazzonelli 2011; Schaub et al. 2018), and the pathway of carotenoid metabolism in plants has been thoroughly described (Rodriguez-Concepcion 2010; Ruiz-Sola and Rodríguez-Concepción 2012). Regulation of carotenoid biosynthesis and accumulation is complex and has not been fully elucidated. It involves a cross-talk between the 2-C-methyl-D-erythritol 4-phosphate (MEP) pathway delivering substrates for carotenogenesis and the carotenoid pathway delivering signal molecules for the feedback response. Environmental factors regulate carotenoid biosynthesis that is then manifested in qualitative and quantitative changes of these metabolites (Nisar et al. 2015). Sunlight is the primary modulator affecting the transcription level of key genes such as phytoene synthase (*PSY*) through phytochrome and cytochrome receptors transducing the light signal to induce or repress gene expression (Llorente et al. 2017). Developmental regulation is common and clearly observed in ripening fruits while changing their colour due to altered pigment accumulation accompanying chloroplast degradation and chromoplast development (Cazzonelli and Pogson 2010; Sun et al. 2018). Direct evidence that carotenoid accumulation is regulated by genetic determinants related to plastid biogenesis was found in cauliflower (Lu et al. 2006), but plastid differentiation is additionally affected by environmental stimuli (Li and Yuan 2013). Plastids may undergo transition from initial proplastids to non-green leucoplasts and amyloplasts, and green chloroplasts. In non-green tissues, chromoplasts originating from chloroplasts or non-green plastids have the capacity to sequester carotenoids and store them safely for a long period (Egea et al. 2010). Chromoplasts are the primary location of carotenogenesis, with most enzymes associated with membranes, although some of them remain active in stroma or are associated with plastid sub-structures (Shumskaya and Wurtzel 2013; van Wijk and Kessler 2017).

Carrot (*Daucus carota* L.) is a vegetable accumulating high amounts of carotenoids in its storage root; thus it is one of a few plant species synthesizing these pigments in an underground organ. The ability of carrots to accumulate large quantities of predominantly provitamin A carotenoids has been intriguing for decades, but its mechanism still remains not fully elucidated although structural genes and quantitative trait loci (QTL) were identified and mapped (Just et al. 2007; Cavagnaro et al. 2011). The activity of carotenoid genes changes during carrot root development, but increased transcript levels only partially explain massive carotenoid sequestration (Clotault et al. 2008). Recently, a mutant gene outside the carotenoid biosynthesis pathway and related to photomorphogenesis has been proposed as a putative regulator essential for carotenoid accumulation in the orange storage root (Iorizzo et al. 2016). The lack of a direct correlation between transcript and carotenoid levels indicates the essential role of plastid biogenesis in carotenoid biosynthesis, accumulation and storage. This was also shown in dark-grown and de-etiolated carrot roots where carotenoid level was coordinated with light control and chromoplast development (Fuentes et al. 2012; Rodriguez-Concepcion and Stange 2013). Typical chromoplasts in an intact carrot root contain mainly crystalline sub-structures resulting from overproduction of carotenes which are then stored in lipoprotein sheets, and their unidirectional growth causes the formation of needle-like, broad ribbon-like, and tube-like structures that expand along the plastid envelope (Frey-Wyssling and Schwegler 1965). Recent studies confirmed that carrot chromoplasts contain carotenoids in a solid-crystalline physical state (Schweiggert et al. 2012). The crystals are composed predominantly of β-carotene and may also contain α-carotene as identified using spectroscopy (Roman et al. 2015; Rygula et al. 2018). Globular chromoplasts containing lipid-dissolved carotenoids in plastoglobuli were also found in carrot root cells, but they were small in size and number (Kim et al. 2010). A direct relationship between chromoplast type and carotenoid content and composition has also been observed in other species, confirming that carotenogenesis is a species-specific process (Kilcrease et al. 2013; Schweiggert and Carle 2017).

Carrot callus cultures have been widely used in research for almost 80 years, which began when carrot became one of the first species reported to develop a callus in vitro and was used for the establishment of a cell suspension culture to prove the concept of plant cell totipotency (Ikeuchi et al. 2013). Callus cells' ability to differentiate into different types of cells makes this tissue a feasible model for basic research at a cellular level. Carrot callus can be easily propagated and exposed to different stress factors. It can also serve as a source of released cells and protoplasts, and is amenable to genetic transformation (Baranski 2008). These features make carrot callus a convenient laboratory-based model system that has been recently demonstrated for precise gene editing purposes (Klimek-Chodacka et al. 2018). Genetically modified callus was also valuable for studying physiological processes and their molecular control in other species, including carotenoid biosynthesis, regulation and accumulation (Kim et al. 2013; Schaub et al. 2018).

Carrot callus developing from cambium of root explants is poor in carotenoids and has a pale yellow colour, even when discs of orange root are cultured in vitro (Baranska et al. 2006; Baranski et al. 2006). Recently, we have established a pair of stable callus lines derived from the same orange

carrot root that accumulate either low or high amounts of carotenoids, the latter being essentially similar to that in the carrot root. These lines can serve as a unique model for plant carotenoid research, and both chemical and structural differences of carotenoid crystals have already been demonstrated in this orange callus by applying simultaneously three non-destructive and complementary techniques: Raman imaging, atomic force microscopy (AFM) and scanning near-field optical microscopy (SNOM). Moreover, SNOM observations of intact cells in carotenoid-rich callus have indicated the presence of carotenoid-containing subcellular structures that resembled not only crystalline but also membranous and tubular chromoplasts (Rygula et al. 2018).

The results presented in this work demonstrate unique histology, ultrastructure and chromoplast diversity accompanying high carotenoid contents of the established carotenoid-rich carrot callus. A distinct expression pattern of carotenoid-associated genes is shown, including variant roles of some paralogues. The results provide evidence that this cell system may constitute a novel model for basic research on carotenogenesis and chromoplast biogenesis.

Materials and methods

Plant materials

Orange roots of the DH1 doubled haploid carrot (*Daucus carota* L. subsp. *sativus* Hoffm.) line (Fig. 1a) were surface sterilized and cut transversally into 5 mm thick discs, which were then cultured on BI medium (Gamborg B5 mineral medium with vitamins; Duchefa, Haarlem, The Netherlands) supplemented with 1 mg/L 2,4-dichlorophenoxyacetic acid, 0.0215 mg/L kinetin and 30 g/L sucrose, pH 5.8, solidified with 2.7% Phytagel, at 26 °C in the dark. After 2 months, pale yellow (p-y) callus developing along the cambium was transferred to BI medium and cultured in the same conditions, producing stable lines (Fig. 1b, c). Within consecutive subculture periods, small orange-coloured cell foci appeared in the p-y callus line. Orange cell clumps were subsequently transferred to BI medium until a dark orange (d-o) callus line was established (Fig. 1d, e). Visual selection of orange cells was necessary to eliminate non-pigmented cells, which otherwise overgrew the tissue, and to obtain a stable orange callus line. Callus transfer to fresh medium was done every 4 weeks.

Isolation of terpenoids and UPLC analysis

Tissue was ground in liquid nitrogen and lyophilized in the dark. Aliquots of 50 mg were extracted using successively methanol, acetone and petroleum, and ultra performance liquid chromatography (UPLC) was then used to detect terpenoids as described in detail by Boba et al. (2018).

Abscisic acid isolation and quantification

Abscisic acid (ABA) was extracted from 200 mg of fresh tissue ground in liquid nitrogen according to Boba et al. (2018). ABA content was determined spectrophotometrically at

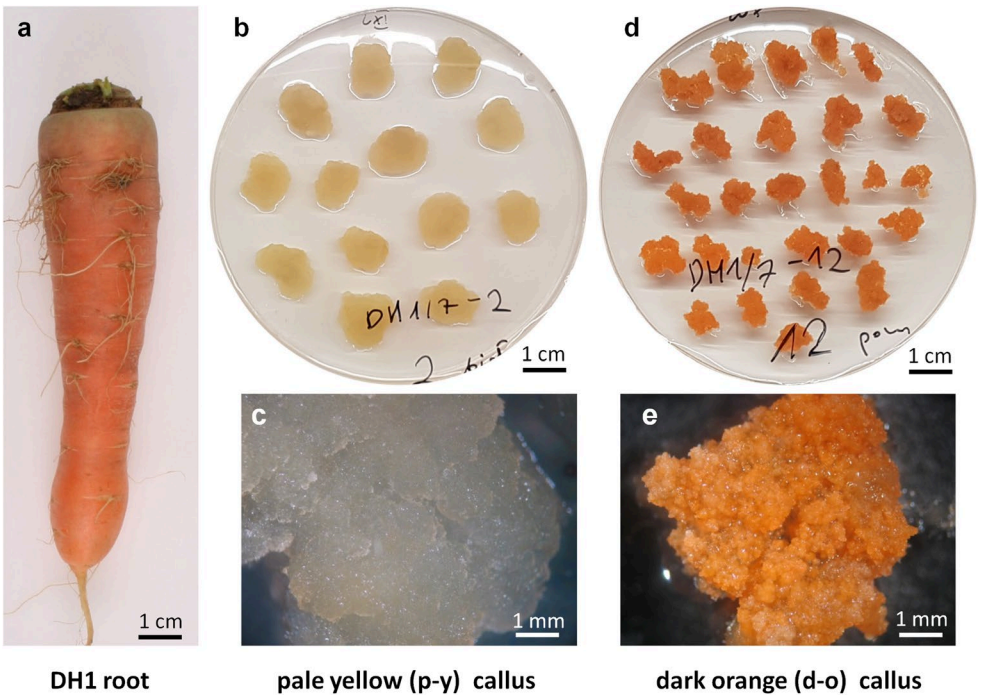

Fig. 1 Root of DH1 carrot line used for callus induction (**a**). Pale yellow (p-y) callus developed from cambium of root discs and cultured on BI mineral medium in vitro (**b**), and observed under higher magnification (**c**). Dark orange (d-o) callus line established from p-y callus by visual selection and subsequent subculture (**d**), and observed under higher magnification (**e**)

37:8117938288

$\lambda = 450$ nm in a Varioscan Microplate Reader (Thermo Fisher Scientific) using the Abscisic Acid Immunoassay Detection Kit (Sigma-Aldrich) according to the producer's protocol.

Microscopic identification of carotenoid crystals

A fresh callus sample was placed on a microscopic slide in a drop of demineralised water, covered with a cover glass and observed without any processing using the Axiovert S100 (Carl Zeiss) bright-field microscope and the Axioskop 40 (Carl Zeiss) polarizing microscope equipped with the MOTICAM580 5.0 MP digital camera with the corresponding software (Nikon).

Histological observation of cells

Samples for histological analyses were collected at various callus areas and fixed in a mixture of 4% (w/v) paraformaldehyde (PFA; Polysciences) and 1% (v/v) glutaraldehyde (GA; Sigma-Aldrich) in phosphate buffered saline (PBS, pH 7.0) at 4 °C for 24 h. Then samples were washed in PBS, dehydrated in a graded ethanol series and infiltrated in LR White resin (Polysciences). Later, polymerization samples were cut into 1.5 µm thick sections using the Leica EM UC6 ultramicrotome, mounted on microscope slides, stained with aqueous solutions of 0.05% Toluidine Blue O (TBO; Sigma-Aldrich) for 10 min, rinsed with distilled water, covered with a cover glass and analyzed with the Nikon Eclipse Ni-U bright-field microscope equipped with the Nikon Digital DS-Fi1-U3 camera with corresponding software. At least three samples were collected and analyzed from each callus line.

Transmission electron microscopy (TEM)

Samples for TEM were fixed in 2.5% glutaraldehyde and 2.5% paraformaldehyde in 0.05 M cacodylate buffer (Sigma-Aldrich) (pH 7.2), kept at 4 °C for 24 h, post-fixed in 1% osmium tetroxide (Sigma-Aldrich) in distilled water at 4 °C overnight, dehydrated in a graded series of ethanol and gradually embedded in Epon resin (Poly/Bed 812; Polysciences) according to a method described previously (Milewska-Hendel et al. 2017). Ultrathin 70-nm thick sections were obtained with the Leica EM UC6 ultramicrotome and collected onto carbon-coated copper grids (300 mesh, Electron Microscopy Science, Hatfield, PA, USA). Grids with sections were stained with a saturated solution of uranyl acetate (Polysciences) in 50% ethanol for 15 min and 0.04% lead citrate agents (Sigma-Aldrich) for 10 min and analyzed in a Jeol JEM-3010 high resolution electron microscope (HRTEM) (300 kV) equipped with an EDS spectrometer and a 2 k × 2 k Orius 833 SC200D CCD camera (Gatan, Pleasanton, CA, USA). TEM images were taken for at least three samples from each callus line.

Significant differences in the mean number of plastids or plastoglobuli between two callus tissues were determined using a *t* test. Frequencies of chromoplasts containing plastoglobuli were compared using a test for significant differences between two proportions.

Gene expression

Tissue samples were frozen in liquid nitrogen and ground in a mortar. Total RNA was isolated using the Direct-zol RNA MiniPrep Plus kit with TRI Reagent (Zymo Research, Irvine, CA, USA) and followed by DNase I treatment (Thermo Fisher Scientific). Lack of DNA contamination was verified by PCR and qPCR on the RT control. cDNA was synthesized from 1 µg of RNA using the iScript cDNA Synthesis Kit (Bio-Rad). Real-time quantitative PCR (qPCR) was conducted using the StepOnePlus (Applied Biosystems) thermocycler with the Maxima SYBR Green/ROX qPCR Master Mix (Thermo Fisher Scientific). Primers were validated for single product specificity and their effectiveness to range between 90 and 105% (Electronic Suppl. Table S1). qPCR thermal cycling conditions were: initial denaturation at 95 °C for 10 min, 40 cycles of 95 °C for 15 s and 55 °C for 60 s. Amplification was followed by melt curve analysis to verify single product amplification. Normalization was done to the expression of the actin gene. qPCR reactions were done in at least three biological replications. Relative gene expression was calculated using the REST 2009 (Qiagen) software.

Results

Carotenoid content in orange callus is similar as in carrot root

Root discs of orange carrot DH1 line (Fig. 1a) were exposed to a mineral medium in vitro, which resulted in the development of pale yellow (p-y) callus tissue along the cambium (Fig. 1b, c), as expected. However, during subsequent subcultures of this tissue, orange-coloured cell foci appeared and they were separated from the host tissue for further growth (Fig. 1c, d). In consequence, a pair of p-y callus and dark orange (d-o) callus lines was established. Carotenoid contents in both p-y and d-o callus lines were determined and compared to the amounts in DH1 roots. The total carotenoid content in the roots was high (1985 µg/g dry weight; DW) and resulted from the presence of three main compounds (Fig. 2). β-carotene predominated and constituted 90% of total carotenoids while α-carotene and lutein constituted only 8 and 2%,

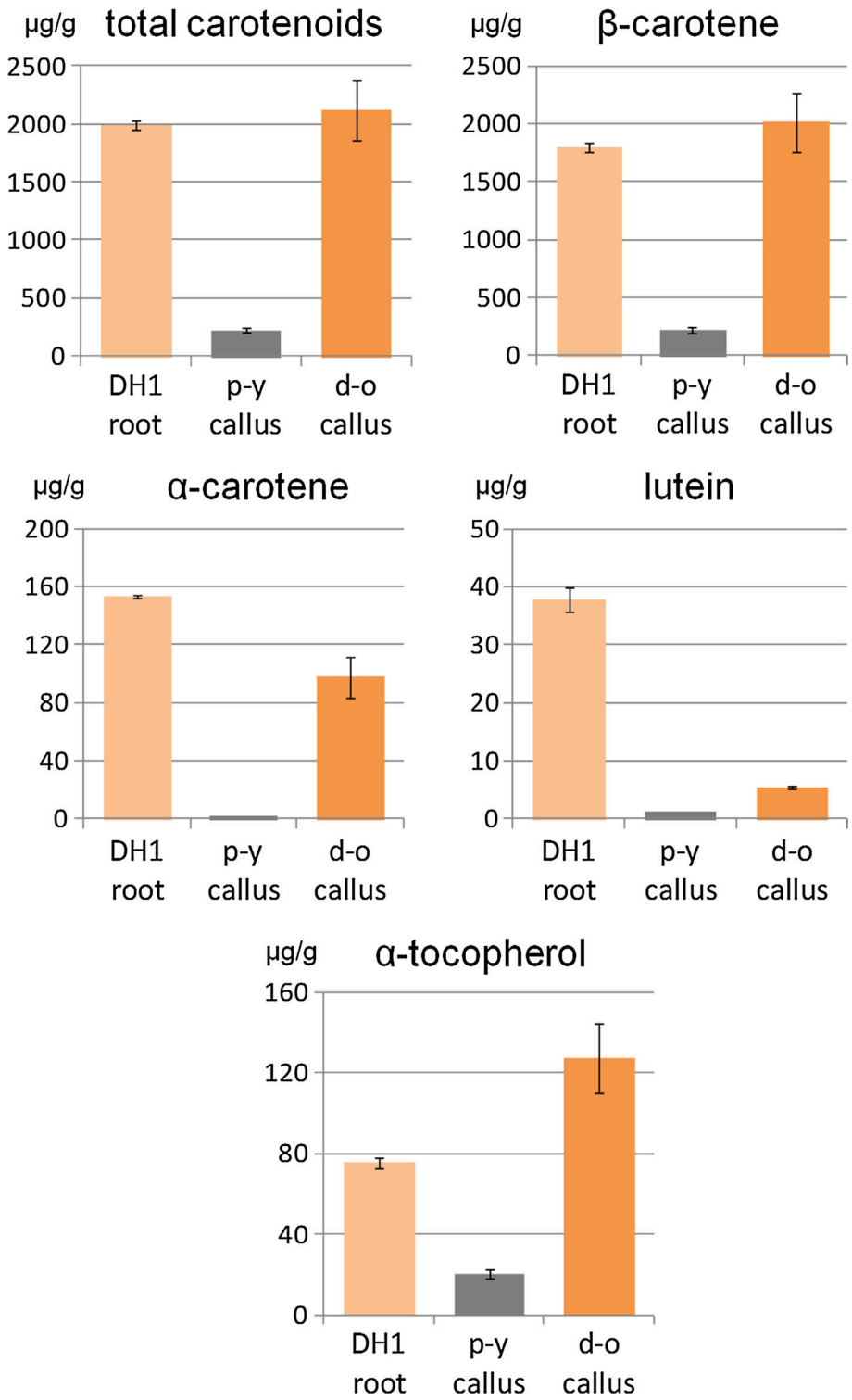

Fig. 2 Carotenoid and α-tocopherol contents in roots of the DH1 carrot line and in callus derived from them. p-y—pale yellow callus developed from cambium of DH1 root disc incubated on BI medium in vitro, d-o—dark orange callus selected from p-y callus. Means with standard errors per g tissue dry weight; $n = 8$ (roots), $n = 5$ (p-y callus), $n = 10$ (d-o callus)

respectively. In contrast, p-y callus was poor in carotenoids and contained 8.5-fold lower amounts of carotenoids (232 µg/g DW) than the roots. The contents of α-carotene, lutein, other xanthophylls and phytoene in p-y callus were very low, and thus β-carotene was mainly present (95% of total carotenoids). The selected d-o callus line contained similar amounts of β-carotene (2015 µg/g DW) and total carotenoids (2150 µg/g DW) as the roots ($P = 0.486$ and 0.668, respectively) with β-carotene being the main carotenoid (94%). α-Branch carotenoids accounted for 5% of total carotenoids, and their amounts were lower than in the root by 36 and 85% for α-carotene and lutein, respectively.

The comparison of both callus tissues showed that d-o callus contained more total carotenoids (9.3-fold), β-carotene (9.1-fold), α-carotene (48.8-fold), lutein (4.3-fold), other xanthophylls (1.6-fold) and phytoene (3.7-fold) than p-y callus. Additionally, the level of ABA was 3.4-fold higher ($P < 0.001$) in d-o callus (0.41 nmol/g FW) than in p-y callus (0.12 nmol/g FW). The content of α-tocopherol was 3.7-fold lower in p-y callus than in the roots and 6.4-fold lower than in the d-o callus while in d-o callus the content was 1.7-fold higher ($P = 0.017$) than in the roots (Fig. 2).

These results show that the observed orange colour in d-o callus was due to accumulation of carotenoid pigments that were present in similar amounts as in the roots. It was mainly attributed to the presence of β-carotene, slightly elevated amounts of which compensated for the lower α-branch carotenoid contents.

Differences in p-y callus and d-o callus are prominent at histological and ultrastructural levels

Microscopic observations revealed that cells of p-y callus were almost transparent when observed in a bright field, and that they did not show birefringent crystals when observed using a polarizing microscope (Fig. 3a, c). In some cells, orange, irregular, amorphous and rarely crystalline carotenoids were spotted. In contrast, cells of d-o callus were rich mainly in orange-coloured crystalloid structures of regular shapes (Fig. 3b), which were also clearly visible in polarizing light (Fig. 3d). They occurred in cells either individually or arranged in groups, often closely packed (Fig. 3d).

Both callus tissues differed in their histological and cellular structures. The p-y callus was composed of loosely connected cells, which were large and rounded, with a prominent central vacuole (Fig. 3e). Some cells located deeper

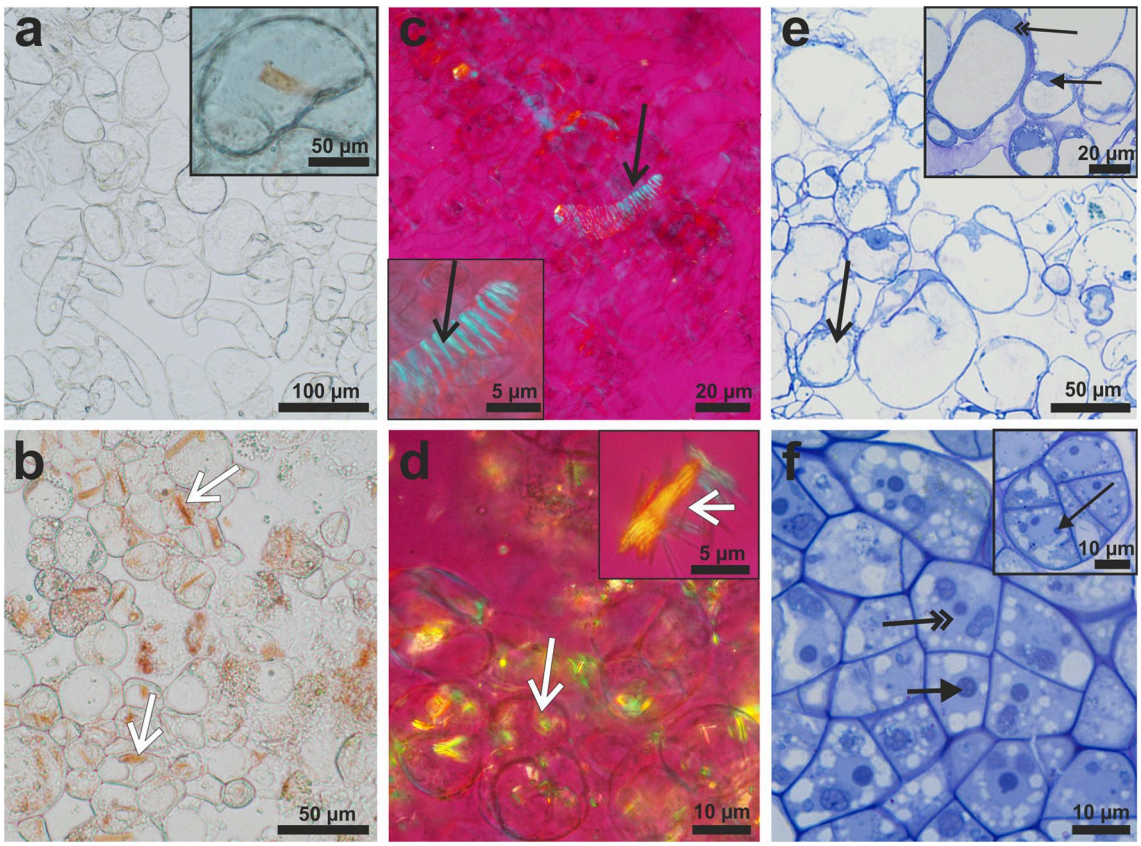

Fig. 3 Callus cells in bright-field (**a**, **b**, **e**, **f**) and polarizing microscopy (**c**, **d**). Cells from p-y callus (upper row) almost devoid of carotenoid crystals (**a**, **c**) with rarely observed crystals in single cells (**a** inset). Some callus cells differentiated into tracheary elements (**c** inset: open arrow). In contrast, d-o callus cells (bottom row) were filled with crystals (**b**, **d**, white, open arrows; inset: magnification of crystals released from the cell). Histology of callus tissue stained with toluidine blue O (**e**, **f**). Highly vacuolated and loosely attached cells in p-y callus (**e**). Many cells located at the callus surface presented features resembling those of cell decay (**e**, black, open arrow). Inside p-y callus alive cells with large vacuole, narrow layer of cytoplasm (**e** inset: double arrow) and nucleus (**e** inset: black arrow) were present. Dark orange callus composed of compact arrangement of cells (**f**) having dense cytoplasm, large nucleus (double arrow) with prominent nucleolus (arrow) that indicates their embryogenic character. Some cells from d-o callus were characterized by a dense cytoplasm and a large nucleus with nucleoli (**f** inset: arrow) that indicate their meristematic character

in the callus mass also possessed cytoplasm heavily stained with Toluidine Blue O (TBO), and with a clearly visible nucleus (Fig. 3e inset). Many cells were characterized by a large size, prominent vacuole and a narrow strand of cytoplasm in the vicinity of the walls (Fig. 3e), also visible in greater detail at an ultrastructural level, described below. In contrast, d-o callus was composed mainly of embryogenic-like cells characterized by a dense cytoplasm, large nucleus with a prominent nucleolus, small starch grains and a fragmented vacuome (Fig. 3f). Meristematic cells were also present and they were characterized by a dense cytoplasm, large nucleus with at least two nucleoli and small vacuoles. Meristematic and embryogenic cells formed cell aggregates within callus tissue (Fig. 3f).

Both types of calli also differed at the ultrastructural level. In p-y callus most cells were highly vacuolated, with one prominent vacuole (Fig. 4a). Cytoplasm was electron-lucent, with only some mitochondria and plastids. The plastid ultrastructure was very simple, with a limited internal membrane system and a few plastoglobuli (Fig. 4a, inset). These plastids were classified as proplastids and were most abundant in p-y callus cells (Fig. 4a; Table 1). Amyloplasts containing large starch grains were less frequent, and plastids with crystal remnants were found occasionally. In some callus regions, cells with dense cytoplasm with a very well-preserved tonoplast, endoplasmic reticulum (ER) profiles and mitochondria were also present (Fig. 4b). Cells showing disruption of the tonoplast membrane continuity (Fig. 4c; open arrow) but with still preserved plasma membrane continuity (Fig. 4c; arrow) were detected. The ultrastructure of d-o callus cells varied. Cells had a dense cytoplasm, numerous mitochondria and high number of Golgi apparatus dictyosomes, indicating intensive exocytosis (Fig. 4d–f). They comprised numerous rough ER (rER) profiles, ribosomes and small vacuoles. Microtubules occurred in the vicinity of the plasma membrane, and plasmodesmata traversing the neighbouring cell walls were also abundant (Fig. 4d). The number of plastids per cell was two-fold higher than in p-y callus and chromoplasts dominated (Table 1). Their number was 2.7-fold higher than the number of amyloplasts and proplastids, while the later were almost three-fold less frequent in d-o callus than in p-y callus. Also the proportion of plastids with plastoglobuli was higher ($P = 0.032$) in d-o callus (0.55) than in p-y callus (0.38), and these plastids contained different average numbers ($P = 0.026$) of plastoglobuli, 3.9 and 2.5, respectively.

Orange callus cells contain various chromoplast types

Plastids in d-o callus cells differed in their ultrastructure, and chromoplasts of various types occurred often in the same cell. Crystalline chromoplasts were the most abundant (Table 1) and they were clearly distinguished by the presence of membranes resembling ribbon-like (Fig. 5a) or needle-like shapes (Fig. 5b). These preserved structures were the remnants of dissolved carotene crystals resulting from the use of a destructive preparation procedure for TEM; however, in some chromoplasts, unaffected crystals or their parts were still present (Fig. 5b). Globular chromoplasts had an ellipsoid shape and a few plastoglobuli enclosed inside the stroma. They were three times less frequently observed than crystalline chromoplasts (Table 1; Fig. 5c). Two other chromoplast types, membranous (Fig. 5d) and tubular (Fig. 5e) were infrequent. Membranous chromoplasts were characterized by several to over a dozen concentric internal double membranes (Fig. 5c and inset). Tubular chromoplasts were characterized by internal elements of an elongated tube-shaped appearance and aligned to bundles (Fig. 5e, inset 1). Transverse sections revealed that the outer tubule layer was electron dense and the inner part was electron translucent (Fig. 5e, inset 2). Very often undulated membranes located distant from the chromoplasts were detected in the cytoplasm (Fig. 5f). Such membrane shape indicates that carotene crystals could be very long, which was congruent with observations done using bright-field and polarized light microscopes. Phytoferritin crystals were occasionally detected in some chromoplasts (Fig. 5g). Moreover, large plastoglobuli were detected, and in some of them crystal remnants were present (Fig. 5g, inset).

Unique pattern of carotenoid gene expression exists in orange callus cells

Transcript levels of 33 genes associated with carotenoid biosynthesis (Electronic Suppl. Table S1) were measured using a quantitative RT-PCR approach in carotenoid-poor and carotenoid-rich callus and in the orange root which p-y callus was derived from, and differential expression was found among these materials. Genes involved in the biosynthesis of carotenoid precursors were expressed at similar levels in d-o callus and the roots, and *IPI* expression was similar in all three tissues, including p-y callus (Fig. 6; Electronic Suppl. Table S2). Three out five geranylgeranyl diphosphate (*GGPS*) paralogues were highly upregulated in carotenoid-rich tissues, i.e. *GGPS1.5* and particularly two genes located on chromosomes Ch1 (*GGPS1.1*) and Ch8 (*GGPS1.8*). The full nucleotide homology between *GGPS1.1* and *GGPS1.8* in the carrot genome did not allow separate quantification of their transcripts, whose levels were 14–16-fold higher in both tissues in comparison to the carotenoid-poor p-y callus.

The expression of most of 24 genes, including paralogues, of the main pathway for carotenoid biosynthesis and metabolism was much higher (2–72-fold) in the roots than in p-y callus (Fig. 6; Electronic Suppl. Table S2). Only two genes, ζ-carotene desaturase (*ZDS2*) and

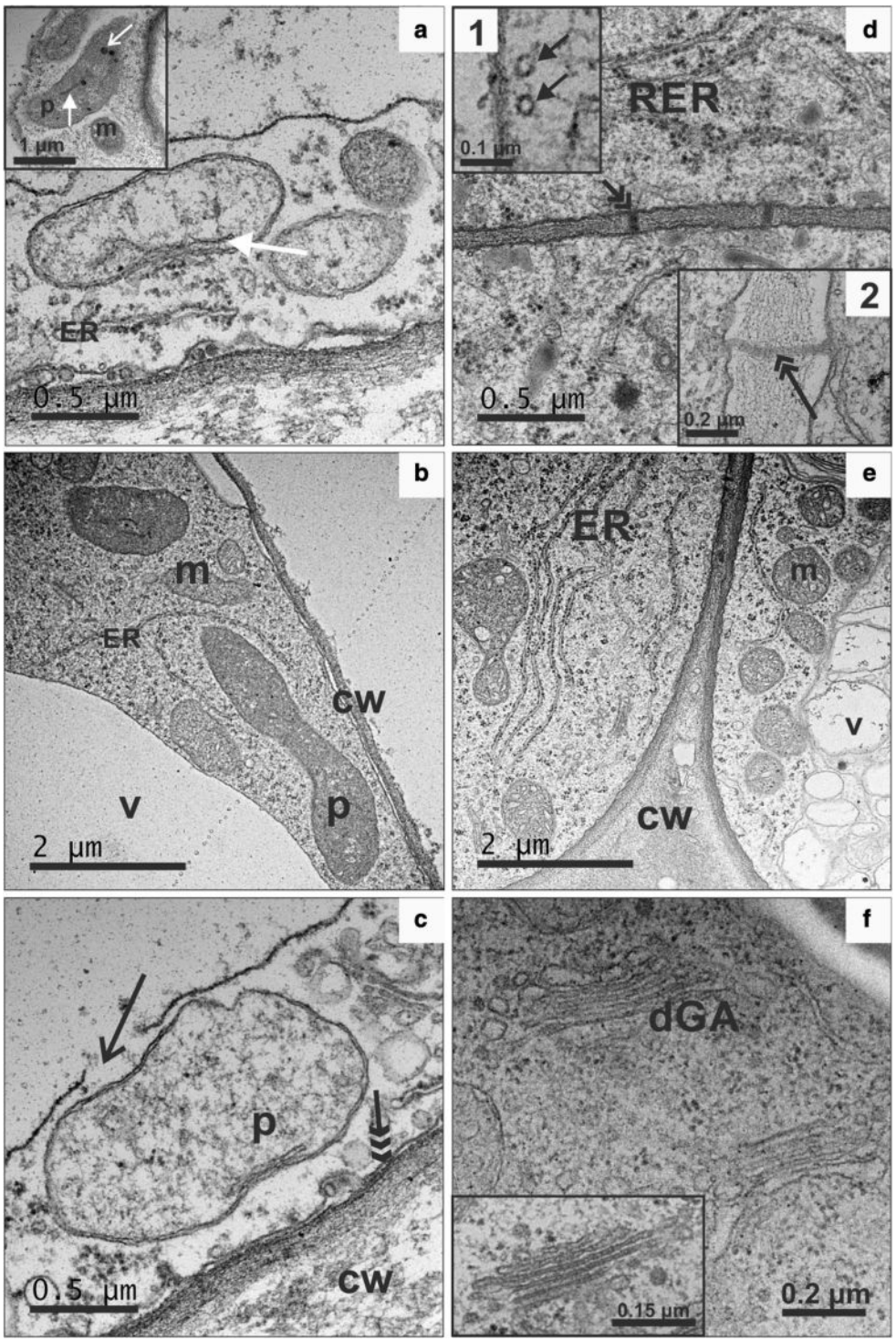

Fig. 4 Ultrastructure of cells from p-y (**a-c**) and d-o callus (**d-f**). Cells from p-y calli had electron-lucent cytoplasm with some ER membranes (**a**), mitochondria, a large vacuole, plastids with limited internal membranes and a few plastoglobuli (**a** inset). Cells with a narrow layer of electron-dense cytoplasm filled with numerous ribosomes, ER, plastids, mitochondria and a prominent vacuole were also detected (**b**). In some cells of p-y callus symptoms of cell decay were found (**c**). Cells from d-o callus were characterized by electron-dense cytoplasm (**d**–**f**) with numerous profiles of rough ER (**d**), microtubules, plasmodesmata (PD) [**d,** inset 1: black arrows, higher magnification of microtubules; inset 2: black, double arrow, higher magnification of PD], numerous mitochondria, vacuoles (**e**) and dictyosomes of the Golgi apparatus (**f**, **f** inset). *cw* cell wall, *dGA* dictyosomes of Golgi apparatus, *ER* endoplasmic reticulum, *m* mitochondria, *p* plastids, *RER* rough endoplasmic reticulum, *v* vacuole. Black open arrow, discontinuity of tonoplast; black double arrow, plasmodesmata; black triple arrow, plasma membrane; white arrow, plastid membranes; white open arrow, plastoglobuli

42:1150800241

Table 1 Number of plastids in p-y and d-o callus

Plastid type	p-y callus	d-o callus	P^a
Proplastids	38.0[b]	13.3	0.002
Amyloplasts	9.7	16.3	0.022
Chromoplasts	3.0	78.7	< 0.001
Crystalline	3.0	43.3	< 0.001
Globular	0.0	16.3	–
Membranous	0.0	9.3	–
Tubular	0.0	9.7	–

[a] *t* test significance level for difference between means

[b] Mean values from three replications of 40 cells each

zeaxanthin epoxidase (*ZEP.4*) were downregulated in the roots, and transcript levels of five genes, phytoene synthase *PSY1*, phytoene desaturase (*PDS*), prolycopene isomerase (*CRTISO*), β-carotene hydroxylase *BCH1.3*, and carotene ε-monooxygenase (*CHXE*), were similar in both materials. The most downregulated genes in p-y callus were epoxycarotenoid dioxygenases (*NCED*s), *BCH2* and *PSY2*.

Both carotenoid-poor and carotenoid-rich callus lines had similar expression levels of 12 genes but the next nine genes had higher expression in d-o callus. Only two of them, *PSY2* and *ZDS1*, are involved at early steps of carotene biosynthesis and had 4.0-fold and 2.0-fold higher expression, respectively. Lycopene ε-cyclase (*LCYE*) and some xanthophyll cycle and *NCED* genes were upregulated in d-o callus. Two genes had lower expression in d-o callus than in p-y callus, i.e. *PSY1* (4.6-fold lower expression) and *BCH2* (11.9-fold), involved in β-carotene conversion to xanthophylls.

Notable differences in expression levels were observed between d-o callus and the roots despite both materials accumulating similar amounts of carotenoids. Transcripts of most genes in d-o callus were at the same or lower levels than in the roots, and the most prominent differences were observed for genes involved in carotenoid catabolism (*NCED*s), including *BCH2* (155-fold lower expression in d-o callus). The expression level of another paralogue, *BCH1.6*, was only slightly higher (1.6-fold) in the roots while expression of the *BCH1.3* gene was at a similar level in both tissues, apparently not different from that observed in p-y callus. Both *PSY1* and *PSY2* were differentially expressed in carotenoid-accumulating tissues, and their expression was about three-fold higher in the roots. *PSY1* expression in d-o callus was also lower than in p-y callus. In the α-branch carotenoid pathway, a higher *LCYE* transcript level was found in d-o callus than in both p-y callus and the roots, while *CHXE* expression was stable among all tissues.

A candidate gene (*Y*, DCAR_032551) regulating carotenoid accumulation in orange storage carrot root (Iorizzo et al. 2016) was also highly expressed in the root used in our study. Its transcript level was 238-fold and 49-fold lower in p-y callus and d-o callus, respectively.

Transcript levels of geranylgeranyl diphosphate reductase (*GGred*) variants involved in metabolite flux to the biosynthesis of phytyl chain compounds were seven-to-ten-fold lower in p-y callus, and 5–12-fold lower in d-o callus in comparison to the levels determined for root tissue.

Discussion

Chromoplasts were rarely found in p-y callus cells, and thus only low amounts of carotenoids could be accumulated in this tissue. The small number of plastids and their simple organisation may explain the low carotenoid contents in carrot callus, also reported previously (Hanchinal et al. 2008). In contrast, cells of d-o callus contained high carotenoid amounts, notably being as high as in the carrot root. This carotenoid-rich d-o callus was distinguished from typical carrot callus at morphological, histological and ultrastructural levels, showing cell organisation common in embryogenic and meristematic tissues, and had a higher ABA content. Elevated ABA amounts were reported earlier in embryogenic calli derived from carrot hypocotyls, in contrast to non-embryogenic calli (Jimenez and Bangerth 2001). Thus, it was shown that cell organisation in the callus is related to the level of this plant hormone, which is a product of carotenoid catabolism. Due to its embryogenic character, d-o callus architecture was compact, so the increase of callus volume during the culture was slower than in the case of p-y callus, having larger cells and a loose structure. Higher ABA content could additionally explain slower d-o callus growth, as this hormone affects many physiological processes, including repressing the synthesis of cytokinin, whose limited availability in the tissue results in delayed cell division (Ha et al. 2012).

Chromoplasts are classified as four main types, i.e. crystalloid, globular, tubular and membranous, depending on their ultrastructure and chemical composition (Egea et al. 2010; Solymosi and Keresztes 2012; Schweiggert and Carle 2017). Usually one type of chromoplasts dominates in the tissue, but the coexistence of some other types, even in the same cell, is known. It is broadly accepted that the occurrence of different chromoplast types is a result of plastid differentiation and transition from one plastid type to another (Ljubesic et al. 1991; Pyke 2007). All four chromoplast types were observed in d-o callus, which is unusual and indicates highly complex plastid biogenesis occurring in this tissue, although crystalloid chromoplasts were the most abundant, unlike in p-y callus where they were hardly identified. It is well documented that in carrot root, crystalloid chromoplasts possess carotenoids in their crystalline form of different shapes (Frey-Wyssling and Schwegler

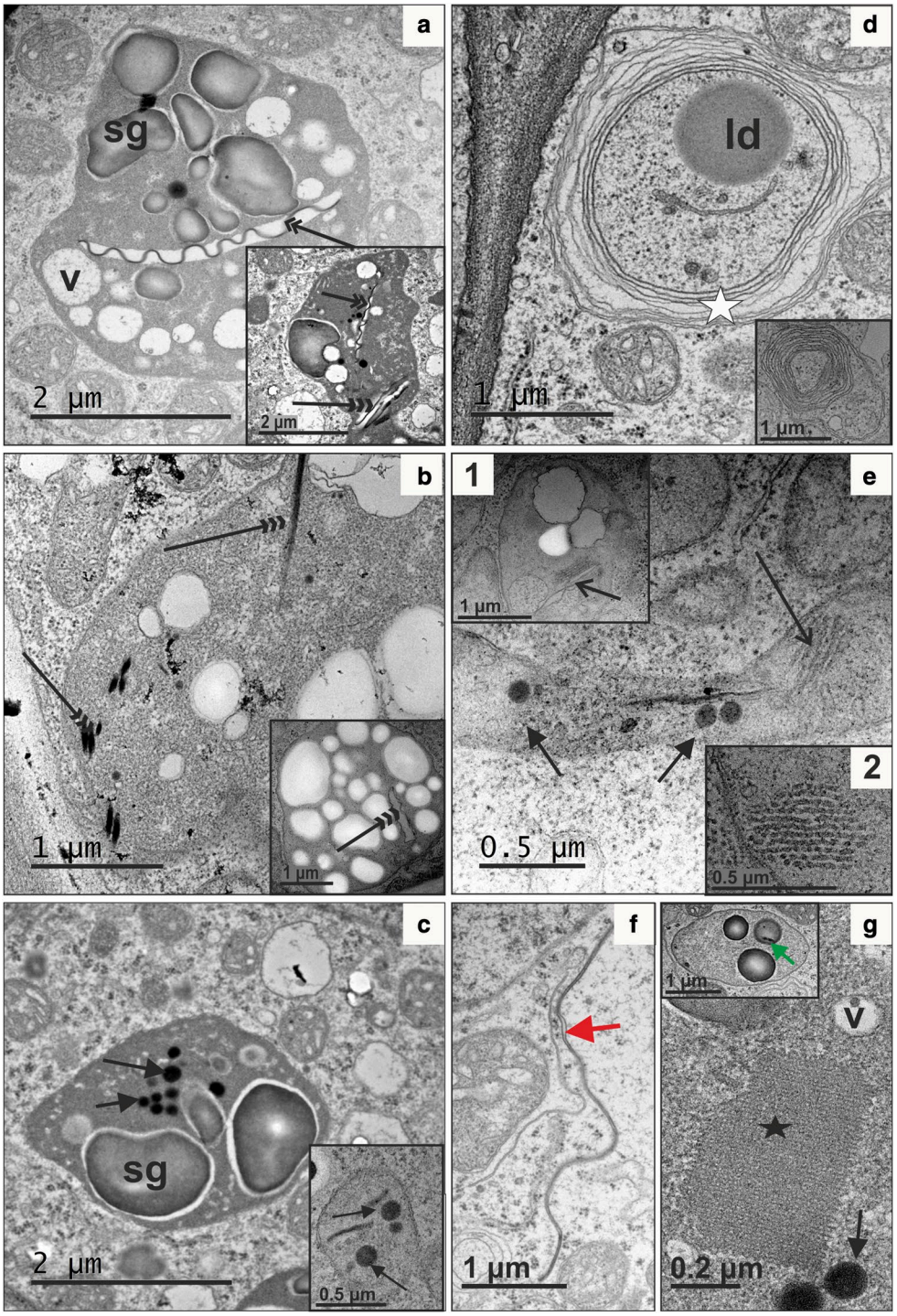

Fig. 5 Ultrastructural diversity of chromoplast types in d-o callus: crystalline (**a**, **b**), globular (**c**), membranous (**d**) and tubular (**e, e** inset 2: transverse section). Chromoplast membranes devoid of crystals were frequently quite long and extended outward from the chromoplast membrane (**f**, red arrow). Phytoferritin crystals were occasionally observed (**g**, black star); also large plastoglobuli were detected and in some of them crystal remnants were present (**g** inset: green arrow). Arrow, plastoglobuli; open arrow, tubules inside a chromoplast; double arrow, membrane remnants after removal of carotene crystals during microscopic preparation; triple arrow, preserved crystals; white star, membranes inside a membranous chromoplast. *ld* lipid droplet, *sg* starch grain, *v* vacuole

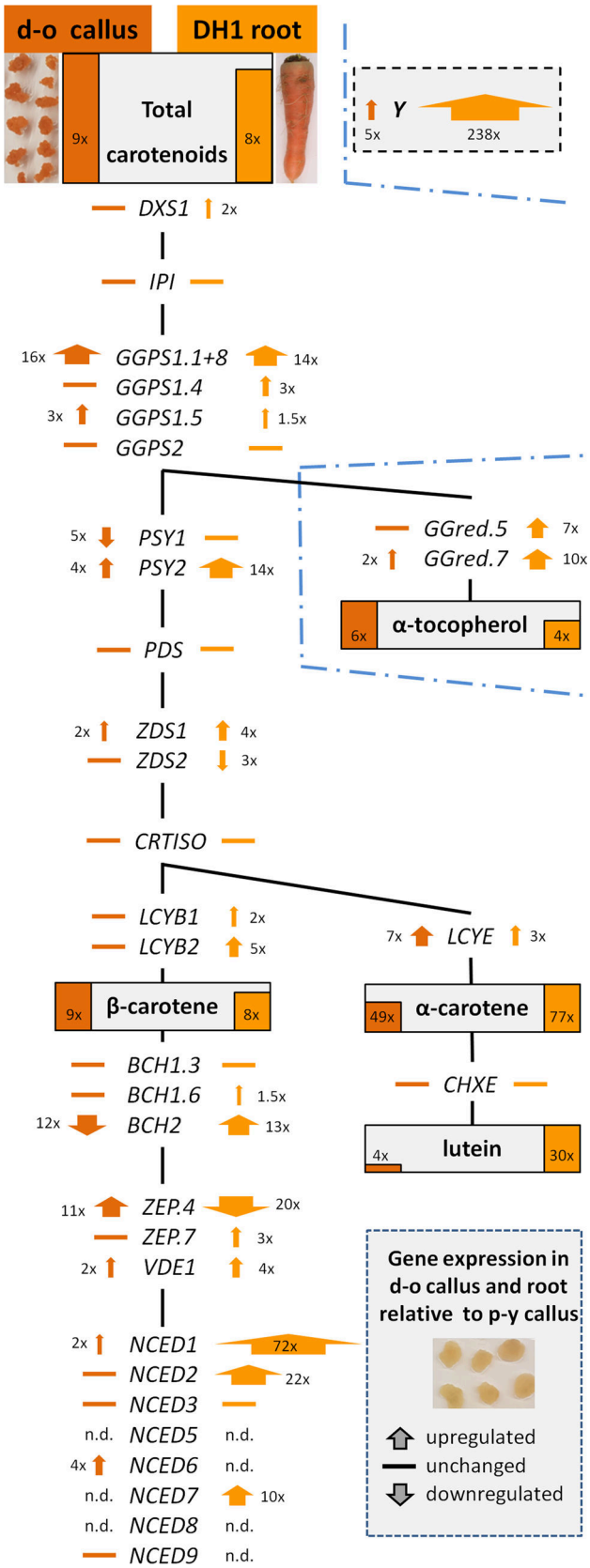

Fig. 6 Schematic comparison of relative gene expression (to that in pale yellow callus) and carotenoid contents in dark orange (d-o) callus and roots. A simplified biosynthesis pathway of carotenoids and their precursors are shown with genes analyzed in this paper and listed in Suppl. Table S1. Carotenoid and α-tocopherol contents in d-o callus and roots are represented by dark orange and orange bars, respectively. The bar height is proportional to the relative content of a given compound in both tissues. Numbers show the compound content ratios relative to the contents in p-y callus. Gene expression levels, relative to the expression in pale yellow (p-y) callus, are represented by arrows with numbers indicating fold difference and arrow widths proportional to expression levels, or by a horizontal line if there is no significant change in expression level in comparison to p-y callus. Relative expression of the candidate regulatory *Y* gene is shown in the box with a dashed border. *n.d.* transcripts not detected. Exact expression values are given in Suppl. Table S2

1965; Paolillo et al. 2004; Vasquez-Caicedo et al. 2006; Roman et al. 2015). When the concentration of carotenoids increases, they start to crystallize inside the chromoplast, and the growing crystals often heavily distort the shape of the chromoplast, which may extend to a large size (Li and Yuan 2013). Confirmation of crystalline carotenoid presence in TEM images is, however, indirect, as during sample fixation carotenoids dissolve and only some crystal remnants can be preserved and observed as electron-dense structures of regular shape. When carotenoids are completely washed out, chromoplast membranes surrounding the crystal collapse and are visible as characteristic undulating, electron-dense membrane spanning along the electron-lucent area void of the crystal (Kim et al. 2010). Crystalline structures have been frequently observed in d-o callus using light and polarizing microscopy, and partially using TEM. Both electron-dense and electron-lucent structures were clearly identified and often coexisted in one cell, indicating massive crystal accumulation. Recent spectroscopic measurements of crystals in d-o callus showed that they were composed predominantly of β-carotene accompanied by α-carotene, while co-occurrence of lutein was unlikely but their composition depended on the crystal structure (Rygula et al. 2018). Thus, measurements of carotenoid crystals in model d-o callus provided evidence supporting the previous hypothesis of heterogeneous composition of crystals accumulated in carrot root (Marx et al. 2003; Roman et al. 2015).

Other types of carotenoid-containing chromoplasts can be identified based on their ultrastructure visualized by TEM, and their classification is well presented (Schweiggert and Carle 2017). However, spectroscopic measurements using non-destructive approaches applied to intact cells provide additional support in carotenoid identification. It was revealed that carotenoid crystals and their lipoprotein complexes coexist in carrot root cells (Marx et al. 2003; Baranska et al. 2011; Roman et al. 2015). The presence of amorphous carotenoids, whose spectra indicate lipoprotein complexes, is congruent with observations of the

non-crystalline chromoplasts in TEM images of d-o callus. Moreover, scanning near-field optical microscopy (SNOM) coupled with Raman spectroscopy applied directly to d-o callus cells revealed numerous, small and carotenoid-rich, membranous and tubular-like structures, which thus most likely were chromoplasts (Rygula et al. 2018), which is also congruent with the TEM results presented here.

Kim et al. (2010) observed the presence of globular chromoplasts in carrot root tissue, although their number was small. Globular chromoplasts contain numerous plastoglobuli and only fragments of membranes (Camara et al. 1995). Lipid-rich plastoglobuli are a suitable environment for the biosynthesis and deposition of many lipophilic constituents, and they are believed to have little function beyond lipid storage, although they are also considered as the most common carotenoid-containing structures in the chromoplasts (Schweiggert and Carle 2017). Cells of carrot d-o callus described in this paper also contained globular chromoplasts with electron-dense plastoglobuli and embedded small crystals visible in TEM images. The formation of carotene crystals inside plastoglobuli was also reported for tulip tree (*Liriodendron tulipifera*) flowers and squash (*Cucurbita maxima*) fruit (Ljubesic et al. 1991). As crystals in plastoglobuli in d-o callus were small, these structures are most likely involved in accumulation of soluble carotenoids and other lipophilic compounds, including tocopherols. Carotenoids stored within plastoglobuli exhibit much higher light stability than those associated with membranes, so plastoglobuli play an important role mainly in light-exposed plant organs (Vasquez-Caicedo et al. 2006). Thus, the smaller number of plastoglobuli found in d-o callus chromoplasts might result from tissue culture in the dark. Unexpectedly, membranous chromoplasts were identified in d-o callus cells. These plastids have a distinguished structure of multiple, usually up to 20, internal double membranes arranged concentrically (Schweiggert and Carle 2017). They are rarely found in plants and have been uniquely reported in some flowers and selected pepper and tomato cultivars (Sitte et al. 1980). Chromoplasts of the *Or* cauliflower (*Brassica oleracea* L. var. *botrytis*) mutant were classified as membranous (Paolillo et al. 2004). To our best knowledge, typical membranous chromoplasts have never been observed in carrot. Thus, the presence of membranous chromoplasts in carrot d-o callus is unique. Tubular chromoplasts were also observed in TEM images of d-o callus cells. They resembled a system of tubules of crystalline-like appearance and about 30 nm in diameter (see Fig. 5e) corresponds to a typical morphology known from other species where the average tube diameter range is 20–60 nm (Sitte et al. 1980). Tubular chromoplasts are bundles of elongated, sometimes branched, tubes that can reach up to 10 µm in length (Sitte et al. 1980) and have been found in many flowers and fruits (Camara et al. 1995; Schweiggert and Carle 2017). They are anisotropic structures with a birefringence property due to the presence of liquid-crystalline carotenoids, including β-carotene, and are sinks of lipid-dissolved carotenoid esters (Schweiggert et al. 2012; Hempel et al. 2017; Schweiggert and Carle 2017). The composition of tubes can be diverse, and lutein may constitute even a half of the lipophilic fraction, as was found in *Palisota barteri* (Knoth et al. 1986). The relatively low frequency of tubular chromoplasts in d-o callus may thus be related to low lutein content present in this tissue.

The presence of composed amylochromoplasts as well as typical crystalline, globular, membranous and tubular chromoplasts in d-o callus cells implies that carotenoid biosynthesis, sequestration and storage take place in chromoplasts of different ultrastructure. Such diversity supports the conclusion that chromoplast development can proceed in various ways (Solymosi and Keresztes 2012) and makes d-o callus a valuable model tissue for research on plastid biogenesis as it can be easily exposed to a range of stimuli. According to Kumar et al. (1984) amyloplasts may serve as chromoplast precursors; thus developing chromoplasts (amylochromoplasts) maintain small starch grains and can include globular and crystalline structures, making classification of chromoplasts ambiguous (Hempel et al. 2014). Amyloplasts were abundant in p-y callus while chromoplasts and amylochromoplasts were frequent in d-o callus. A large number of amylochromoplasts containing either plastoglobuli or crystalline structures, or both, indicates chromoplasts' origin from amyloplasts in d-o callus. This route of chromoplast biogenesis has already been proposed to operate in carrot root. Amyloplasts were identified in young carrot roots but they disappeared during root development and were not observed in mature, carotenoid-rich, orange storage root. However, roots of white carrot, which are free of carotenoids, retained large amyloplasts (Kim et al. 2010). The authors hypothesized that the amyloplast-to-chromoplast transition occurred during carotenoid accumulation. The presence of amylochromoplasts in d-o callus cells supports this hypothesis and provides evidence of intermediate stages of chromoplast development that have not been demonstrated in carrot root so far, but were found in other species (Horner et al. 2007). The process of chromoplast development in d-o callus was also captured in ultrastructure images. Usually, the size of plastoglobuli ranges from 30 nm to more than 1000 nm (Sitte et al. 1980), although it depends on plastid type, species, organ and even environment (Brehelin et al. 2007), and the number of plastoglobuli increases with chromoplast maturation (Solymosi and Keresztes 2012). Thus, globular chromoplasts in d-o callus possessing a few small plastoglobuli seem to exemplify chromoplasts at their early stages of development. Chromoplast development can also be seen in the ultrastructure of membranous chromoplasts, which in d-o callus had a smaller number of concentric

membrane layers than mature chromoplasts described in other species (Schweiggert and Carle 2017). This callus tissue also contained cells with ageing chromoplasts. The detection of large phytoferritin aggregates in some chromoplasts may be evidence of chromoplast senescence, which has not been reported in carrot root cells before. This conclusion is congruent with elevated ABA content in d-o callus that mediates senescence, including chlorophyll degradation and plastid degeneration, and non-toxic, protein–iron phytoferritin complexes present in the stroma are characteristic for ageing chromoplasts (Ljubesic 1982).

Several genes related to carotenogenesis were identified within the analysis of the carrot genome sequence (Iorizzo et al. 2016). A set of genes chosen for expression analyses in this work are primarily congruent with that list. It includes genes and their paralogues involved in biosynthesis of carotenoids and their precursors, and those involved in the main carotenoid degradation route through xanthophyll cycle carotenoids to ABA. Carotenoids may also be enzymatically degraded by carotenoid cleavage dioxygenases (CCDs), which affect carotenoid levels, as observed in *Arabidopsis* callus (Schaub et al. 2018). The existence of several *CCD* genes with paralogues in carrot makes their discrimination troublesome when using a qPCR approach; hence they were not included in this work. In the carrot genome, a region linked to the *Y* gene (DCAR_032551) associated with carotenoid accumulation has also been mapped recently, and its sequence analysis indicated homology to *Arabidopsis* PEL protein involved in photomorphogenesis. Only carrots possessing a mutant, putatively non-functional PEL accumulated carotenoids (Iorizzo et al. 2016). The authors hypothesized that the *yy* mutant plant was not able to repress photomorphogenesis, and thus plastids, either chloroplasts in the light or chromoplasts in the dark, can develop, synthesize, and sequester carotenoids. The hypothesis was supported by transcriptome analysis showing coordinated expression of other genes, such as COP1 and HY5 cytochrome-associated proteins, known to be involved in photomorphogenesis, and interacting with PSY expression (Llorente et al. 2017). We used the same genetic material, i.e. a homozygous recessive *yy* mutant as described by Iorizzo et al. (2016). The relative expression of the *Y* (DCAR_032551) gene in d-o callus was almost five-fold higher than in p-y callus and over 50-fold lower than in the root of the growing DH1 plant. The higher expression in d-o callus than in p-y callus partially corresponds to the higher carotenoid level. However, the much more pronounced lower expression in d-o callus than in the root, containing similar carotenoid amounts, indicates that accumulation of carotenoids is unlikely to be related to the differences in DCAR_032551 expression. These results are not contradictory to the above-mentioned hypothesized role of DCAR_032551 assuming this gene codes for a non-functional protein, although conclusions based on the comparison of the callus model system to the growing plant must be drawn with caution.

Gene upregulation in the upstream pathway causing carotenoid precursors' flux is essential for downstream metabolite biosynthesis and in consequence their accumulation (Rodriguez-Concepcion 2010). One of the most prominent differences in transcript levels between both carotenoid-rich d-o callus and roots, and carotenoid-poor p-y callus was identified for *GGPS*. The transcript levels of mainly *GGPS1* present in two copies in the carrot genome were essentially similar in both carotenoid-rich d-o callus and roots, and about 15-fold higher than in carotenoid-poor p-y callus. Thus, their high expression most likely enhanced biosynthesis of geranylgeranyl diphosphate molecules, which are substrates for PSY, the first enzyme in the carotenoid pathway. Usually, PSY is the major rate-limiting factor of carotenoid biosynthesis in many organisms (Giuliano 2014). The key role of this gene was shown in non-green *Arabidopsis* tissues, including callus. The overexpression of the *AtPSY* gene resulted in an increased PSY protein level and in consequence carotenoid contents, although the expression of other carotenoid genes remained unaffected. Callus accumulated high β-carotene amounts deposited also as crystals that resembled sequestration as observed in carrot root (Maass et al. 2009). The differential role of PSY isoforms depending on the plant organ was also shown with plastid localization associated mainly with plastoglobuli (Shumskaya and Wurtzel 2013). Two *PSY* genes, *PSY1* and *PSY2*, have been described in carrot, and their expression has been reported (Maass et al. 2009; Iorizzo et al. 2016). Additionally, a partial *PSY2* sequence was predicted after genome sequencing, also known as *PSY3* in the NCBI nucleotide database, but it has a low homology to *PSY3* genes in other species and there is no confirmation of its functional role, so it was not included in our investigation. PSY1 seems more important in green tissues than in the root as *PSY1* expression is upregulated in leaves (Wang et al. 2014). Moreover, it responds to light regulation and becomes active in de-etiolated root tissues. The expression of *PSY2* in the root remains unaffected by light while it is repressed in leaves (Fuentes et al. 2012; Wang et al. 2014). However, Maass et al. (2009) showed that the *PSY1* transcript level was two-to-three-fold higher than *PSY2* in cultivars with white and orange roots. In our work, *PSY1* was downregulated in the dark-grown d-o callus in comparison to p-y callus, and thus its expression could not contribute to the increase of carotenoid level in d-o callus. In contrast, comparing both callus lines, *PSY2* was upregulated in orange tissue, which corresponded to enhanced phytoene biosynthesis. The increased *PSY2* expression in the dark indicates different activity of *PSY1* and *PSY2* genes depending on the tissue. This corroborates differential *PSY* gene expression found in carrot root

phloem tissue containing higher carotenoid contents than xylem. The expression of *PSY2* in phloem was much higher relative to xylem, while *PSY1* was stable or only slightly increased (Perrin et al. 2017). However, high carotenoid accumulation in d-o callus can be only partially explained by *PSY2* upregulation, as its transcript level was almost four-fold lower than in the root, containing similar amounts of carotenoids. This is congruent with the incomplete correlation found between *PSY* transcript levels and carotenoid contents in white and orange roots (Bowman et al. 2014). Moreover, reduced PSY enzyme levels did not correspond to unchanged PSY transcript levels, indicating that the protein level is modulated by carotenoid metabolites (Arango et al. 2014). Recent application of another callus-based system in *Arabidopsis* indicated that low carotenoid contents in callus may result from non-enzymatic carotene degradation, which was compensated by only high PSY overexpression enabling carotenoid accumulation (Schaub et al. 2018).

Conversion of cyclic carotenes to xanthophylls is mediated by hydroxylases and BCH is the main enzyme hydroxylating β-carotene (Moise et al. 2014); thus the repression of BCH may also result in higher β-carotene accumulation (Giuliano 2014). The *BCH1* expression levels were similar in both callus tissues and in the roots, while the *BCH2* expression was highly repressed in d-o callus compared to the root, and its level was additionally 12-fold lower than in carotenoid-poor p-y callus. These results indicate that β-carotene accumulated in d-o callus mainly as the result of repressed β-carotene hydroxylation due to *BCH2* downregulation. This mechanism is thus analogous to that observed at a late stage of carrot root development where after 12 weeks of vegetation the *BCH2* expression was highly repressed in the dark-grown roots, preventing β-carotene catabolism and contributing to carotenoid accumulation (Fuentes et al. 2012).

Interestingly, the amounts of α-branch carotenoids in d-o callus were lower than in the root despite higher LCYE expression in callus. Two enzymes, lycopene β-cyclase (LCYB) and LCYE, responsible for lycopene cyclisation compete for the substrate. LCYB is responsible for lycopene to β-carotene conversion, while both LCYB and LCYE are involved in the biosynthesis of α-carotene possessing one β- and one ε-ionone ring (Moise et al. 2014). Thus, relative activities of both enzymes affect β-carotene to α-carotene ratio (Giorio et al. 2013). It was shown that LCYE overexpression led to higher lutein accumulation in tomato (Giorio et al. 2013) while its downregulation elevated β-carotene amounts in potato, channelling the substrate to the β-branch pathway (Diretto et al. 2007; Kim et al. 2013). A significant increase of *LCYE* expression was also observed during carrot root maturation, which partially explained the increase of α-branch carotenoids (Fuentes et al. 2012). The results presented here show that *LCYB* genes were expressed at the same level in carotenoid-poor and carotenoid-rich callus lines, but the *LCYE* transcript level was significantly increased in d-o callus, notably also in relation to the roots. Nevertheless, α-carotene level was lower than in the roots. As LCYE may also exhibit activity for β-ionone ring formation (Bai et al. 2009) it could partially contribute to the enhanced β-carotene biosynthesis, making α-carotene biosynthesis less effective.

Lower α-carotene availability may only partially explain low lutein content in the callus. Hydroxylation of α-carotene at both β- and ε-ionone rings is required for lutein biosynthesis, and the conversion is preferentially catalyzed by CYP97 haem-containing cytochrome P450 hydroxylases (Kim and DellaPenna 2006; Moise et al. 2014). It was also shown in rice that interaction of CYP97A4 and CYP97C2 is required for efficient hydroxylation of both β- and ε-ionone rings, respectively (Quinlan et al. 2012). The carrot CHXE amino acid sequence shows homology to CYP97C enzyme family (Rodriguez-Concepcion and Stange 2013), while a mutant *CYP97A3* gene coding for a non-functional hydroxylase was identified in developing orange roots, and its presence correlated with high α-carotene content due to restricted α-carotene to lutein conversion (Arango et al. 2014). As CYP97A3 is not functional in carrot, most likely lutein biosynthesis in carrot requires coordinated activity of BCH and CHXE. However, in d-o callus the *BCH2* expression was highly repressed, which could not only enhance β-carotene accumulation but simultaneously restrict α-carotene hydroxylation at the β-ring, hence limiting lutein biosynthesis.

The results presented here indicate that two callus lines developed from the same orange carrot root have contrasting potential for carotenogenesis that coincides with differential expression of some genes associated with carotenoid biosynthesis and metabolism. A differential role of gene paralogues was found in a high-carotene, orange callus. This tissue had a pronounced cell organisation with abundant crystalline chromoplasts common also in carrot root. Additionally, membranous chromoplasts, rarely occurring in plants, accompanied globular and tubular chromoplasts, and amylochromoplasts. Hence, this orange callus accumulating similar amounts of carotenoids as carrot root is a unique model tissue possessing chromoplasts representing all known ultrastructural types, whose co-occurrence has not been observed in carrot root tissue until now. Carrot callus can be conveniently maintained in laboratory conditions, so the d-o callus described here can be highly advantageous for elucidating both chromoplast biogenesis and associated carotenogenesis when it is exposed to a range of environmental factors. Moreover, it can be easily genetically manipulated and may serve as a valuable material for implementing CRISPR technology enabling precise, targeted genome editing aimed at elucidating the role of carotenogenesis-associated genes.

Author contributions statement TO, MK-Ch and RB designed the research; TO performed callus culture in vitro; the following authors performed, analyzed and interpreted results: TO, AM-H and EK: light microscopy; AM-H and EK: polarizing microscopy and histology; AM-H, MZ, DS and EK: transmission electron microscopy; AB and JS: UPLC; TO and MK-Ch: bioinformatics and RT-qPCR; RB interpreted results and coordinated work; TO, MK-Ch, AM-H, EK and RB wrote the manuscript.

Acknowledgements The authors thank Prof. P.W. Simon (University of Wisconsin-Madison, Madison, WI, USA) for providing the reference DH1 carrot. The financial support of the National Science Centre, Poland is acknowledged (decision no. DEC-2013/09/B/NZ9/02379).

Compliance with ethical standards

Conflict of interest The authors declare that they have no conflict of interest.

References

Arango J, Jourdan M, Geoffriau E, Beyer P, Welsch R (2014) Carotene hydroxylase activity determines the levels of both α-carotene and total carotenoids in orange carrots. Plant Cell 26(5):2223–2233. https://doi.org/10.1105/tpc.113.122127

Bai L, Kim E, DellaPenna D, Brutnell T (2009) Novel lycopene epsilon cyclase activities in maize revealed through perturbation of carotenoid biosynthesis. Plant J 59(4):588–599. https://doi.org/10.1111/j.1365-313X.2009.03899.x

Baranska M, Baranski R, Schulz H, Nothnagel T (2006) Tissue-specific accumulation of carotenoids in carrot roots. Planta 224(5):1028–1037. https://doi.org/10.1007/s00425-006-0289-x

Baranska M, Baranski R, Grzebelus E, Roman M (2011) In situ detection of a single carotenoid crystal in a plant cell using Raman microspectroscopy. Vib Spectrosc 56(2):166–169. https://doi.org/10.1016/j.vibspec.2011.02.003

Baranski R (2008) Genetic transformation of carrot (*Daucus carota*) and other Apiaceae species. Trans Plant J 2:18–38

Baranski R, Klocke E, Schumann G (2006) Green fluorescent protein as an efficient selection marker for *Agrobacterium rhizogenes* mediated carrot transformation. Plant Cell Rep 25(3):190–197. https://doi.org/10.1007/s00299-005-0040-2

Boba A, Kostyn K, Preisner M, Wojtasik W, Szopa J, Kulma A (2018) Expression of heterologous lycopene β-cyclase gene in flax can cause silencing of its endogenous counterpart by changes in gene-body methylation and in ABA homeostasis mechanism. Plant Physiol Biochem 127:143–151. https://doi.org/10.1016/j.plaphy.2018.03.023

Bowman M, Willis D, Simon P (2014) Transcript abundance of phytoene synthase 1 and phytoene synthase 2 is associated with natural variation of storage root carotenoid pigmentation in carrot. J Am Soc Hortic Sci 139(1):63–68

Brehelin C, Kessler F, van Wijk KJ (2007) Plastoglobules: versatile lipoprotein particles in plastids. Trends Plant Sci 12:260–266. https://doi.org/10.1016/j.tplants.2007.04.003

Camara B, Hugueney P, Bouvier F, Kuntz M, Monéger R (1995) Biochemistry and molecular biology of chromoplast development. Int Rev Cytol 163:175–247. https://doi.org/10.1016/s0074-7696(08)62211-1

Cavagnaro P, Chung S, Manin S, Yildiz M, Ali A, Alessandro M, Iorizzo M, Senalik D, Simon P (2011) Microsatellite isolation and marker development in carrot—genomic distribution, linkage mapping, genetic diversity analysis and marker transferability across Apiaceae. BMC Genomics 12:386. https://doi.org/10.1186/1471-2164-12-386

Cazzonelli C (2011) Carotenoids in nature: insights from plants and beyond. Funct Plant Biol 38(11):833–847. https://doi.org/10.1071/FP11192

Cazzonelli C, Pogson B (2010) Source to sink: regulation of carotenoid biosynthesis in plants. Trends Plant Sci 15(5):266–274. https://doi.org/10.1016/j.tplants.2010.02.003

Clotault J, Peltier D, Berruyer R, Thomas M, Briard M, Geoffriau E (2008) Expression of carotenoid biosynthesis genes during carrot root development. J Exp Bot 59(13):3563–3573. https://doi.org/10.1093/jxb/ern210

Diretto G, Welsch R, Tavazza R, Mourgues F, Pizzichini D, Beyer P, Giuliano G (2007) Silencing of beta-carotene hydroxylase increases total carotenoid and beta-carotene levels in potato tubers. BMC Plant Biol 7:11. https://doi.org/10.1186/1471-2229-7-11

Egea I, Barsan C, Bian W, Purgatto E, Latche A, Chervin C, Bouzayen M, Pech J (2010) Chromoplast differentiation: current status and perspectives. Plant Cell Physiol 51(10):1601–1611. https://doi.org/10.1093/pcp/pcq136

Frey-Wyssling A, Schwegler F (1965) Ultrastructure of the chromoplasts in the carrot root. J Ultrastruct Res 13:543–559

Fuentes P, Pizarro L, Moreno J, Handford M, Rodriguez-Concepcion M, Stange C (2012) Light-dependent changes in plastid differentiation influence carotenoid gene expression and accumulation in carrot roots. Plant Mol Biol 79(1–2):47–59. https://doi.org/10.1007/s11103-012-9893-2

Giorio G, Yildirim A, Stigliani A, D'Ambrosio C (2013) Elevation of lutein content in tomato: a biochemical tug-of-war between lycopene cyclases. Metabolic Eng 20:167–176. https://doi.org/10.1016/j.ymben.2013.10.007

Giuliano G (2014) Plant carotenoids: genomics meets multi-gene engineering. Curr Opin Plant Biol 19:111–117. https://doi.org/10.1016/j.pbi.2014.05.006

Giuliano G (2017) Provitamin A biofortification of crop plants: a gold rush with many miners. Curr Opin Biotechnol 44:169–180. https://doi.org/10.1016/j.copbio.2017.02.001

Ha S, Vankova R, Yamaguchi-Shinozaki K, Shinozaki K, Tran L (2012) Cytokinins: metabolism and function in plant adaptation to environmental stresses. Trends Plant Sci 17(3):172–179. https://doi.org/10.1016/j.tplants.2011.12.005

Hanchinal V, Survase S, Sawant S, Annapure U (2008) Response surface methodology in media optimization for production of β-carotene from *Daucus carota*. Plant Cell Tissue Org Cult 93(2):123–132. https://doi.org/10.1007/s11240-008-9350-8

Hempel J, Amrehn E, Quesada S, Esquivel P, Jimenez V, Heller A, Carle R, Schweiggert R (2014) Lipid-dissolved γ-carotene, β-carotene, and lycopene in globular chromoplasts of peach palm (*Bactris gasipaes* Kunth) fruits. Planta 240(5):1037–1050. https://doi.org/10.1007/s00425-014-2121-3

Hempel J, Schadle CN, Sprenger J, Heller A, Carle R, Schweiggert RM (2017) Ultrastructural deposition forms and bioaccessibility of carotenoids and carotenoid esters from goji berries (*Lycium*

barbarum L.). Food Chem 218:525–533. https://doi.org/10.1016/j.foodchem.2016.09.065

Horner HT, Healy RA, Ren G, Fritz D, Klyne A, Seames C, Thornburg RW (2007) Amyloplast to chromoplast conversion in developing ornamental tobacco floral nectaries provides sugar for nectar and antioxidants for protection. Am J Bot 94:12–24. https://doi.org/10.3732/ajb.94.1.12

Ikeuchi M, Sugimoto K, Iwase A (2013) Plant callus: mechanisms of induction and repression. Plant Cell 25(9):3159–3173. https://doi.org/10.1105/tpc.113.116053

Iorizzo M, Ellison S, Senalik D, Zeng P, Satapoomin P, Huang J, Bowman M, Iovene M, Sanseverino W, Cavagnaro P, Yildiz M, Macko-Podgorni A, Moranska E, Grzebelus E, Grzebelus D, Ashrafi H, Zheng Z, Cheng S, Spooner D, Van Deynze A, Simon P (2016) A high-quality carrot genome assembly provides new insights into carotenoid accumulation and asterid genome evolution. Nat Genet 48(6):657. https://doi.org/10.1038/ng.3565

Jimenez V, Bangerth F (2001) Endogenous hormone levels in explants and in embryogenic and non-embryogenic cultures of carrot. Physiol Plant 111(3):389–395. https://doi.org/10.1034/j.1399-3054.2001.1110317.x

Just B, Santos C, Fonseca M, Boiteux L, Oloizia B, Simon P (2007) Carotenoid biosynthesis structural genes in carrot (*Daucus carota*): isolation, sequence-characterization, single nucleotide polymorphism (SNP) markers and genome mapping. Theor Appl Genet 114(4):693–704. https://doi.org/10.1007/s00122-006-0469-x

Kilcrease J, Collins A, Richins R, Timlin J, O'Connell M (2013) Multiple microscopic approaches demonstrate linkage between chromoplast architecture and carotenoid composition in diverse *Capsicum annuum* fruit. Plant J 76(6):1074–1083. https://doi.org/10.1111/tpj.12351

Kim J, DellaPenna D (2006) Defining the primary route for lutein synthesis in plants: the role of *Arabidopsis* carotenoid β-ring hydroxylase CYP97A3. Proc Natl Acad Sci USA 103(9):3474–3479. https://doi.org/10.1073/pnas.0511207103

Kim JE, Rensing KH, Douglas CJ, Cheng KM (2010) Chromoplasts ultrastructure and estimated carotene content in root secondary phloem of different carrot varieties. Planta 231:549–558. https://doi.org/10.1007/s00425-009-1071-7

Kim S, Kim Y, Ahn Y, Ahn M, Jeong J, Lee H, Kwak S (2013) Down-regulation of the lycopene ε-cyclase gene increases carotenoid synthesis via the β-branch-specific pathway and enhances salt-stress tolerance in sweet potato transgenic calli. Physiol Plant 147(4):432–442. https://doi.org/10.1111/j.1399-3054.2012.01688.x

Klimek-Chodacka M, Oleszkiewicz T, Lowder LG, Qi Y, Baranski R (2018) Efficient CRISPR/Cas9-based genome editing in carrot cells. Plant Cell Rep 37(4):575–586. https://doi.org/10.1007/s00299-018-2252-2

Knoth R, Hansmann P, Sitte P (1986) Chromoplasts of *Palisota barteri*, and the molecular structure of chromoplast tubules. Planta 168:167–174. https://doi.org/10.1007/BF00402960

Kumar A, Bender L, Neumann K (1984) Growth-regulation, plastid differentiation and the development of a photosynthetic system in cultured carrot root explants as influenced by exogenous sucrose and various phytohormones. Plant Cell Tissue Org Cult 3(1):11–28. https://doi.org/10.1007/BF00035917

Li L, Yuan H (2013) Chromoplast biogenesis and carotenoid accumulation. Arch Biochem Biophys 539(2):102–109. https://doi.org/10.1016/j.abb.2013.07.002

Ljubesic N (1982) Phytoferritin accumulations in chromoplasts of *Sorbus aucuparia* L. fruits. Acta Bot Croat 41:29–32

Ljubesic N, Wrischer M, Devide Z (1991) Chromoplasts—the last stages in plastid development. Int J Dev Biol 35:251–258

Llorente B, Martinez-Garcia J, Stange C, Rodriguez-Concepcion M (2017) Illuminating colors: regulation of carotenoid biosynthesis and accumulation by light. Curr Opin Plant Biol 37:49–55. https://doi.org/10.1016/j.pbi.2017.03.011

Lu S, Van Eck J, Zhou X, Lopez A, O'Halloran D, Cosman K, Conlin B, Paolillo D, Garvin D, Vrebalov J, Kochian L, Kupper H, Earle E, Cao J, Li L (2006) The cauliflower *Or* gene encodes a DnaJ cysteine-rich domain-containing protein that mediates high levels of β-carotene accumulation. Plant Cell 18(12):3594–3605. https://doi.org/10.1105/tpc.106.046417

Maass D, Arango J, Wust F, Beyer P, Welsch R (2009) Carotenoid crystal formation in *Arabidopsis* and carrot roots caused by increased phytoene synthase protein levels. PLoS One 4(7):e6373. https://doi.org/10.1371/journal.pone.0006373

Marx M, Stuparic M, Schieber A, Carle R (2003) Effects of thermal processing on trans-cis-isomerization of β-carotene in carrot juices and carotene-containing preparations. Food Chem 83(4):609–617. https://doi.org/10.1016/S0308-8146(03)00255-3

Milani A, Basirnejad M, Shahbazi S, Bolhassani A (2017) Carotenoids: biochemistry, pharmacology and treatment. Br J Pharmacol 174(11):1290–1324. https://doi.org/10.1111/bph.13625

Milewska-Hendel A, Zubko M, Karcz J, Stroz D, Kurczynska E (2017) Fate of neutral-charged gold nanoparticles in the roots of the *Hordeum vulgare* L. cultivar Karat. Sci Rep 7:3014. https://doi.org/10.1038/s41598-017-02965-w

Moise A, Al-Babili S, Wurtzel E (2014) Mechanistic aspects of carotenoid biosynthesis. Chem Rev 114(1):164–193. https://doi.org/10.1021/cr400106y

Nisar N, Li L, Lu S, Khin N, Pogson B (2015) Carotenoid metabolism in plants. Mol Plant 8(1):68–82. https://doi.org/10.1016/j.molp.2014.12.007

Paolillo DJ Jr, Garvin DF, Parthasarathy MV (2004) The chromoplasts of *Or* mutants of cauliflower (*Brassica oleracea* L. var. *botrytis*). Protoplasma 224:245–253. https://doi.org/10.1007/s00709-004-0059-1

Perrin F, Hartmann L, Dubois-Laurent C, Welsch R, Huet S, Hamama L, Briard M, Peltier D, Gagné S, Geoffriau E (2017) Carotenoid gene expression explains the difference of carotenoid accumulation in carrot root tissues. Planta 245:737–747. https://doi.org/10.1007/s00425-016-2637-9

Pyke K (2007) Plastid biogenesis and differentiation. In: Bock R (ed) Cell and molecular biology of plastids, vol 19. Springer, Berlin, pp 1–28. https://doi.org/10.1007/4735_2007_0226

Quinlan R, Shumskaya M, Bradbury L, Beltran J, Ma C, Kennelly E, Wurtzel E (2012) Synergistic interactions between carotene ring hydroxylases drive lutein formation in plant carotenoid biosynthesis. Plant Physiol 160(1):204–214. https://doi.org/10.1104/pp.112.198556

Rodriguez-Concepcion M (2010) Supply of precursors for carotenoid biosynthesis in plants. Arch Biochem Biophys 504(1):118–122. https://doi.org/10.1016/j.abb.2010.06.016

Rodriguez-Concepcion M, Stange C (2013) Biosynthesis of carotenoids in carrot: an underground story comes to light. Arch Biochem Biophys 539(2):110–116. https://doi.org/10.1016/j.abb.2013.07.009

Roman M, Marzec K, Grzebelus E, Simon P, Baranska M, Baranski R (2015) Composition and (in)homogeneity of carotenoid crystals in carrot cells revealed by high resolution Raman imaging. Spectrochim Acta A 136:1395–1400. https://doi.org/10.1016/j.saa.2014.10.026

Ruiz-Sola MÁ, Rodríguez-Concepción M (2012) Carotenoid biosynthesis in *Arabidopsis*: a colorful pathway. Arabidopsis Book/American Society of Plant Biologists 10:e0158. https://doi.org/10.1199/tab.0158

Rygula A, Oleszkiewicz T, Grzebelus E, Pacia MZ, Baranska M, Baranski R (2018) Raman, AFM and SNOM high resolution imaging of

carotene crystals in a model carrot cell system. Spectrochim Acta A 197:47–55. https://doi.org/10.1016/j.saa.2018.01.054

Schaub P, Rodriguez-Franco M, Cazzonelli CI, Alvarez D, Wust F, Welsch R (2018) Establishment of an *Arabidopsis* callus system to study the interrelations of biosynthesis, degradation and accumulation of carotenoids. PLoS One 13(2):e0192158. https://doi.org/10.1371/journal.pone.0192158

Schweiggert R, Carle R (2017) Carotenoid deposition in plant and animal foods and its impact on bioavailability. Crit Rev Food Sci Nutr 57(9):1807–1830. https://doi.org/10.1080/10408398.2015.1012756

Schweiggert R, Mezger D, Schimpf F, Steingass C, Carle R (2012) Influence of chromoplast morphology on carotenoid bioaccessibility of carrot, mango, papaya, and tomato. Food Chem 135(4):2736–2742. https://doi.org/10.1016/j.foodchem.2012.07.035

Shumskaya M, Wurtzel E (2013) The carotenoid biosynthetic pathway: thinking in all dimensions. Plant Sci 208:58–63. https://doi.org/10.1016/j.plantsci.2013.03.012

Sitte P, Falk H, Liedvogel B (1980) Chromoplasts. In: Czygan FGC (ed) Pigments in plants. Fischer-Verlag, Stuttgart, pp 117–148

Solymosi K, Keresztes A (2012) Plastid structure, diversification and interconversions II. Land plants. Curr Chem Biol 6:187–204. https://doi.org/10.2174/2212796811206030003

Sun T, Yuan H, Cao H, Yazdani M, Tadmor Y, Li L (2018) Carotenoid metabolism in plants: the role of plastids. Mol Plant 11(1):58–74. https://doi.org/10.1016/j.molp.2017.09.010

van Wijk K, Kessler F (2017) Plastoglobuli: plastid microcompartments with integrated functions in metabolism, plastid developmental transitions, and environmental adaptation. Annu Rev Plant Biol 68:253–289. https://doi.org/10.1146/annurev-arplant-043015-111737

Vasquez-Caicedo AL, Heller A, Neidhart S, Carle R (2006) Chromoplast morphology and β-carotene accumulation during postharvest ripening of mango cv. 'Tommy Atkins'. J Agric Food Chem 54:5769–5776. https://doi.org/10.1021/jf060747u

Wang H, Ou C, Zhuang F, Ma Z (2014) The dual role of phytoene synthase genes in carotenogenesis in carrot roots and leaves. Mol Breed 34(4):2065–2079. https://doi.org/10.1007/s11032-014-0163-7

Publikacja 2: Repression of carotenoid accumulation by nitrogen and NH_4^+ supply in carrot callus cells *in vitro*

Oleszkiewicz T., Kruczek M., Baranski R. Repression of carotenoid accumulation by nitrogen and NH_4^+ supply in carrot callus cells *in vitro*.

Plants **2021**, 10, 1813

https://doi.org/10.3390/plants10091813

IF_{2020}: 3,935

Materiały uzupełniające dostępne online

https://www.mdpi.com/article/10.3390/plants10091813/s1

Table S1: Composition of Gamborg B5 and Murashige and Skoog (MS) media and their modified variants, BI and R, respectively

Table S2: Nitrogen salts composition of BI media with a modified N content or NO3:NH4 ratio

Figure S1: HPLC chromatogram at 452 nm of the sample from callus grown on a BI (control) medium.

plants

MDPI

Article

Repression of Carotenoid Accumulation by Nitrogen and NH_4^+ Supply in Carrot Callus Cells In Vitro

Tomasz Oleszkiewicz *, Michał Kruczek and Rafal Baranski

Department of Plant Biology and Biotechnology, Faculty of Biotechnology and Horticulture, University of Agriculture in Krakow, 31-425 Krakow, Poland; kruczek.michael@gmail.com (M.K.); rafal.baranski@urk.edu.pl (R.B.)

* Correspondence: tomasz.oleszkiewicz@urk.edu.pl

Abstract: The effect of mineral nutrition on the accumulation of the main health beneficial compounds in carrots, the carotenoid pigments, remains ambiguous; here, a model-based approach was applied to reveal which compounds are responsible for the variation in carotenoid content in carrot cells in vitro. For this purpose, carotenoid-rich callus was cultured on either BI (modified Gamborg B5) or R (modified Murashige and Skoog MS) mineral media or on modified media obtained by exchanging compounds between BI and R. Callus growing on the BI medium had abundant carotene crystals in the cells and a dark orange color in contrast to pale orange callus with sparse crystals on the R medium. The carotenoid content, determined by HPLC and spectrophotometrically after two months of culture, was 5.3 higher on the BI medium. The replacement of media components revealed that only the N concentration and the NO_3:NH_4 ratio affected carotenoid accumulation. Either the increase of N amount above 27 mM or decrease of NO_3:NH_4 ratio below 12 resulted in the repression of carotenoid accumulation. An adverse effect of the increased NH_4^+ level on callus growth was additionally found. Somatic embryos were formed regardless of the level of N supplied. Changes to other media components, i.e., macroelements other than N, microelements, vitamins, growth regulators, and sucrose had no effect on callus growth and carotenoid accumulation. The results obtained from this model system expand the range of factors, such as N availability, composition of N salts, and ratio of nitrate to ammonium N form, that may affect the regulation of carotenoid metabolism.

Keywords: *Daucus carota*; carotene; nitrate; ammonium; somatic embryogenesis

Citation: Oleszkiewicz, T.; Kruczek, M.; Baranski, R. Repression of Carotenoid Accumulation by Nitrogen and NH_4^+ Supply in Carrot Callus Cells In Vitro. *Plants* **2021**, *10*, 1813. https://doi.org/10.3390/plants10091813

Academic Editors: Laura Pistelli and Kalina Danova

Received: 10 August 2021
Accepted: 27 August 2021
Published: 31 August 2021

1. Introduction

The carrot is a well-known vegetable grown around the world for its nutritious storage root. The roots of the most common carrot varieties accumulate carotenoids, mainly β-carotene and α-carotene, which give them their orange color. Both carotenes have provitamin A activity and, together with other carotenoids, play beneficial roles in human health [1]. The high carotene content makes carrots one of the most important sources of carotenoids in the human diet [2], and knowledge on carotenoid biosynthesis, accumulation, and regulation of these processes is essential for the development of high-quality carrot varieties.

Carotenoids exist widely in nature. They are 40-carbon molecules built from eight base isoprenoid units. They are classified to two main groups: carotenes, being hydrocarbons such as β-carotene and α-carotene, and xanthophylls, which are oxidized carotenes [3]. The processes of carotenoid biosynthesis in plants, including carrot, have been well described [4]. In recent years, research has focused on understanding the regulation of biosynthetic pathway and carotenoid sequestration. Currently, it is known that developmental and environmental factors, such as light, influence carotenoid accumulation in carrot cells [5,6]. Field conditions and genotype have a pronounced effect on carotenoid

accumulation in carrot storage roots in contrast to plant fertilization [7]. However, fertilization with calcium ammonium nitrate increased carotenoid content [8]. The effect of other N salts was equivocal unless an additional foliar nutrition with a complex fertilizer was applied [9]. Variation in carotenoid content among carrot cultivars was also reported depending on the applied urea dose [10]. Thus, the conclusions regarding the effect of nutrition on carotenoid metabolism in carrot remain ambiguous. Recently, it was demonstrated that ammonium ions negatively affect carotenoid accumulation in *Calendula officinalis* callus cultured in vitro [11]. Another genetic research based on callus response to changes in the composition of mineral medium indicated that N supply affected pigment accumulation [12].

For more than 60 years, the carrot has been considered a model species in research on totipotency, somatic embryogenesis, and horizontal gene transfer (for review see [13] and [14]), while broad genetic research, including the recent genome sequencing project [15], led to the development of high-quality varieties [16]. Carrot is amenable to cell and tissue culture on mineral media in vitro. Callus can be induced in in vitro culture from various explants by the supplementation of mineral medium with growth regulators and then it can be easily propagated [17], hence, it has become a convenient material for research on stress factors, genetic transformation, and genome editing, including genes of the carotenoid pathway [18,19]. Carrot callus usually accumulates low amounts of carotenoids, as do the storage root meristematic cells used to induce callus [20,21]. However, the development of carotenoid-rich callus was also reported [22–24], and recently, it has been successfully used for structural studies of carotene crystals [25,26], regulation of carotenoid biosynthesis, sequestration, and interaction of carotenoid and cell wall composition when it was subjected to targeted mutagenesis using novel tools of genome editing, i.e., clustered regularly interspaced short palindromic repeats (CRISPR) and CRISPR associated (Cas9) proteins [19,24].

Inorganic components in the medium are necessary for the growth of plant tissues and organs in vitro. Their contents and composition influence tissue and plantlet development, hence, the proper balance of medium components is required [27]. For the induction of carrot callus development, and for its further propagation, a medium based on Gamborg B5 [28] mineral salts and vitamin composition is more effective and more often used than the Murashige and Skoog (MS; [29]) medium [30]. The MS medium is recommended for somatic embryogenesis and carrot plant regeneration [31,32]. Our preliminary experiments showed that attempts of plant regeneration using a modified MS medium, the R medium, led to a visually paler color of callus due to a reduced carotenoid accumulation in comparison to callus grown on the B5-based BI medium. Both media, BI and R, differ in the composition of salts, vitamins, plant growth regulators, and in the sucrose concentration. Thus, in this study we sought for an answer to which component of the R medium is responsible for the repression of carotenoid accumulation. For this purpose, we used a model carotenoid-rich callus [23] and exposed it to media with modified compositions. A substantial reduction of carotenoid content was observed on the B5 medium with altered composition of nitrogen salts, thus, we show here that the amount of N and NO_3:NH_4 ratio are key factors affecting carotenoid accumulation in carrot cells.

2. Results

2.1. Callus Growth and Morphology

Carrot callus cultured on both BI (modified Gamborg B5) and R (modified MS) media (Supplementary Table S1) grew with a similar rate. Callus cultured on the BI medium retained its characteristic morphology throughout all experiments. It had dense and lumpy structure, with small parts being more friable. It retained orange color, although rarely, friable callus was paler (Figure 1a). Callus growing on the R medium differed from callus on the BI medium in color, which became paler and eventually light orange over the course of time (Figure 1b). Microscopic observations revealed that regardless of the medium, callus cells were densely packed in aggregates (Figure 2a,b). Carotene crystals, clearly

distinguishable due to their intense orange color, were sequestered in the cells of dark orange callus on the BI medium (Figure 2c). Cells of callus maintained on the R medium contained only small crystals, and they were not abundant (Figure 2d). Additionally, proembryogenic tissue was identified in callus on the R medium. Embryoid structures were visible (Figure 1b inset); however, their development was arrested at early stages. They did not convert into plants, turned brown, and often died or dedifferentiated to new callus cell layers.

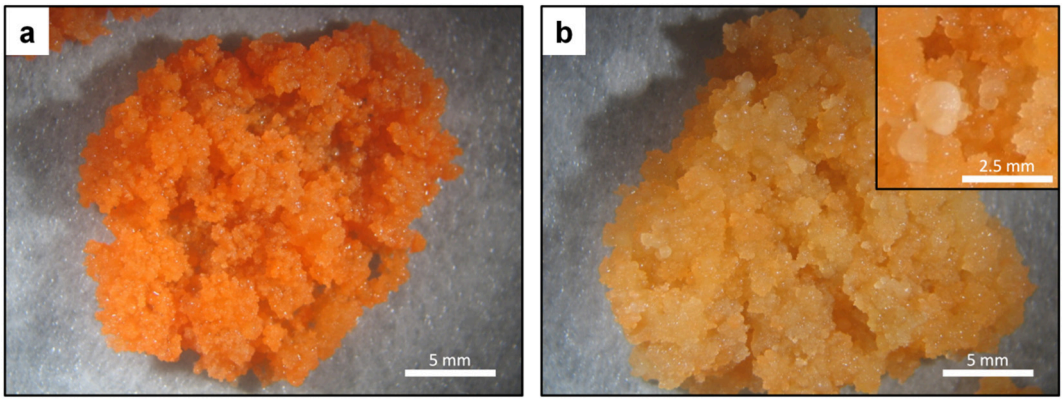

Figure 1. Carrot callus growing on mineral media. (**a**) BI medium; (**b**) R medium; (**b-inset**) embryo-like structure.

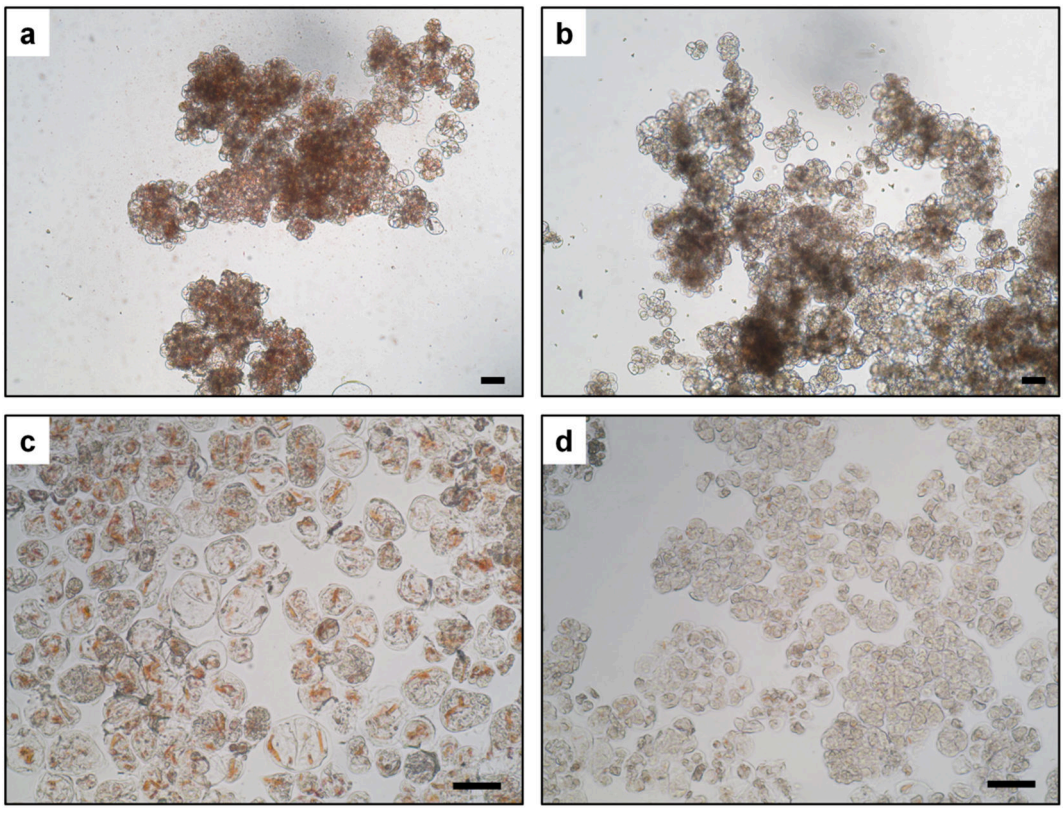

Figure 2. Densely packed carrot callus cells (not macerated tissue) growing on either the BI (**a**) or R medium (**b**). Easily noticeable carotene crystals in cells growing on the BI medium (**c**) and sparse crystals in cells growing on the R medium (**d**). Bar = 100 μm.

2.2. Carotenoid Content in Callus

Two main carotenes were identified in callus using HPLC (Table 1 and Supplementary Figure S1). The sum of α- and β-carotene contents in callus growing on the BI medium was very high (2264 µg/g DW) and exceeded that in callus on the R medium (425 µg/g DW) by 5.3 times, which corresponded to differences in color observed between calli on both media. The β/α carotene ratio (2.6) was also higher for the BI medium than for the R medium (1.5) (Table 1). The sum of α- and β-carotenes determined by HPLC highly correlated ($r = 0.98$, $p < 0.001$) with the total carotenoid content, determined spectrophotometrically, although it was usually higher. A linear relationship was described by a well fitted regression line ($p < 0.001$) with the coefficient of determination $R^2 = 0.96$ (Figure 3). Hence, quantitative determination of carotenoid content in further experiments was done using spectrophotometry.

Table 1. Carotenoid content [µg/g DW] in callus growing on the BI and R media.

Medium	α-carotene [1]	β-carotene [1]	β:α Ratio	Total Carotenoids [2]
BI (modified Gamborg B5 medium)	627 ± 73 a	1637 ± 305 a	2.6	1169 ± 89 a
R (modified MS medium)	172 ± 55 b	253 ± 113 b	1.5	404 ± 62 b
BI/MS-macro (BI with macroelements as in MS (R))	304 ± 35 b	529 ± 101 b	1.7	531 ± 44 b
R/B5-macro (R with macroelements as in B5 (BI))	725 ± 55 a	2191 ± 182 a	3.0	1322 ± 99 a
BI:R ratio	3.6	6.5	nd [3]	2.9

[1] determined by HPLC, [2] determined spectrophotometrically; means ± std. error ($n = 4$); means followed by different letters within column are significantly different at $p = 0.05$; [3] not determined.

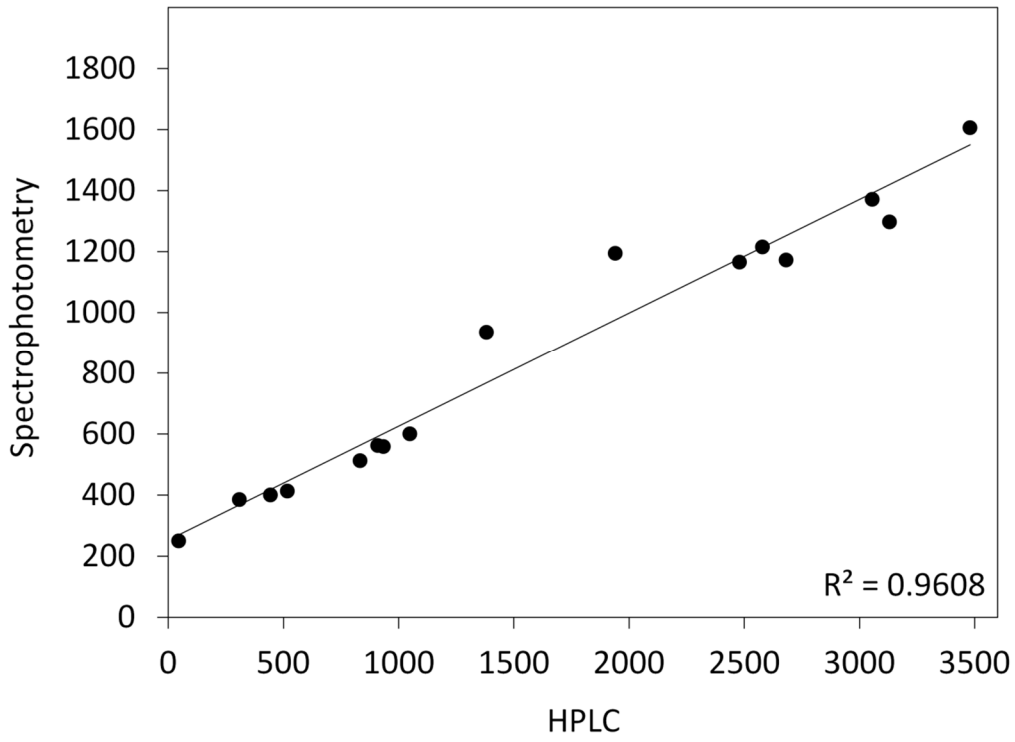

Figure 3. Fitted linear regression model for carotenoid content (µg/g DW) in carrot callus, determined based on HPLC (sum of α- and β-carotene) and spectrophotometric measurements (total carotenoids).

2.3. Effect of Medium Composition

To identify compounds that affected the carotenoid content in callus, 12 media varying in the composition of main compound groups were compared. For this purpose, the composition and amounts of macroelements, microelements, vitamins, growth regulators, or sucrose in the BI medium were replaced by the corresponding compound groups, and in the same amounts, as present in the R medium (Table 2). Analogous modifications were applied to the R medium by replacing compound groups to be the same as in the BI medium. Callus growing on the modified media showed changes in color and carotene contents ($p < 0.001$). The replacement of macroelements in the BI medium caused callus discoloration and the decrease of carotenoid content by 54.6% to a level similar to the R medium (Table 2). The effect of B5 macroelements added to the R medium was also significant. Callus growing on the R/B5-macro medium had an intense orange color and over 3-fold increased carotenoid content in comparison to the unmodified R medium, reaching the carotenoid level present in callus on the BI medium (Table 2). Thus, the Gamborg B5 composition of macroelements stimulated carotenoid accumulation in contrast to the MS formulation of macroelements. Any other changes done to either the BI or R media composition (microelements, vitamins, growth regulators, sucrose) did not significantly affect carotenoid content (Table 2). These results indicated that macroelement composition in the medium was critical for carotenoid accumulation in callus. The only other effect of modified media was the formation of embryoid structures on the BI medium free of 2,4-D and kinetin that resembled structures observed in callus on the R medium.

Table 2. Modified media used for callus culture and the carotenoid content in callus after eight-week culture (mean ± std. error).

Experiment	Medium	Medium Modification	Carotenoid Content (µg/g DW)	%BI [1]	*P* (BI) [2]	*P* (R) [2]
Modification of compound groups	BI [3]	Modified Gamborg B5 medium	1169 ± 89	100.0	ref	*
	BI/MS-macro	BI with macroelements as in MS (R)	531 ± 44	45.4	*	ns
	BI/MS-micro	BI with microelements as in MS (R)	1292 ± 64	110.5	ns	*
	BI/MS-vit	BI with vitamins as in MS (R)	1226 ± 80	104.8	ns	*
	BI/MS-pgr	BI without growth regulators as in R	1279 ± 91	109.4	ns	*
	BI/MS-suc	BI with 2% sucrose as in R	1386 ± 225	118.5	ns	*
	R [4]	Modified MS medium	404 ± 62	34.5	*	ref
	R/B5-macro	R with macroelements as in B5 (BI)	1322 ± 99	113.0	ns	*
	R/B5-micro	R with microelements as in B5 (BI)	554 ± 44	47.4	*	ns
	R/B5-vit	R with vitamins as in B5 (BI)	485 ± 51	41.5	*	ns
	R/B5-pgr	R with growth regulators as in BI	505 ± 56	43.2	*	ns
	R/B5-suc	R with 3% sucrose as in BI	512 ± 99	43.8	*	ns

Table 2. *Cont.*

Experiment	Medium	Medium Modification	Carotenoid Content (µg/g DW)	%BI [1]	*P* (BI) [2]	*P* (R) [2]
Modification of macro-elements	BI	as above	1210 ± 71	100.0	ref	*
	R	as above	656 ± 52	54.3	*	ref
	R+K	R suppl. with 2.35 mM K_2SO_2	736 ± 128	60.8	*	ns
	BI/MS-N	BI with nitrogen salts as in MS (R)	753 ± 178	62.2	*	ns
	BI/MS-N+K	BI with nitrogen salts as in MS (R) suppl. with 2.97 mM K_2SO_2	736 ± 83	60.8	*	ns
	BI/MS-P	BI with phosphorus salts as in MS (R)	1216 ± 202	100.5	ns	*
	BI/MS-Mg	BI with magnesium salts as in MS (R)	1300 ± 162	107.5	ns	*
	BI/MS-Ca	BI with calcium salts as in MS (R)	1435 ± 107	118.6	ns	*

[1] %BI—carotenoid content expressed as the percentage of the content in callus growing on the BI medium; [2] *P*—significant at $p < 0.05$ (*) or not significant (ns) difference from either BI or R considered as the reference (ref) according to the Dunnett test; [3] Modified Gamborg B5 [28] medium; [4] Modified MS [29] medium.

2.4. Effect of Macroelements

Various salts of macroelements were present in the BI and R media, thus, any element or their combination could affect carotene content. The contents of individual macroelements in the BI medium were modified to get the same molar concentrations as in the R medium. Modifications to either P, K, Ca, or Mg contents did not result in changes either of callus morphology, color, or carotenoid content. A noticeable callus discoloration was observed only on the medium with a modified composition of N salts. Callus exposed to the BI/MS-N medium developed more white or pale orange cell aggregates. It accumulated almost 40% less carotenoids than callus on the BI medium and had similar amounts of carotenoids as callus on the R medium (Table 2). The N content depends on the amounts of NH_4NO_3 and KNO_3 salts, and KNO_3 supplementation results in the increased concentration of both N and K. To verify the effect of K on carotenoid content, the R and BI/MS-N media were supplemented with K_2SO_4 (R+K and BI/MS-N+K, respectively). No effect of additional K amounts on carotenoid level was found.

2.5. Effect of N Concentration and NO_3:NH_4 Ratio

The N content in the R medium (60.02 mM) was more than doubled in comparison to the BI medium (26.76 mM) (Table 3). To verify the effect of N concentration on carotenoid accumulation, media differing in composition of N salts were compared (Supplementary Table S2). The increase of N amount in the range from 27 mM to 80 mM did not affect callus growth but significantly reduced carotene content from 1252 µg/g DW to 411 µg/g DW. Such changes were highly significant independent from whether the NO_3:NH_4 ratio in all comparing media was the same, i.e., 12.19 (the same as in the BI medium) or it was increasing in the range from 12.19 up to 38.5 (both $p < 0.001$). In both sets of media, the observed reduction of carotene content followed similar trends described by logarithmic functions with R^2 of 0.8249 and 0.9490, respectively (Figure 4).

The R medium contained NH_4NO_3 not present in the BI medium, which had NH_4^+ ions supplied in a low amount of $(NH_4)_2SO_4$ not present in the R medium (Table 3). In consequence, the R medium had more N, mainly due to the use of an amount 10.2 times higher of the ammonium form while the nitrate form was only 1.6 times higher. The effect of N form in the medium on the carotene content was verified by using media containing 26.76 mM N, the same as in the BI medium, adjusted by using both nitrate and ammonium salts in various ratios. While decreasing the NO_3:NH_4 ratio down to 1.91 (the same as in the

R medium), callus grew similar to the callus exposed to the BI medium with the NO_3:NH_4 ratio of 12.19. Further elevation of the NH_4^+ amount in the media restricted callus growth, which was eventually inhibited on the medium with the 1:1 NO_3:NH_4 ratio. The increasing NH_4^+ level also highly reduced carotenoid content in callus ($p < 0.001$). In comparison to the BI medium, the carotenoid content was reduced 3.0-fold at the NO_3:NH_4 ratio of 1.91 (the same as in the R medium), and a further increase of NH_4^+ to the 1:1 NO_3:NH_4 ratio reduced the carotenoid content by 11.5-fold to the level of 115 µg/g DW. Such changes in the carotenoid content followed a trend described by a well fitted logarithmic function with $R^2 = 0.9685$ (Figure 5).

Table 3. The BI and R media composition with regard to nitrogen content.

N Form	Compound/Ion/N	BI (mM)	R (mM)	BI:R Ratio
Salt	KNO_3	24.73	18.79	1.3
	$(NH_4)_2SO_4$	1.01	0	nd [1]
	NH_4NO_3	0	20.61	nd
Ion	NO_3^-	24.73	39.41	0.6
	NH_4^+	2.02	20.61	0.1
Element	N	26.76	60.02	0.4
Ratio	NO_3:NH_4	12.19	1.91	6.4

[1] not determined.

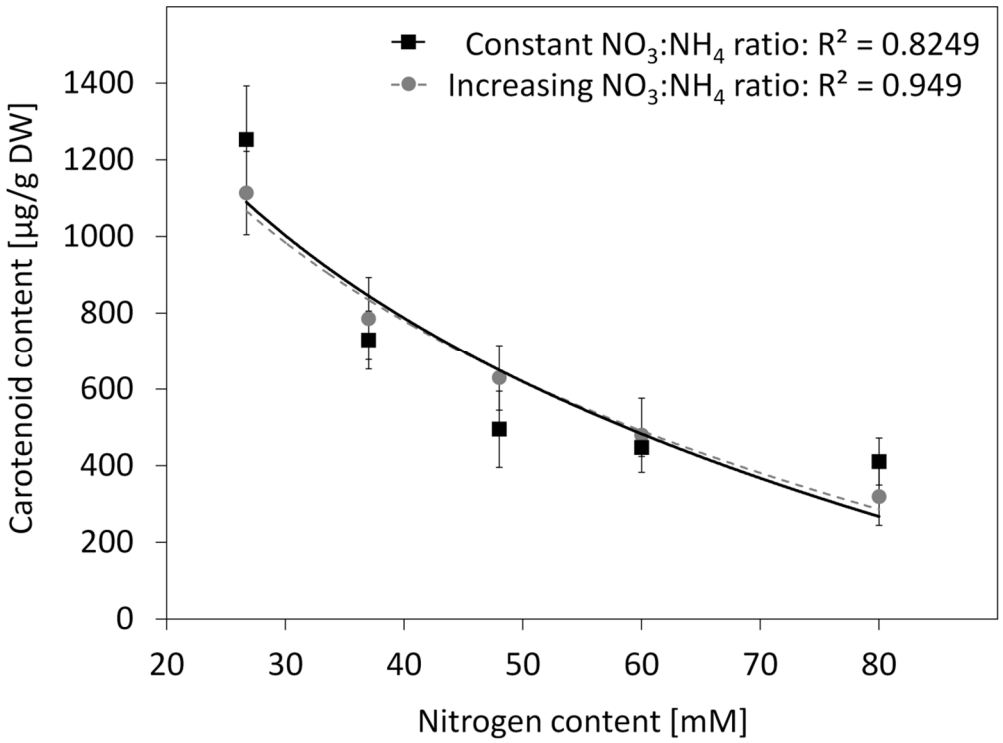

Figure 4. Carotenoid content in callus grown on the BI media with modified N content and with the constant (12.2) NO_3:NH_4 ratio (squares, solid line) or with increasing NO_3:NH_4 ratio from 12.2 to 38.5 (dots, dashed line). Lines represent logarithmic functions: $y = 3551.5 - 749.5\ln(x)$ for the constant NO_3:NH_4 ratio and $y = 3852 - 820.7\ln(x)$ for the increasing NO_3:NH_4 ratio; whiskers—std. error.

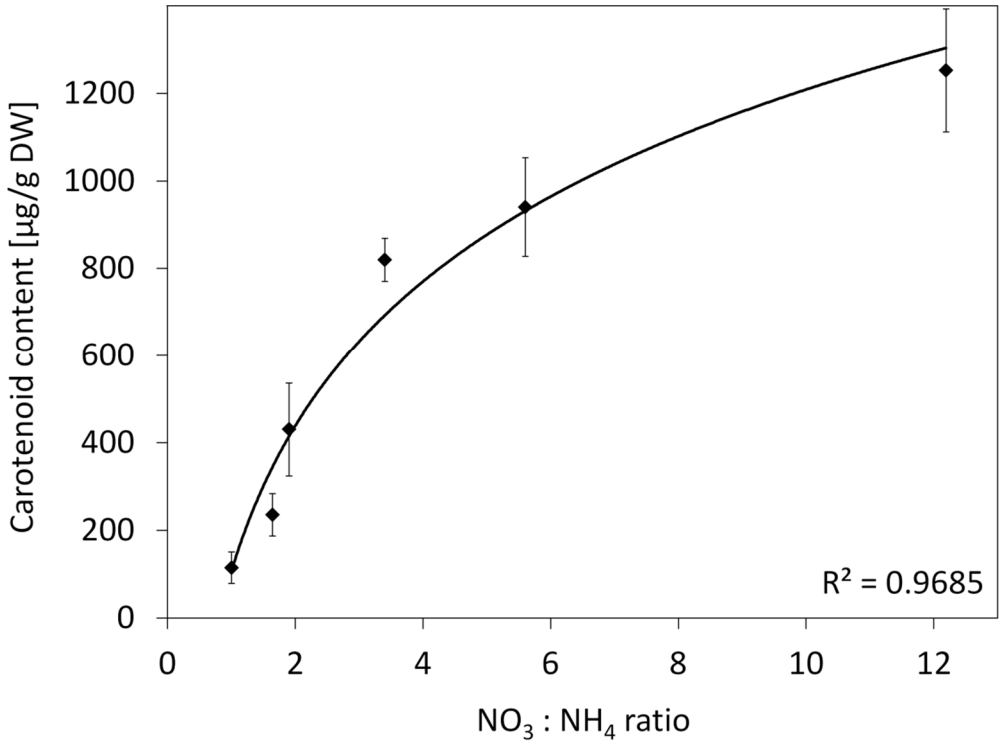

Figure 5. Carotenoid content in callus grown on BI media with a modified NO_3:NH_4 ratio and with the constant N content (26.8 mM). The line represents a logarithmic function y = 107.65 + 478.27ln(x); whiskers—std. error.

3. Discussion

Nutrient supply and their uptake by plants determine yield and quality of agricultural products, including carrot, and available data indicate that fertilization, in particular with N, may also affect carotenoid accumulation in carrot storage roots. Previous evaluations of NPK fertilization showed that genotype and environmental conditions affected carotenoid accumulation rather than N supply [7]. These conclusions were supported by results of a multiyear field trial using various N fertilizers, although significant increase of carotenoid content was achieved after foliar nutrition [9]. Fertilization with urea suggested variation in carotenoid content in used cultivars depending on the urea dose, although differences between overall means were insignificant [10], while fertilization with calcium ammonium nitrate increased carotenoid accumulation in two cultivars in a two-year trial [8]. The conclusions of field studies on plant nutrition remain ambiguous as the results are highly affected by complex environmental factors, additionally interacting with variety.

Experiments utilizing cell and tissue culture in vitro allow to apply controlled conditions that, in particular, are essential in plant nutrition research, and which are not possible to obtain in field conditions. Therefore, we have applied a research model to elucidate at cellular level the role of nutrition on the accumulation of the main carrot health beneficial compounds, the carotenoid pigments. The MS-based mineral media had already been used to culture cell suspension or to induce callus for carotenoid research. The cell suspension or callus from a red storage root carrot variety accumulated mainly β-carotene and lycopene; the level of these pigments highly varied and was clone-dependent [33,34]. For *Arabidopsis thaliana*, the carotenoid content in wild type callus cultured on the medium containing MS salts was low, 200–550 µg/g DW [35]. For *Tagetes erecta* [36], individual carotenoids were identified and not quantified, but the assessment of color and HPLC profiles also indicated low amounts of pigments. The Gamborg B5-based mineral media were used to induce development of light-orange [24] and dark-orange, carotenoid-rich, carrot callus accumulating up to the same amounts of carotenoids (2150 µg/g DW) as the storage root from which

such callus was derived [23]. Thus, carotenogenesis was ongoing in materials cultured on the MS-based media, but the B5-based media were much more efficient for pigment accumulation. The observed color variation of carrot callus cultured on different mineral media in vitro have indicated that accumulation of carotenoid pigments is stimulated or repressed by media components. The mineral compositions of BI and R media, used in this work, differed significantly as they were essentially based on the Gamborg B5 and MS formulations, respectively. Both media differed mainly in their N salts composition. The amount of N was 2.24 times higher in the MS medium, and N was supplied in NH_4NO_3 and KNO_3 salts, of which the former was present in a higher concentration, thus, the NO_3:NH_4 ratio in MS was 1.91 (Table 3). The B5 medium was richer in the nitrate salt by 32% but contained a low amount of ammonium $(NH_4)_2SO_4$ salt, thus, the NO_3:NH_4 ratio in B5 was 12.19. Hence, the B5 medium contained 10.2 times less ammonium N form than MS. In this study, we found that callus grown on the BI medium and on any modified BI medium containing N salts according to the Gamborg B5 formulation accumulated many more carotenoids than when using MS-based N salts.

Both BI and R media differed also in the composition of other compounds. The MS medium contained three times more $CaCl_2$, 50% more $MgSO_4$, and had KH_2PO_4 instead of NaH_2PO_4. Although these differences are less pronounced than differences in N salts composition, they were also taken into account in this study. It was previously reported that a reduction of Ca supply promoted carotenoid accumulation in the roots of carrot plants, but this effect was variety dependent, with the most significant effect on lycopene content in a lycopene accumulating variety [37]. When using a lycopene accumulating carrot cell suspension, it was shown that increasing the initial P content in the medium or resupplying P during the culture increased carotenoid accumulation [38]. It was also shown that the increase of 2,4-D up to 10 ppm promoted carotenoid accumulation in carrot cells [33]. A higher sucrose concentration increased carotenoid content, with 3%−5% sucrose being optimal, while 8% sucrose had adverse effects on carrot cells growth and their size [39]. Additionally, the carotenoid accumulation increased in *Calendula officinalis* callus when sucrose concentration was raised from 4% to 7% [11]. In our work, no significant changes in carotenoid accumulation in carrot callus was found when modifying the compositions of Ca, P, K, and Mg salts. Further BI medium modifications by replacing microelements, vitamins, elimination of growth regulators, and reduction of sucrose from 3% to 2%, as present in the R medium, had no significant impact. No response of carrot callus to all these modifications supports the conclusion that N availability is the prime factor affecting carotene accumulation. This finding is in contrary to the results presented by Hanchinal et al. [40], who modified N, P, and sucrose concentrations and used a response surface methodology to optimize β-carotene production by carrot cells in suspension. A doubled N concentration to 50 mM with increased sucrose content from 2% to 3% increased β-carotene production up to 13.61 μg/g DW. However, it must be underlined that they used cells accumulating very low amounts of carotenoids, two magnitude lower than callus in our work, which may highly bias the conclusions.

Our results showed also that a gradual increase of N from 26.76 mM to 80.04 mM restricts carotenoid accumulation, which eventually decreased 3-fold. Nitrogen was supplied mainly in the form of KNO_3, thus, the amounts of N and K in the medium were interrelated. Further media adjustments with K salts to keep this element at the same level while increasing N concentration showed that K did not affect carotenoid accumulation, confirming that the N amount in the medium is a critical factor and, moreover, its effect is independent on the NO_3:NH_4 ratio in the range from 12.2 to 38.5. Additionally, the amount of N did not alter callus growth. Recent study on grape callus showed that the reduced N amount in the MS medium from 60 mM to 40–50 mM enhanced accumulation of other pigments, anthocyanins, in red-pod okra callus; however, further reduction to 30 mM had an adverse effect [41]. Additionally, N starvation promoted anthocyanin accumulation in grape callus [42]. In contrary, other reports showed that the increase of total N content by doubling KNO_3 in the MS medium increased anthocyanin content by 135% [12], which

was congruent with results showing the highest accumulation of anthocyanins using an elevated N amount (70 mM) in the medium [43].

The N content in a medium depends on the combination of supplied ammonium and nitrate salts. The ammonium N form is preferred by plants as it can be directly used, and its incorporation by a cell requires less energy. However, it can become toxic to plant cells at higher concentrations, and plant sensitivity to ammonia varies greatly depending on species, plant age, and environment pH [44]. Hairy roots of carrot, red beet, and madder in the presence of NH_4^+ available in the amounts in the MS medium had a reduced growth [45]. A similar effect of restricted growth was observed for anthocyanin accumulating carrot callus cultured on MS [12]. No growth changes were reported only when carrot cell suspension was exposed to a doubled amount of ammonium N form than present in MS [46]. The comparison of a wide range of NO_3:NH_4 ratios in our work demonstrates that when keeping the optimum N level (26.76 mM) for carotenoid accumulation, as in the B5 medium, the callus growth is restricted with increasing amounts of NH_4^+, as is the carotenoid content. This adverse effect of the ammonium form led to an over 10-fold reduction of carotenoids and such response intensified logarithmically with the NH_4^+ concentration. A similar adverse effect of high NH_4^+ concentration was found in *Calendula officinalis* callus. The 50% decrease of NH_4^+ amount, in comparison to MS, induced carotenoid biosynthesis, and the complete removal of NH_4^+ from the medium further promoted carotenoid accumulation [11]. An analogous effect of increasing NH_4^+ concentration was reported in relation to anthocyanin accumulation. Lower anthocyanin contents were recorded in carrot cells in suspension exposed to media with a low NO_3:NH_4 ratio, and the increase of the ratio to 4:1 led to the highest pigment content [43]. In callus induced from rose leaves, the reduction of NH_4^+ and increase of NO_3^- concentrations in the MS-based medium enhanced anthocyanin accumulation [47]. Conversely, doubling the concentration of NH_4^+ in the MS medium restricted the anthocyanin content by one third in carrot callus [12].

Nitrogen is required by plants for their growth, but the composition and concentrations of N salts in a culture medium affect also morphogenesis and embryogenesis [27]. It was previously shown that a reduced form of N, present in high amounts in MS, is required for the development of somatic embryos from carrot hypocotyl explants. Three N salts with reduced N were compared and two of them, NH_4NO_3 and NH_4Cl, favored somatic embryogenesis, while $(NH_4)_2SO_4$ did not [48]. However, contrary to these results, nearly 20 times more plants developed on the B5 medium, which contained much less of the reduced N form and was supplied with $(NH_4)_2SO_4$ salt only, than on the MS-based medium [49]. The comparison of several media free of growth regulators in our work has shown that the formation of proembryogenic tissue and globular embryos is ongoing regardless of the medium mineral composition. Somatic embryos were observed on both, carotenoid-rich callus and low carotenoid accumulating callus, thus, there was no clear relationship between somatic embryogenesis and N salt composition, hence, carotenoid accumulation, although quantitative comparison was not the subject of this work.

4. Materials and Methods

4.1. Plant Material, Media Preparation, and Experiment Design

Dark-orange callus derived from the root of DH1 (doubled haploid) carrot (*Daucus carota* L.) line accumulating high amounts of carotenoids and described previously [23] was used. Callus was maintained on filter paper disks laid down on the surface of solidified mineral medium in 9 cm Petri dishes and cultured at 26 °C in the dark. In each experiment, callus was grown for eight weeks with one transfer to a fresh medium after four weeks. Two main media were used: (1) the BI medium consisting of Gamborg B5 macro- and microelements with vitamins, 30 g/L sucrose, 1 mg/L 2,4-D, and 0.0215 mg/L kinetin, and (2) the R medium consisting of MS macro- and microelements with vitamins (with an increased glycine content to 3 mg/L), 20 g/L sucrose, and free of growth regulators (Supplementary Table S1). Both media had pH adjusted to 5.8 and were solidified with

2.7 g/L phytagel. Macro- and microelements, including vitamin mixtures, separate macro- and microelement mixtures, vitamins, and plant growth regulators were purchased from Duchefa Biochemie (Haarlem, The Netherlands). Media modifications were done by exchanging group of components between BI and R media (12 media variants; Table 2), or by exchanging individual compounds (eight variants; Table 2), or by changing nitrogen salts composition and their concentration (14 variants) (Supplementary Table S2).

4.2. Microscopic Observations

To observe callus structure, small callus pieces were placed on a microscopic slide in a water drop under the cover slide. Carotenoid crystals were observed in single cells after tissue maceration in 1N HCl at 50 °C for 5 min. Observations were done in a bright-field using the Zeiss Axiovert S100 microscope with ×10 objective. Images were collected by using the attached digital camera.

4.3. Determination of Carotenoid Content

Eight-week-old callus was lyophilized and ground into a fine powder in a beading mill for 5 min. Carotenoids were extracted from 5–10 mg samples with 500 µL of acetone in 1.5 mL tubes. Samples were vortexed for 30 s and centrifuged at 18,000 g for 5 min. Acquired extracts were transferred to fresh tubes. The procedure was repeated to ensure complete extraction, and then, obtained extracts were combined. The absorbance of extracts was measured in a 1 cm QS quartz cuvette (Hellma Analytics, Müllheim, Germany) at 450 nm using the NanoDrop 2000c (ThermoScientific, Waltham, MA, USA) spectrophotometer. Extractions and measurements were done for each sample in triplicate and the readouts were averaged before statistical analysis. The total carotenoid content was calculated based on the β-carotene extinction coefficient ($A^{1\%}_{1cm}$ = 2500) using the formula:

$$\frac{\frac{absorbance\ (450\ nm)}{2500} \times extract\ volume\ (ml) \times 10000}{sample\ mass\ (g)}$$

The results are presented in µg of carotenes per gram of callus dry weight.

High performance liquid chromatography (HPLC) measurements were done using the same callus samples as for spectrophotometry. HPLC was performed as previously described [19]. Briefly, the extraction was performed using ethanol:*n*-hexane (1:1, *v*:*v*) and HPLC was performed using Shimadzu LC–20AD chromatograph equipped with a C18 RP (5 µm) column and the Shimadzu SPDM–20A–DAD photodiode-array detector. The identification of β-carotene was based on the retention time of the standard and confirmed by analysis of absorption spectra. The identification of α-carotene was based on the analysis of the absorption spectra. Quantification of β-carotene was done using a standard curve, while α-carotene was quantified in relation to β-carotene.

4.4. Statistical Analysis

Each experiment was set up in four replicates, each consisting of five calli, and having a completely randomized design. A one-way ANOVA was performed to test effects of media composition on carotene contents in callus using the Statistica v.13.1 software (TIBCO; Palo Alto, CA, USA). Differences between means were verified at the significance level $p = 0.05$ using the Dunnett test. Means are presented with their standard errors.

5. Conclusions

In this study, we sought for the answer to which component of the culture medium affects carotenoid accumulation in carrot callus. A compound by compound replacement in the MS and Gamborg B5 media have revealed that the only critical element is nitrogen, and either the increase of the total N concentration or the decrease of NO_3:NH_4 ratio restricts carotenoid accumulation. Thus, the highest carotenoid content was achieved in the medium with 26.76 mM N and 12.19:1 NO_3:NH_4 ratio, regardless of whether the other

media components were supplied according to the MS or Gamborg B5 formulation. These model-based obtained results pave the way for further elucidation of biological processes related to regulation of carotenoid metabolism. The observed effects might be limited to a simplified in vitro model; hence, further confirmation in planta may be required. However, they can be useful for research or application purposes using cell or tissue culture where stimulation of valuable secondary metabolites, such as carotenoids, is required.

Supplementary Materials: The following are available online at https://www.mdpi.com/article/10.3390/plants10091813/s1, Table S1: Composition of Gamborg B5 and Murashige and Skoog (MS) media and their modified variants, BI and R, respectively; Table S2: Nitrogen salts composition of BI media with a modified N content or NO_3:NH_4 ratio; Figure S1: HPLC chromatogram at 452 nm of the sample from callus grown on a BI (control) medium.

Author Contributions: Conceptualization, T.O.; methodology, T.O. and M.K.; formal analysis, T.O. and R.B.; investigation, T.O. and M.K.; resources, T.O.; data curation, T.O.; writing—original draft preparation, T.O.; writing—review and editing, R.B.; visualization, T.O.; supervision, R.B.; project administration, T.O.; funding acquisition, T.O. All authors have read and agreed to the published version of the manuscript.

Funding: This Research was financed by the Ministry of Science and Higher Education of the Republic of Poland. This research was supported by the National Science Centre, Poland (grant No. 2018/31/N/NZ9/02368).

Institutional Review Board Statement: Not applicable.

Informed Consent Statement: Not applicable.

Data Availability Statement: Not applicable.

Acknowledgments: Tomasz Oleszkiewicz received financial funding for a doctoral scholarship from the National Science Centre, Poland (Etiuda No. 2019/32/T/NZ9/00463).

Conflicts of Interest: The authors declare no conflict of interest.

References

1. Eggersdorfer, M.; Wyss, A. Carotenoids in human nutrition and health. *Arch. Biochem. Biophys.* **2018**, *652*, 18–28. [CrossRef]
2. Simon, P.W. Carrots and Other Horticultural Crops as a Source of Provitamin A Carotenes. *HortScience* **1990**, *25*, 1495–1499. [CrossRef]
3. Rodriguez-Amaya, D.B. Structures and Analysis of Carotenoid Molecules. In *Carotenoids in Nature: Biosynthesis, Regulation and Function*; Stange, C., Ed.; Springer International Publishing: Cham, Switzerland, 2016; pp. 71–108. [CrossRef]
4. Rosas-Saavedra, C.; Stange, C. Biosynthesis of carotenoids in plants: Enzymes and color. In *Carotenoids in Nature: Biosynthesis, Regulation and Function*; Stange, C., Ed.; Springer International Publishing: Cham, Switzerland, 2016; pp. 35–69. [CrossRef]
5. Rodriguez-Concepcion, M.; Stange, C. Biosynthesis of carotenoids in carrot: An underground story comes to light. *Arch. Biochem. Biophys.* **2013**, *539*, 110–116. [CrossRef]
6. Perrin, F.; Hartmann, L.; Dubois-Laurent, C.; Welsch, R.; Huet, S.; Hamama, L.; Briard, M.; Peltier, D.; Gagné, S.; Geoffriau, E. Carotenoid gene expression explains the difference of carotenoid accumulation in carrot root tissues. *Planta* **2017**, *245*, 737–747. [CrossRef]
7. Evers, A.-M. Effects of different fertilization practices on the carotene content of carrot. *Agric. Food Sci.* **1989**, *61*, 7–14. [CrossRef]
8. Boskovic-Rakocevic, L.; Pavlovic, R.; Zdravkovic, J.; Zdravkovic, M.; Pavlovic, N.; Djuric, M. Effect of nitrogen fertilization on carrot quality. *Afr. J. Agric. Res.* **2012**, *7*, 2884–2900. [CrossRef]
9. Smoleń, S.; Sady, W. The effect of various nitrogen fertilization and foliar nutrition regimes on the concentrations of sugars, carotenoids and phenolic compounds in carrot (*Daucus carota* L.). *Sci. Hortic.* **2009**, *120*, 315–324. [CrossRef]
10. Gajewski, M.; Węglarz, Z.; Sereda, A.; Bajer, M.; Kuczkowska, A.; Majewski, M. Carotenoid Accumulation by Carrot Storage Roots in Relation to Nitrogen Fertilization Level. *Not. Bot. Horti Agrobot. Cluj-Napoca* **2010**, *38*, 71–75. [CrossRef]
11. Legha, M.R.; Prasad, K.V.; Singh, S.K.; Kaur, C.; Arora, A.; Kumar, S. Induction of carotenoid pigments in callus cultures of *Calendula officinalis* L. in response to nitrogen and sucrose levels. *Vitr. Cell. Dev. Biol.-Plant* **2012**, *48*, 99–106. [CrossRef]
12. Saad, K.R.; Kumar, G.; Giridhar, P.; Shetty, N.P. Differential expression of anthocyanin biosynthesis genes in *Daucus carota* callus culture in response to ammonium and potassium nitrate ratio in the culture medium. *3 Biotech* **2018**, *8*, 431. [CrossRef]
13. Baranski, R. Genetic Transformation of Carrot (Daucus carota) and Other *Apiaceae* Species. *Transgenic Plant J.* **2008**, *2*, 18–38.
14. Baranski, R.; Lukasiewicz, A. Genetic Engineering of carrot. In *The Carrot Genome*; Simon, P., Iorizzo, M., Grzebelus, R., Baranski, R., Eds.; Springer International Publishing: Cham, Switzerland, 2019; pp. 149–186. [CrossRef]

15. Iorizzo, M.; Ellison, S.; Senalik, D.; Zeng, P.; Satapoomin, P.; Huang, J.; Bowman, M.; Iovene, M.; Sanseverino, W.; Cavagnaro, P.; et al. A high-quality carrot genome assembly provides new insights into carotenoid accumulation and asterid genome evolution. *Nat. Genet.* **2016**, *48*, 657–666. [CrossRef]
16. Simon, P.W. Classical and Molecular Carrot Breeding. In *The Carrot Genome*; Simon, P., Iorizzo, M., Grzebelus, R., Baranski, R., Eds.; Springer International Publishing: Cham, Switzerland, 2019; pp. 137–147. [CrossRef]
17. Ikeuchi, M.; Sugimoto, K.; Iwase, A. Plant Callus: Mechanisms of Induction and Repression. *Plant Cell* **2013**, *25*, 3159–3173. [CrossRef]
18. Klimek-Chodacka, M.; Oleszkiewicz, T.; Lowder, L.G.; Qi, Y.; Baranski, R. Efficient CRISPR/Cas9-based genome editing in carrot cells. *Plant Cell Rep.* **2018**, *37*, 575–586. [CrossRef] [PubMed]
19. Oleszkiewicz, T.; Klimek-Chodacka, M.; Kruczek, M.; Godel-Jędrychowska, K.; Sala, K.; Milewska-Hendel, A.; Zubko, M.; Kurczyńska, E.; Qi, Y.; Baranski, R. Inhibition of Carotenoid Biosynthesis by CRISPR/Cas9 Triggers Cell Wall Remodelling in Carrot. *Int. J. Mol. Sci.* **2021**, *22*, 6516. [CrossRef] [PubMed]
20. Baranska, M.; Baranski, R.; Schulz, H.; Nothnagel, T. Tissue-specific accumulation of carotenoids in carrot roots. *Planta* **2006**, *224*, 1028–1037. [CrossRef] [PubMed]
21. Baranski, R.; Klocke, E.; Schumann, G. Green fluorescent protein as an efficient selection marker for Agrobacterium rhizogenes mediated carrot transformation. *Plant Cell Rep.* **2006**, *25*, 190–197. [CrossRef]
22. Shimizu, K.; Kikuchi, T.; Sugano, N.; Nishi, A. Carotenoid and Steroid Syntheses by Carrot Cells in Suspension Culture. *Physiol. Plant.* **1979**, *46*, 127–132. [CrossRef]
23. Oleszkiewicz, T.; Klimek-Chodacka, M.; Milewska-Hendel, A.; Zubko, M.; Stróż, D.; Kurczyńska, E.; Boba, A.; Szopa, J.; Barański, R. Unique chromoplast organisation and carotenoid gene expression in carotenoid-rich carrot callus. *Planta* **2018**, *248*, 1455–1471. [CrossRef]
24. Xu, Z.-S.; Feng, K.; Xiong, A.-S. CRISPR/Cas9-Mediated Multiply Targeted Mutagenesis in Orange and Purple Carrot Plants. *Mol. Biotechnol.* **2019**, *61*, 191–199. [CrossRef] [PubMed]
25. Rygula, A.; Oleszkiewicz, T.; Grzebelus, E.; Pacia, M.Z.; Baranska, M.; Baranski, R. Raman, AFM and SNOM high resolution imaging of carotene crystals in a model carrot cell system. *Spectrochim. Acta A* **2018**, *197*, 47–55. [CrossRef] [PubMed]
26. Dudek, M.; Machalska, E.; Oleszkiewicz, T.; Grzebelus, E.; Baranski, R.; Szcześniak, P.; Mlynarski, J.; Zajac, G.; Kaczor, A.; Baranska, M. Chiral amplification in nature: Studying cell-extracted chiral carotenoid microcrystals via the resonance Raman optical activity of model systems. *Angew. Chem. Int. Ed.* **2019**, *58*, 8383–8388. [CrossRef]
27. George, E.F.; Hall, M.A.; Klerk, G.J.D. The Components of Plant Tissue Culture Media I: Macro- and Micro-Nutrients. In *Plant Propagation by Tissue Culture*; George, E.F., Hall, M.A., Klerk, G.J.D., Eds.; Springer International Publishing: Dordrecht, The Netherlands, 2008; pp. 65–113. [CrossRef]
28. Gamborg, O.L.; Miller, R.A.; Ojima, K. Nutrient requirements of suspension cultures of soybean root cells. *Exp. Cell. Res.* **1968**, *50*, 151–158. [CrossRef]
29. Murashige, T.; Skoog, F. A Revised Medium for Rapid Growth and Bio Assays with Tobacco Tissue Cultures. *Phys. Plant.* **1962**, *15*, 474–497. [CrossRef]
30. Hardegger, M.; Sturm, A. Transformation and regeneration of carrot (*Daucus carota* L.). *Mol. Breed.* **1998**, *4*, 119–127. [CrossRef]
31. Grzebelus, E.; Szklarczyk, M.; Baranski, R. An improved protocol for plant regeneration from leaf- and hypocotyl-derived protoplasts of carrot. *Plant Cell Tiss. Organ Cult.* **2012**, *109*, 101–109. [CrossRef]
32. Kiełkowska, A.; Grzebelus, E.; Lis-Krzyścin, A.; Maćkowska, K. Application of the salt stress to the protoplasts cultures of the carrot (*Daucus carota* L.) and the evaluation of the response of regenerants to soil salinity. *Plant Cell Tiss. Organ Cult.* **2019**, *137*, 379–395. [CrossRef]
33. Sugano, N.; Miya, S.; Nishi, A. Carotenoid synthesis in a suspension culture of carrot cells. *Plant Cell Physiol.* **1971**, *12*, 525–531. [CrossRef]
34. Nishi, A.; Kurosaki, F. *Daucus carota* L. (Carrot): In Vitro Production of Carotenoids and Phytoalexins. In *Medicinal and Aromatic Plants V. Biotechnology in Agriculture and Forestry*; Bajaj, Y.P.S., Ed.; Springer: Berlin/Heidelberg, Germany, 1993; pp. 178–191. [CrossRef]
35. Schaub, P.; Rodriguez-Franco, M.; Cazzonelli, C.I.; Álvarez, D.; Wüst, F.; Welsch, R. Establishment of an Arabidopsis callus system to study the interrelations of biosynthesis, degradation and accumulation of carotenoids. *PLoS ONE* **2018**, *13*, e0192158. [CrossRef]
36. Benítez-García, I.; Vanegas-Espinoza, P.E.; Meléndez-Martínez, A.J.; Heredia, F.J.; Paredes-López, O.; Del Villar-Martínez, A.A. Callus culture development of two varieties of Tagetes erecta and carotenoid production. *Electron. J. Biotechnol.* **2014**, *17*, 107–113. [CrossRef]
37. Singh, D.P.; Beloy, J.; McInerney, J.K.; Day, L. Impact of boron, calcium and genetic factors on vitamin C, carotenoids, phenolic acids, anthocyanins and antioxidant capacity of carrots (*Daucus carota*). *Food Chem.* **2012**, *132*, 1161–1170. [CrossRef]
38. Yoshida, A.; Okamura, S.; Sugano, N.; Nishi, A. Effect of Phosphate Concentration on Growth and Carotenoid Synthesis of Carrot Cells in Suspension Culture. *Environ. Control. Biol.* **1975**, *13*, 47–53. [CrossRef]
39. Yun, J.W.; Kim, J.H.; Yoo, Y.J. Optimizations of carotenoid biosynthesis by controlling sucrose concentration. *Biotechnol. Lett.* **1990**, *12*, 905–910. [CrossRef]

40. Hanchincal, V.M.; Survase, S.A.; Sawant, S.K.; Annapure, U.S. Response surface methodology in media optimization for production of β-carotene from *Daucus carota*. *Plant Cell Tiss. Organ Cult.* **2008**, *93*, 123–132. [CrossRef]
41. Irshad, M.; Debnath, B.; Mitra, S.; Arafat, Y.; Li, M.; Sun, Y.; Qiu, D. Accumulation of anthocyanin in callus cultures of red-pod okra [*Abelmoschus esculentus* (L.) Hongjiao] in response to light and nitrogen levels. *Plant Cell Tiss. Organ Cult.* **2018**, *134*, 29–39. [CrossRef]
42. Zheng, H.-Z.; Wei, H.; Guo, S.-H.; Yang, X.; Feng, M.-X.; Jin, X.-Q.; Fang, Y.-L.; Zhang, Z.-W.; Xu, T.-F.; Meng, J.-F. Nitrogen and phosphorus co-starvation inhibits anthocyanin synthesis in the callus of grape berry skin. *Plant Cell Tiss. Organ Cult.* **2020**, *142*, 313–325. [CrossRef]
43. Narayan, M.S.; Venkataraman, L.V. Effect of Sugar and Nitrogen on the Production of Anthocyanin in Cultured Carrot (*Daucus carota*) cells. *J. Food Sci.* **2002**, *67*, 84–86. [CrossRef]
44. Li, S.-X.; Wang, Z.-H.; Stewart, B.A. Chapter Five—Responses of Crop Plants to Ammonium and Nitrate, N. *Adv. Agron.* **2013**, *118*, 205–397. [CrossRef]
45. Kino-oka, M.; Taya, M.; Tone, S. Evaluation of inhibitory effect of ammonium ion on cultures of plant hairy roots. *J. Chem. Eng. Jpn* **1993**, *26*, 578–580. [CrossRef]
46. Okamura, S.; Sueki, K.; Nishi, A. Physiological Changes of Carrot Cells in Suspension Culture during Growth and Senescence. *Physiol. Plant.* **1975**, *33*, 251–255. [CrossRef]
47. Ram, M.; Prasad, K.V.; Kaur, C.; Singh, S.K.; Arora, A.; Kumar, S. Induction of anthocyanin pigments in callus cultures of *Rosa hybrida* L. in response to sucrose and ammonical nitrogen levels. *Plant Cell Tiss. Organ Cult* **2011**, *104*, 171–179. [CrossRef]
48. Kamada, H.; Harada, H. Studies on the organogenesis in carrot tissue cultures II. Effects of amino acids and inorganic nitrogenous compounds on somatic embryogenesis. *Z. Pflanzenphysiol.* **1978**, *91*, 453–463. [CrossRef]
49. Yau, Y.-Y.; Wang, K.J. Increased regeneration ability of transgenic callus of carrot (*Daucus carota* L.) on B5-based regeneration medium. *J. Appl. Hort.* **2012**, *14*, 3–6. [CrossRef]

Publikacja 3: Inhibition of carotenoid biosynthesis by CRISPR/Cas9 triggers cell wall remodelling in carrot

Oleszkiewicz T., Klimek-Chodacka M., Kruczek M., Godel-Jędrychowska K., Sala K., Milewska-Hendel A., Zubko M., Kurczyńska E., Qi Y., Baranski R. Inhibition of carotenoid biosynthesis by CRISPR/Cas9 triggers cell wall remodelling in carrot.

International Journal of Molecular Sciences **2021**, 22, 6516

https://doi.org/10.3390/ijms22126516

IF_{2020}: 5,923

Materiały uzupełniające dostępne online

https://www.mdpi.com/article/10.3390/ijms22126516/s1

Figure S1: Amino acid sequences of PSY in the wild type and mutant lines

Figure S2: Morphology and structure of the wild type and psy2 mutant callus

Table S1: Primers used for PCR and qPCR

Table S2: Cellular epitopes localization and degree of their occurrence within the callus of different lines.

International Journal of
Molecular Sciences

MDPI

Article

Inhibition of Carotenoid Biosynthesis by CRISPR/Cas9 Triggers Cell Wall Remodelling in Carrot

Tomasz Oleszkiewicz [1], Magdalena Klimek-Chodacka [1], Michał Kruczek [1], Kamila Godel-Jędrychowska [2], Katarzyna Sala [2], Anna Milewska-Hendel [2], Maciej Zubko [3,4], Ewa Kurczyńska [2], Yiping Qi [5] and Rafal Baranski [1,*]

[1] Department of Plant Biology and Biotechnology, Faculty of Biotechnology and Horticulture, University of Agriculture in Krakow, 31-425 Krakow, Poland; tomasz.oleszkiewicz@urk.edu.pl (T.O.); m.chodacka@urk.edu.pl (M.K.-C.); kruczek.michael@gmail.com (M.K.)
[2] Institute of Biology, Biotechnology and Environmental Protection, Faculty of Natural Sciences, University of Silesia in Katowice, 40-032 Katowice, Poland; kamila.godel-jedrychowska@us.edu.pl (K.G.-J.); katarzyna.sala@us.edu.pl (K.S.); anna.milewska@us.edu.pl (A.M.-H.); ewa.kurczynska@us.edu.pl (E.K.)
[3] Institute of Materials Engineering, Faculty of Science and Technology, University of Silesia, 41-500 Chorzów, Poland; maciej.zubko@us.edu.pl
[4] Department of Physics, Faculty of Science, University of Hradec Králové, 500 03 Hradec Králové, Czech Republic
[5] Department of Plant Science and Landscape Architecture, University of Maryland, College Park, MD 20742, USA; yiping@umd.edu
* Correspondence: rafal.baranski@urk.edu.pl

check for updates

Citation: Oleszkiewicz, T.; Klimek-Chodacka, M.; Kruczek, M.; Godel-Jędrychowska, K.; Sala, K.; Milewska-Hendel, A.; Zubko, M.; Kurczyńska, E.; Qi, Y.; Baranski, R. Inhibition of Carotenoid Biosynthesis by CRISPR/Cas9 Triggers Cell Wall Remodelling in Carrot. *Int. J. Mol. Sci.* **2021**, *22*, 6516. https://doi.org/10.3390/ijms22126516

Academic Editors: Robert Hasterok, Alexander Betekhtin and Christophe Dunand

Received: 26 April 2021
Accepted: 14 June 2021
Published: 17 June 2021

Publisher's Note: MDPI stays neutral with regard to jurisdictional claims in published maps and institutional affiliations.

Abstract: Recent data indicate that modifications to carotenoid biosynthesis pathway in plants alter the expression of genes affecting chemical composition of the cell wall. Phytoene synthase (PSY) is a rate limiting factor of carotenoid biosynthesis and it may exhibit species-specific and organ-specific roles determined by the presence of *psy* paralogous genes, the importance of which often remains unrevealed. Thus, the aim of this work was to elaborate the roles of two *psy* paralogs in a model system and to reveal biochemical changes in the cell wall of *psy* knockout mutants. For this purpose, Clustered Regularly Interspaced Short Palindromic Repeats (CRISPR) and CRISPR associated (Cas9) proteins (CRISPR/Cas9) vectors were introduced to carotenoid-rich carrot (*Daucus carota*) callus cells in order to induce mutations in the *psy1* and *psy2* genes. Gene sequencing, expression analysis, and carotenoid content analysis revealed that the *psy2* gene is critical for carotenoid biosynthesis in this model and its knockout blocks carotenogenesis. The *psy2* knockout also decreased the expression of the *psy1* paralog. Immunohistochemical staining of the *psy2* mutant cells showed altered composition of arabinogalactan proteins, pectins, and extensins in the mutant cell walls. In particular, low-methylesterified pectins were abundantly present in the cell walls of carotenoid-rich callus in contrast to the carotenoid-free *psy2* mutant. Transmission electron microscopy revealed altered plastid transition to amyloplasts instead of chromoplasts. The results demonstrate for the first time that the inhibited biosynthesis of carotenoids triggers the cell wall remodelling.

Keywords: arabinogalactan protein; callus; Cas9 protein; chromoplasts; Clustered Regularly Interspaced Short Palindromic Repeats; CRISPR; pectins; phytoene synthase; plastid ultrastructure

1. Introduction

Carotenoids are a vast group of compounds that widely exist in nature. In plants, they play crucial roles in photosynthetic systems and they are precursors of phytohormones [1]. Beneficial effects of carotenoids on human health are extensive. For example, β-carotene and α-carotene have provitamin A activity, and others are beneficial for treatment of age-related macular degeneration or in prevention of cardiovascular disorders and cancer [2]. The biosynthesis and accumulation of carotenoids in plants occurs in plastids and is regulated by developmental and environmental factors [3,4]. Unlike in green tissues

where carotenoids are components of chloroplasts, in non-green tissues they accumulate in chromoplasts that develop from leucoplasts and amyloplasts [5]. The chromoplast ultrastructure is complex due to the transition from one plastid type to another. Carotenoids are sequestered mainly as membrane embedded crystals or as lipid droplets enclosed in plastoglobuli [6].

Several signalling compounds are products of carotenoid degradation such as abscisic acid (ABA) and strigolactones, which regulate plant processes including germination, plant architecture, recognition of arbuscular mycorrhizal fungi, and response to stresses [7,8]. In recent years, there has been an increasing amount of data suggesting a relationship between the biosynthesis of carotenoids and the chemical composition of the cell wall. The available data indicate that the overexpression or disturbance in the expression of carotenoid genes affects, among others, the expression of genes that take part and regulate the biosynthesis of cell wall components [9–11]. Moreover, strigolactones may participate in the secondary wall architecture remodelling [12]. However, to our best knowledge, no direct evidence has been shown linking carotenoid metabolism and primary cell wall remodelling due to changes in wall components such as pectins, arabinogalactan proteins (AGPs), or extensins.

The main carotenoid biosynthesis pathway in plants has been well described [13,14]. The biosynthesis of an acyclic 15-*cis*-phytoene, the first carotene in the pathway, is catalysed in a two-step reaction by phytoene synthase (PSY). Generation of PSY is a rate-limiting step of carotenogenesis [15]. Various PSY isoforms have been described, but their number and activity differ among plant species. Only one *psy* gene was found in Arabidopsis [13] while multiple *psy* genes exist in many other species. In tobacco, PSY1 and PSY2 proteins have some functional redundancy and are mainly expressed in the aerial plant parts [11]. Both *psy1* and *psy2* genes were strongly expressed in potato tubers accumulating carotenoids [16]. However, they may also show organ-specific activities. In tomato, high expression was found for *psy1* in fruits [17], *psy2* in leaves [18], and *psy3* in roots [19]. In melon, *psy1* is expressed in leaves and fruits, and *psy2* in roots [20]. Furthermore, environmental conditions may modulate *psy* expression [3,4]. Phytochrome and cytochrome receptors regulate *psy* transcription in light exposed organs [21]. In carrot, two paralogous genes, *psy1* and *psy2*, have been found to code functional enzymes [22,23], but their differential role and regulation have not been fully investigated. According to the results of phylogenetic analysis, carrot *psy1* has been grouped with the Eudicot *psy2* clade, while *psy2,* being close to *psy* in *Solanum* species, has been grouped with Eudicot *psy1* [19]. The transcript level in carrot cultivars was up to three times higher for *psy1* than for *psy2* [22]. While the expression of both genes positively correlates with carotenoid contents, the *psy1* expression is upregulated by light in leaves, suggesting PSY1 plays more important role in green tissues than in the root. The expression of *psy2* in the root remains unaffected by light while it is repressed in the leaves [24–26]. Besides such organ specificity, *psy2* is also differentially expressed in xylem and phloem tissues in the carrot root [27] and the *psy2* expression is further induced under salt stress through ABA signalling pathway [28]. However, in white and orange carrot roots incomplete correlations between *psy* transcript levels and carotenoid contents were found [25,29]. The expression of both genes occurs in every part of the carrot plant, but it is not known if they complement each other or the carotenogenesis can be realised when either of them is inactive.

Callus obtained and cultured on mineral medium in vitro has been successfully utilized for studying carotenoid metabolism and accumulation [30,31]. However, carrot callus developing from root explants are poor in carotenoids, even if the roots are rich in carotenoids [32,33]. For this reason, the usefulness of such material for research on carotenogenesis is questionable. Recently, we have obtained and characterised a dark orange (d-o) carrot callus containing similar amounts of carotenoids as the root of orange carrot from which it was developed [34]. It differs from callus of low carotenoid content at morphological and ultrastructural levels, with visible carotene crystals in the cells. Several carotenogenesis related genes were expressed at similar levels as in the root. Both *psy* paralogs were expressed in d-o callus, although the expression level of *psy2* was much

higher, resembling the relationship observed in the root. This model d-o callus is suitable for elucidating genetic background of carotenoid biosynthesis and sequestration as it has already been demonstrated in structural studies of carotene crystals [35,36].

The aim of this work is to elaborate the roles of *psy* paralogs in carrot and to verify whether carotenogenesis may occur if either *psy1* or *psy2* are non-functional. By designing and introducing Clustered Regularly Interspaced Short Palindromic Repeats (CRISPR) and CRISPR associated (Cas9) proteins (CRISPR/Cas9) vectors we generated functional mutations in *psy1* and *psy2* genes and demonstrate their effect on carotenoids accumulation and mutual regulation of their expression. Furthermore, having a *psy* functional mutant we show changes in callus histology, and plastid ultrastructure, in particular the development of the amyloplasts instead of chromoplasts. Moreover, we show for the first time, that the inhibited biosynthesis of carotenoids is accompanied by the cell wall remodelling that is manifested by changes in the compositions of AGPs, pectins, and extensins in the wall.

2. Results

2.1. Generating of psy1 and psy2 Mutants by CRISPR/Cas9

The role of two *psy* paralogs in the carotenoid biosynthesis was elucidated in the model callus system and for this purpose both genes were targeted during experiments aiming in the generation of knockout mutations. Two vectors, each with the Cas9 gene and a pair of gRNAs (namely g1 or g2), targeting either the *psy1* or *psy2* gene (Figure 1) were delivered to a dark-orange, carotenoid-rich carrot callus cells using *Agrobacterium*-mediated transformation. Callus incubated with *Agrobacterium* and transferred to a hygromycin selection medium developed new distinguishable cell clumps on the explants surface. They had mainly orange colour, but after subsequent transfers the differences in colour among callus lines became clearly visible. Those transformed with the psy1-g1g2 vector, to target the *psy1* gene, remained predominantly orange but varied from dark to pale orange or yellowish. Similar phenotype was observed for psy2-g1g2 callus, in which the *psy2* gene was targeted, but additionally, several white clumps developed. New white clumps were also developing on the surface of orange psy2-g1g2 callus in a prolonged culture which was not observed for psy1-g1g2 callus. The presence of *aph* and *Cas9* genes was confirmed in PCR. Hence, the developed callus lines were considered transgenic with introduced putatively active CRISPR/Cas9 editing system. Well grown calli were selected (Figures 2A and 3A) for further characterisation regarding carotenoid content, expression of the *psy* genes and occurred mutations.

2.2. Characterisation of the psy1 Mutants

The developing callus lines after transformation with the psy1-g1g2 vector were characterised. Molecular analyses were performed to verify whether mutations were generated in the targeted *psy1* gene. The PCR amplification of DNA resulted in the expected products of either 480 bp or 740 bp depending on whether primers flanking the psy1-g1 or psy1-g2 target sites were used, respectively. The use of primer pair flanking both targets resulted in the expected 1495 bp product. The PCR products were then incubated with specific enzymes recognising restriction sites near protospacer adjacent motif (PAM) at each gRNA targets to reveal the occurrence of site mutations. All samples showed the restriction pattern of fragments whose sizes corresponded to those obtained for the wild type (WT), i.e., non-transgenic callus (Figure 2B).

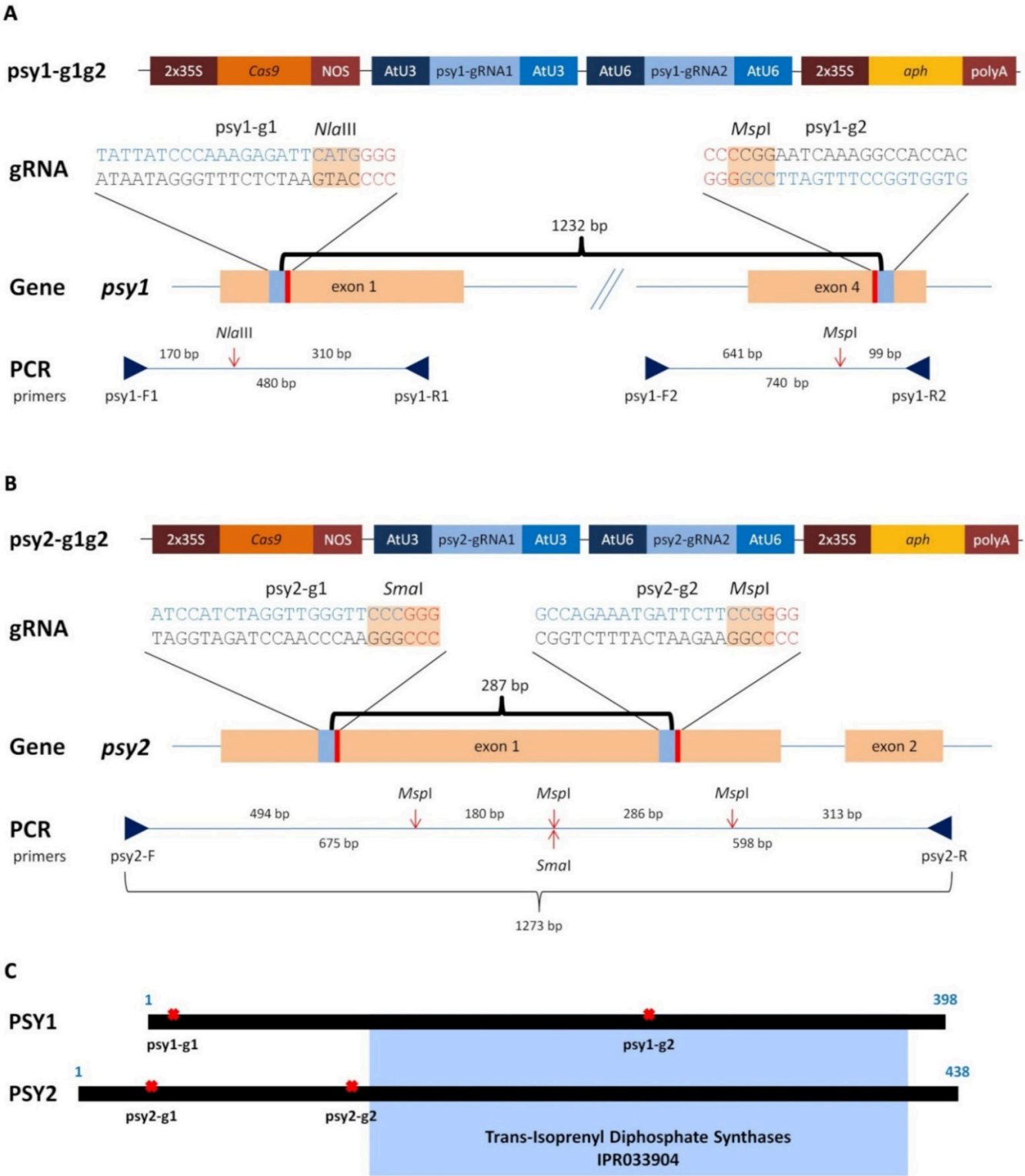

Figure 1. A scheme of Cas9 vectors (psy1-g1g2 and psy2-g1g2), each with two gRNAs (g1 and g2) targeting *psy* carrot genes and the PCR amplified fragments with primer names, restriction sites, and their lengths for (**A**) *psy1* and (**B**) *psy2*. (**C**) A linear scheme of PSY protein with the conserved domain marked in blue. The restriction sites are marked by red arrows and the gRNA:Cas9 target sites are marked by red crosses.

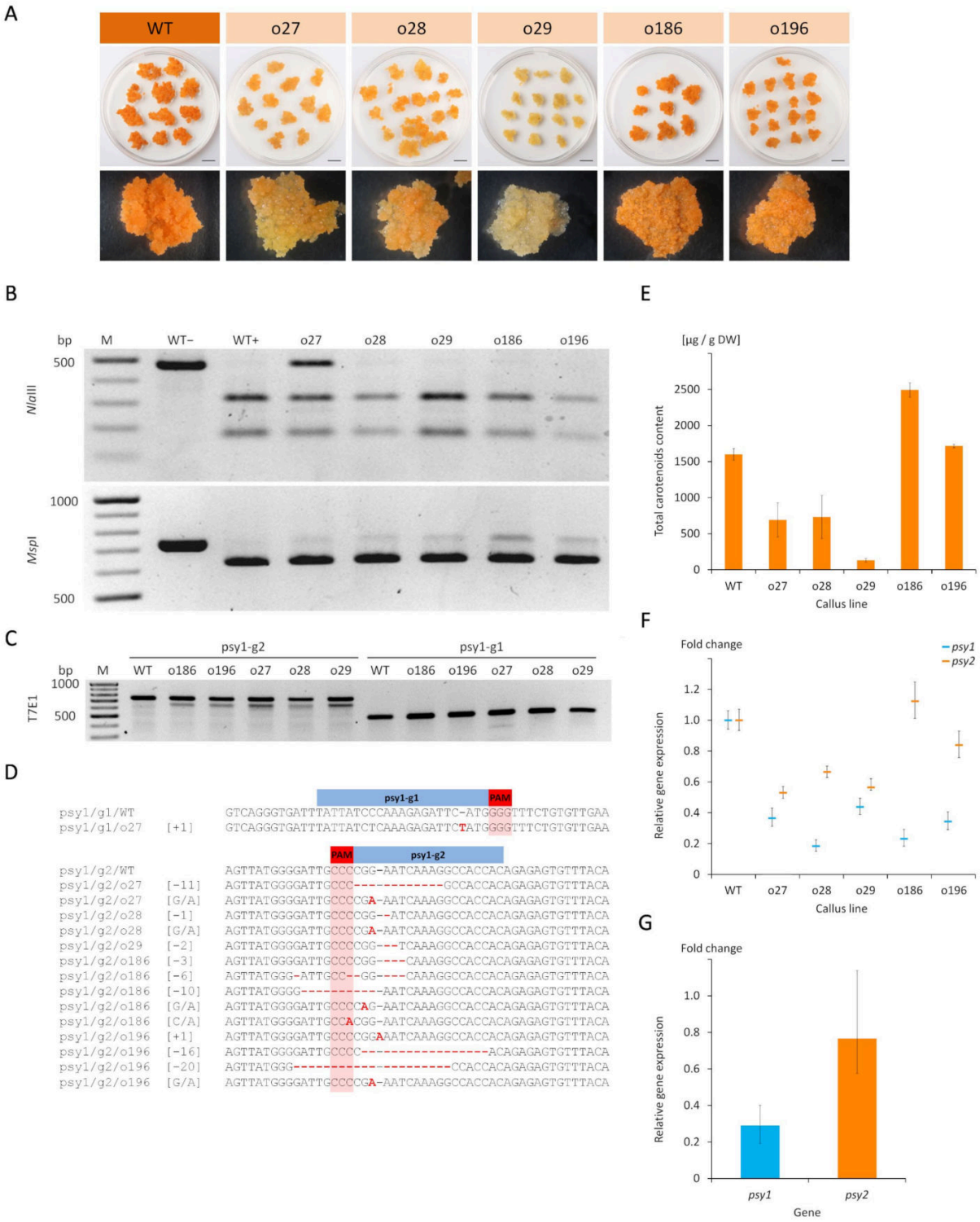

Figure 2. Carrot callus lines selected after transformation using the psy1-g1g2 vector with gRNAs targeting the *psy1* gene. (**A**) Developing callus in vitro. Separation of PCR fragments after restriction with (**B**) specific endonucleases and (**C**) T7EI enzyme. (**D**) Results of Sanger sequencing of target sites in the *psy1* gene. (**E**) Total carotenoid content. Relative *psy1* and *psy2* gene expressions in (**F**) each callus line and (**G**) the mean relative expressions. Scale bars represent 1 cm; WT–wild type callus (not transformed control) before (–) and after (+) restriction; o27-o196–transgenic callus lines; M–GeneRuler DNA Ladder Mix (Thermo Scientific, Waltham, MA, USA) marker.

Additionally, undigested products of various intensities were identified, indicating induced mutations by Cas9. The digestion of psy1-g1 amplicons using *Nla*III resulted in

an intense band of undigested product for o27 line. The digestion of psy1-g2 amplicons using *Msp*I resulted in undigested products for all samples. T7EI assay was applied to reveal mutations that might also occur at sites other than those recognised by *Nla*III or *Msp*I. For WT, amplicons treated with T7EI remained intact and were visible as single band in the gel. When the psy1-g1 amplicons were treated, an additional faint band of shorter products indicating a mutation was obtained for o27 callus. For the psy1-g2 amplicons, all samples produced a single intense band of shorter products, which were not present in WT (Figure 2C). These results indicated the occurrence of mutations caused by Cas9 at the psy1-g2 target site or at both target sites in case of o27 line.

Sanger sequencing was further used to characterise the mutations and it confirmed a single nucleotide (T) insertion at the *Nla*III restriction site in the psy1-g1 region in o27 callus (Figure 2D). All psy1-g1g2 callus lines had mutations at the psy1-g2 region. They were single nucleotide (A) insertions, C/A and G/A substitutions, and deletions ranging from −1 to −20 nt (Figure 2D). Mutations occurred at the *Msp*I restriction site and either upstream or downstream this site. Single mutation was found for o29 callus while 2−5 variants were identified for the other callus lines. In silico translation revealed that the identified single nucleotide insertion in the psy1-g1 region resulted in a reading frame shift, generating a premature stop codon at the 26 amino acid (aa) position (Supplementary Materials, Figure S1A). Indel mutations in the psy1-g2 region resulted in a premature stop codon between 258 and 269 aa or, in case of −3 nt deletion, the deletion of one amino acid at the 250 position. Nucleotide substitutions mostly resulted in amino acid change at the 249 or 250 positions. Single silent mutation was found in o186 callus. Other nonsense mutations occurred in this line as well. Hence, amino acid sequence modifications were identified in all psy1-g1g2 callus lines.

Quantitative determination of carotenoids content was then performed to confirm that callus colour variation was related to the amounts of these pigments and to the induced mutations. WT callus contained carotenoids in the amount of 1599 μg/g DW which consisted of predominantly of β- and α-carotene, and traceable amounts of xanthophylls. In the transgenic psy1-g1g2 callus, the total carotenoids content highly varied among lines ($p < 0.001$) and ranged from 131 to 2493 μg/g DW (Figure 2E). Lines o27 and o28 had reduced amounts of carotenoids by a half (43% and 46% of WT, respectively) while the o29 line had very low amounts at the level of 8% in comparison to WT. Lines o196 did not differ from WT and o186 had higher amounts of carotenoids than WT. The observed variation in callus colour from dark orange to pale orange or yellowish is thus well explained by the total carotenoid content. The different amounts of carotenoids among these transgenic lines indicate different gene knockout levels for *psy1*.

The *psy1* gene expression was considerably down-regulated ($p = 0.002$) in all callus lines and it was at the 0.19−0.46 level relative to WT (Figure 2F) with the mean of 0.29 (Figure 2G). At the same callus, the expression of *psy2* gene did not differ from WT ($p = 0.117$) with the mean relative level of 0.77 (Figure 2G). However, three lines (o27, o28, and o29) had a lower *psy2* expression than WT while for o186 and o196 the *psy2* expression remained unchanged (Figure 2(F)). There was no correlation between the *psy1* and *psy2* expressions ($r = -0.265$; $p = 0.612$). The carotenoids content did not correlate with the *psy1* expression ($r = 0.05$; $p = 0.923$) but highly correlated with the *psy2* expression ($r = 0.94$; $p = 0.006$). The consistent downregulation of *psy1*-edited lines suggests nonsense-mediated mRNA decay (NMD) may play a role in regulating *psy1* expression.

2.3. Characterisation of the psy2 Mutants

Analogously as for the *psy1* mutants, the psy2-g1g2 callus lines were characterised. The PCR amplification of DNA isolated from WT and psy2-g1g2 callus was done using primers flanking both gRNA targets and resulted in the expected 1273 bp products. Additionally, either shorter products of about 300 bp, corresponding to the 286 nt distance between psy2-g1 and psy2-g2 targets, or longer products of about 300 bp were identified for the o270 line, and the product shorter by about 80 bp was found for the o280 line. For WT

callus, the digestion of PCR products with *Sma*I resulted in two expected cleavage products. The same reaction performed for the psy2-g1g2 lines revealed the presence of the same cleaved products and a fainter band of undigested amplicons (Figure 3B). Additionally, the above listed shorter PCR products by about 80 and 300 bp were identified for the o270, o280, and o293 lines. Digestion with *Msp*I resulted in new bands for o270, o280, o298, and o306, but not for WT. Hence, products other than those observed for WT were identified for all white callus lines. The T7EI assay resulted in complex band profiles differing among callus lines, indicating diverse mutations were introduced by Cas9. Additional products ranging from 300 to 1150 bp and not distinguishable in WT were identified for all white callus lines (Figure 3C). The band profile for orange o279 callus was the same for WT, regardless which endonuclease was used. Thus, the obtained results indicated that all white callus lines were mutants.

Sequencing of PCR products confirmed mutations in both gRNA target regions (Figure 3D). Most mutations were single nucleotide insertions (A, T, or G) and deletions, also C/A and C/T substitutions were found. Deletions were either short (−1 to −4 nt) or relatively long (−27 to −82 nt). Additionally, the deletion of the whole fragment spanning between PAMs at both gRNA targets (−286 nt) was found for o270 callus. In the same callus, a duplication of this fragment also occurred. For the o270 and o293 lines, the mutations at the psy2-g1 region resulted in the occurrence of premature stop codons 3−4 aa downstream the mutation sites (Supplementary Materials, Figure S1B). For the o280 and o298 lines, the −27 to −81 nt deletions resulted in the removal of peptide fragments of 9 to 27 aa, and for o270, the −86 nt deletion caused 95 aa fragment removal and reading frame shift. Mutations generated at the psy2-g2 region resulted in the premature stop codons at the locations close to the target site. Hence, all identified mutations considerably affect PSY2 aa sequence and are likely null.

In contrast to the carotenoid-rich WT callus, the psy2-g1g2 white calli were poor in carotenoids. Two lines (o298 and o306) had very low amounts of carotenoids (28 μg/g and 16 μg/g DW, respectively) while carotenoids were hardly detected in the remaining mutants (0.5–4.0 μg/g DW) (Figure 3E).

The expression of *psy2* gene was down-regulated ($p = 0.003$) in all psy2-g1g2 callus lines. It ranged from 0.19 to 0.49 with the mean of 0.29, relative to WT (Figure 3F,G). In the same callus, the expression of *psy1* was also down-regulated ($p = 0.002$) and ranged from 0.27 to 0.48 with the mean relative expression of 0.37. The expression of both genes highly correlated to each other ($r = 0.97$; $p = 0.001$). The carotenoids content also correlated with the expression of both genes, *psy2* ($r = 0.93$; $p = 0.006$) and *psy1* ($r = 0.97$; $p = 0.001$). The downregulation of *psy2*-edited lines may be also caused by NMD. The positive correlation between the expression of *psy1* and *psy2* may suggest also their coordinated regulation.

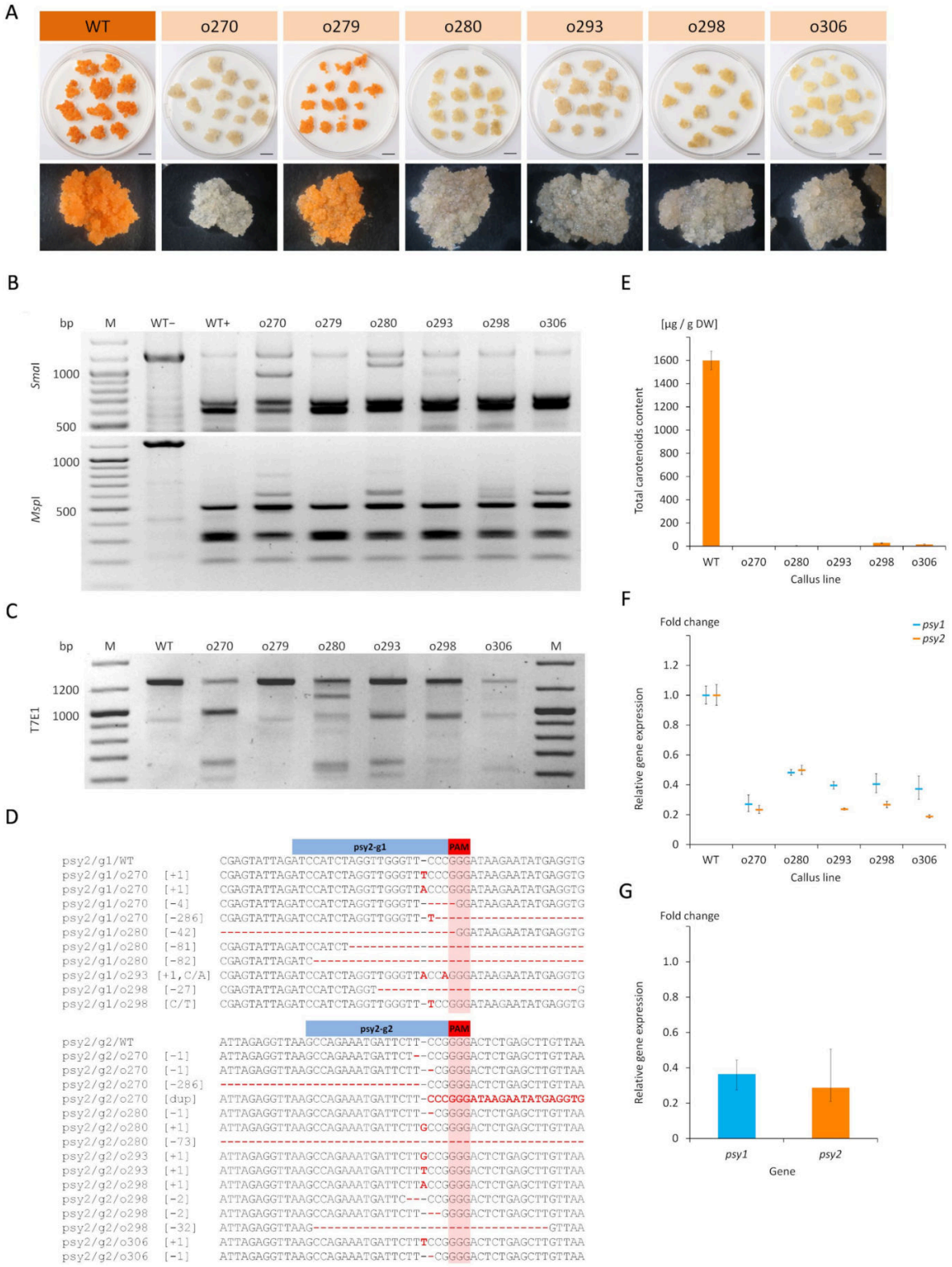

Figure 3. Carrot callus lines selected after transformation using the psy2-g1g2 vector with gRNAs targeting the *psy2* gene. (**A**) Developing callus in vitro. Separation of PCR fragments after restriction with (**B**) specific endonucleases and (**C**) T7EI enzyme. (**D**) Results of Sanger sequencing of target sites in the *psy2* gene. (**E**) Total carotenoid content. Relative *psy1* and *psy2* gene expressions in (**F**) each callus line and (**G**) the mean relative expressions. Scale bars represent 1 cm; WT−wild type callus (not transformed control) before (–) and after (+) restriction; o270-o306–transgenic callus lines; M—GeneRuler DNA Ladder Mix (Thermo Scientific) marker.

2.4. Altered Plastid Ultrastructure in the psy2 Mutants

In non-green tissues, carotenoid accumulation and plastid biogenesis are interrelated, and carotenoids are commonly deposited in crystalloid or globular chromoplasts. To elucidate the effect of the impaired carotenoid biosynthesis on plastid ultrastructure, sections of the white *psy2* mutant and orange WT calli were examined to reveal differences at histological and ultrastructural levels. These callus lines differed in plastid ultrastructure (Figure 4). The plastids in WT callus cells had a structure typical for chromoplasts in the early stages of differentiation and they contained an abundant system of internal membranes, numerous plastoglobuli, and fine vacuoles (Figure 4A). In the later stages of differentiation, the internal membrane system was also clearly visible (Figure 4B). Carotenoid crystals were present in many plastids, which developed into chromoplasts classified to the crystalline type (Figure 4C). In the *psy2* mutant callus, amyloplasts were the most frequent plastid type; they had no internal membrane system and were almost completely filled with starch (Figure 4D–F). Some cells had plastids containing starch grains accompanied by plastoglobuli and small number of internal membranes, indicating an early stage of chromoplast differentiation (Figure 4D–F and insets). Unlike plastids, the cytoplasm ultrastructure of cells in both callus lines was similar. The cytoplasm was electron dense, with numerous mitochondria, vacuoles, abundant Golgi apparatus dictyosomes and endoplasmic reticulum membranes (Figure 4).

Both callus lines were composed of dividing and parenchymatic cells (Supplementary Materials, Figure S2A,B). WT callus consisted essentially of two types of cells. Dividing cells were almost isodiametric in shape and had dense cytoplasm strongly stained with toluidine blue O (TBO), and fine vacuoles (Supplementary Materials, Figure S2A). Many of these cells were at different stages of mitosis (Supplementary Materials, Figure S2C). WT callus also consisted of cells of parenchymatic character, which were oval and had large vacuoles (Supplementary Materials, Figure S2A). Callus of *psy2* mutant consisted of cells of the same two types, but the parenchymatic cells were less common than in WT callus (Supplementary Materials, Figure S2A,B). Regardless of callus line, all dividing cells were tightly attached to each other (Supplementary Materials, Figure S2C,D) and were distinguished based on the number of nuclei, numerous small vacuoles, and mitotic figures (Supplementary Materials, Figure S2C,D). There were two to three nuclei per cell (Supplementary Materials, Figure S2D).

2.5. Altered Cell Wall Composition in the Psy2 Mutants

To reveal whether impairing carotenoid biosynthesis may induce changes in the cell wall composition, AGPs, pectins and extensin spatial distributions in callus cells were assessed. For this purpose, immunohistochemical staining was applied to reveal differences in the cell wall composition between the *psy2* mutant and WT. Low-methylesterified (detected by JIM5 antibody) and highly methylesterified (detected by JIM7 antibody) homogalacturonan (HG, pectins) were present in the cell wall of both callus lines (Figure 5; Supplementary Materials Table S1). The distribution patterns of de-esterified and esterified pectins in cell walls were different and corresponded to the carotenoid contents. Low-methylesterified pectins were abundantly present in walls of each cell in carotenoid-rich WT callus (Figure 5A) but in the white *psy2* mutant they were detected only in some cells (Figure 5B; Supplementary Materials Table S1). In contrast, fluorescence signals coming from highly esterified pectins had similar intensities in WT and mutant calli (Figure 5C,D). Additionally, in the WT callus the JIM7 epitope was present also outside the walls and in cytoplasmic compartments (Figure 5C and inset). The AGP epitopes, recognised by the JIM13 and LM2 antibodies, were abundant in WT callus while their presence in the *psy2* mutant was low (Figure 5E,H; Supplementary Materials Table S1). The extensin epitope recognised by the JIM20 antibody was not abundant, however, it was present in the walls of more cells in the *psy2* mutant than in WT (Figure 5I,J; Supplementary Materials Table S1).

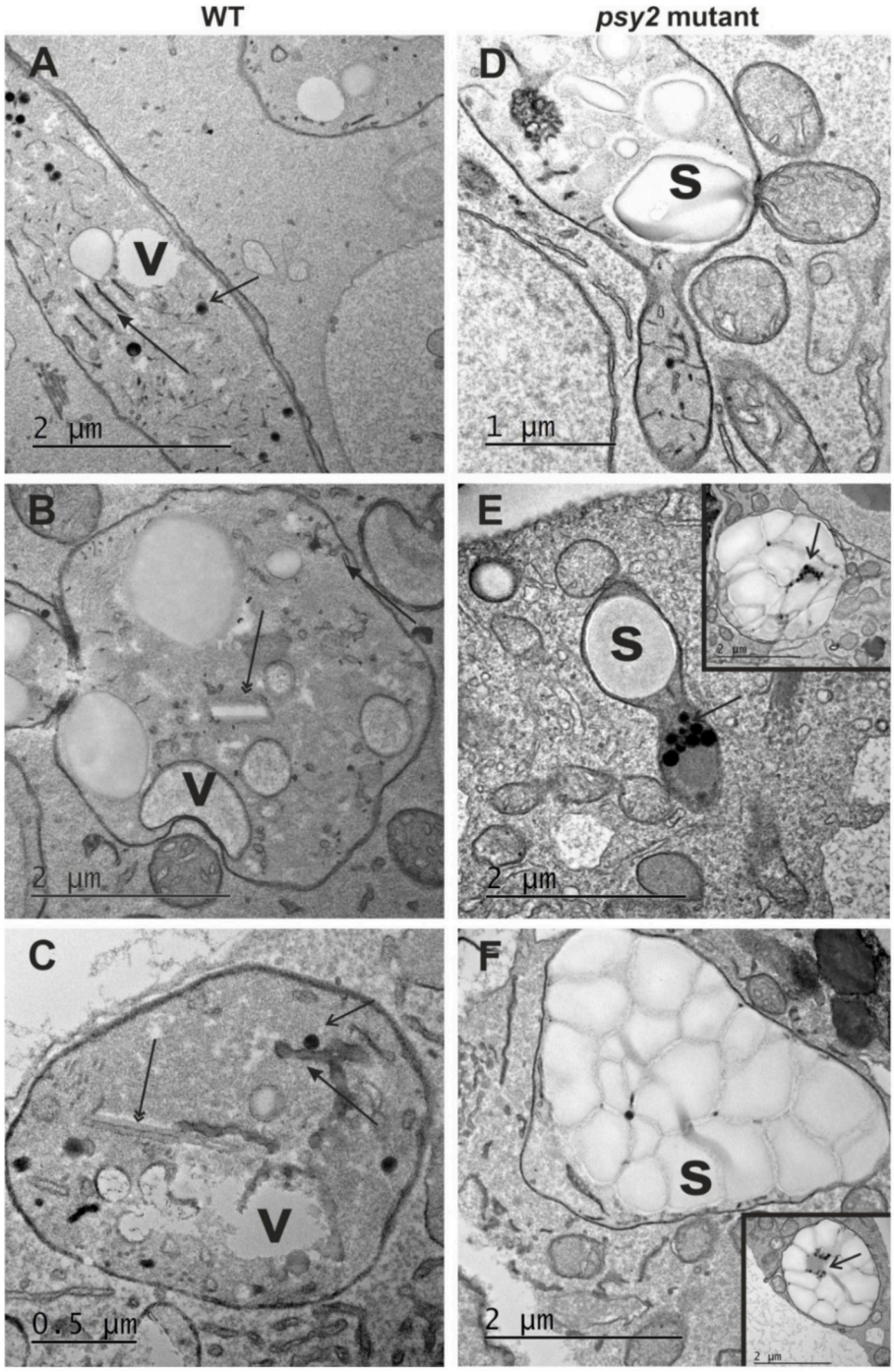

Figure 4. Plastid ultrastructure in callus cells of (**A**–**C**) the WT (not transformed control) and (**D**–**F**) *psy2* mutant. (**A**) Early stage of chromoplast differentiation in WT with plastoglobuli and internal membranes. (**B**) Chromoplast with a well visible carotene crystal. (**C**) Chromoplast with a carotene crystal, numerous plastoglobuli, internal membranes, and vacuoles. (**D**) Plastid in the *psy2* mutant callus cells with simple ultrastructure with the prominent starch grains, some plastoglobuli, and a few internal membranes. (**E**) Plastid with the single prominent starch grain and numerous plastoglobuli (inset–an example of amylochromoplast with numerous starch grains and plastoglobuli). (**F**) A plastid completely filled with starch grains surrounded by numerous mitochondria (inset–an example of plastid filled with the starch grains and numerous plastoglobuli). v-vacuole; s-starch grain; arrow-area with internal membranes; open arrow-plastoglobuli; double arrow-carotene crystal.

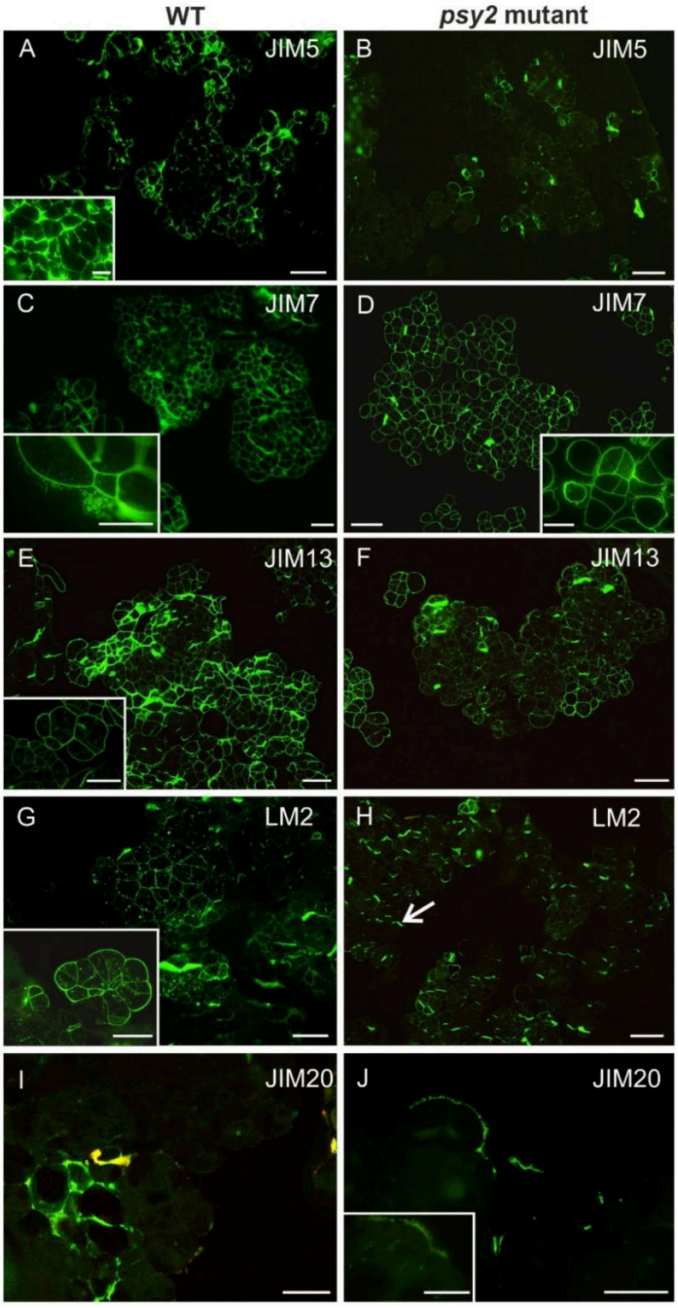

Figure 5. Distribution of pectic, AGPs, and extensin epitopes in callus cells of the WT (not transformed control) and *psy2* mutant. (**A**) The pectic epitope recognised by JIM5 antibody abundantly present in the cell walls (inset–higher magnification). (**B**) The presence of JIM5 epitope in the *psy2* mutant cells restricted only to a few cells. (**C**) JIM7 epitope present in all cells of WT (inset—higher magnification showing the presence of the epitope inside and outside the cells). (**D**) The distribution of JIM7 epitope in the *psy2* mutant cells (inset—higher magnification showing the presence of the epitope inside and outside the cells). (**E**) The presence of AGP epitope recognised by JIM13 antibody in WT cells. The epitope detected in the walls of all cells (inset—higher magnification showing the presence of the epitope also in the cytoplasmic compartments). (**F**) In *psy2* mutant cells the JIM13 epitope detected in much less amount in the cell walls in comparison to WT callus. (**G**) The AGP epitope recognised by LM2 antibody present in the walls of all cells and in the cytoplasmic compartments of WT callus (inset). (**H**) In *psy2* mutant cells this epitope detected mainly in new walls (arrow). (**I**) The extensin epitope recognised by JIM20 antibody was present only in the walls of few cells in WT callus. (**J**) In *psy2* mutant cells this epitope detected also in some cells, within the walls but also outside the walls (inset). Scale bars: (**A**–**H**) 200 μm; (I, J) 100 μm; insets 100 μm.

3. Discussion

To reveal the roles of *psy* paralogs and their effect on the accumulation of carotenoids and metabolites involved in the cell wall composition, two sets of model callus lines with mutations at either *psy1* or *psy2* have been developed in this work using CRISPR/Cas9, which has been extensively utilized for site-directed mutagenesis [37,38]. *Psy* gene knockouts were previously obtained using CRISPR/Cas in other species. In tomato, the *psy1* knockout mutants had reduced accumulation of carotenoids in petals and fruits [39,40]. In maize, *psy* mutations led to the development of albino plants and formation of white seeds [41]. In carrot, the carotenoid pathway genes were targeted using CRISPR/Cas9 [42]. The pioneering work showing CRISPR/Cas-mediated gene editing in carrot was done using callus as a model and the flavanone 3-hydroxylase gene in anthocyanin biosynthesis pathway was edited [43]. The functional mutants had altered pigmentation, including complete discolouration, thus they were identified visually. The same approach has been applied in this work where carotenoid-rich callus distinguished by a dark orange colour was used. The observed colour changes thus indicated putative *psy* knockout due to downregulation of the carotenoid pigments biosynthesis. As expected, several small callus clumps developing on the explant surfaces were light orange and those further developed on psy2-g1g2 calli were white. Visual assessment revealed that discoloured cell foci developed in prolonged culture of orange callus, indicating the occurrence of de novo mutations in non-mutated cells. Such effects of delayed editing could appear due to constitutive expression of Cas9 and gRNAs [44]. White foci were observed only for psy2-g1g2 callus, which was a visible sign of the completely inhibited accumulation of carotenoids that could result from knockout of the carotenoid pathway key genes as shown earlier for a phytoene desaturase knockout [45]. To increase the frequency of potential mutations, we introduced to callus cells two gRNAs targeting the same gene at different locations. Upon successful transformation, various *psy* mutations were identified. They occurred at one of the two gRNA target sites for each gene or at both sites, generating deletions of long DNA fragments spanning between the targets. Several methods are used for the identification of Cas-induced mutants [46]. In the first method, loss of a restriction enzyme site due to Cas9-induced mutations was used. This method, however, could not capture all targeted mutations. Hence, the T7E1 assay was used as an alternative. The T7EI assay however may remain insensitive to long deletions, does not recognise homoduplexes at mutant sites and does not reveal the nature of editing event. Thus, this assay is considered as complementary to other methods to increase the chance for detection of mutants, which were eventually revealed by Sanger sequencing [47]. Hence, the size polymorphism of *psy* restriction fragments obtained after using specific endonucleases accompanied by the T7EI assay and, finally, sequencing, collectively confirmed that the selected callus lines here contained cells with edited *psy* genes.

Long deletions spanning both upstream and downstream the *psy1* and *psy2* target sites were found while the deletion of the whole fragment (−286 nt) between gRNA1 and gRNA2 targets occurred only in the *psy2* mutant lines, probably because of a small distance between targets (<300 bp), which enables such deletions when DSBs at both sites occur simultaneously [48]. The whole fragment duplication (+286 nt) was also found as a rare event. Cas9-induced long fragment insertions and inversions have been reported [42,49]. Most of the mutations detected here resulted in the reading frame shift and the occurrence of premature stop codons. Even a single amino acid modification may affect PSY activity as it was shown in cassava where the A191D amino acid exchange increased 20-fold the carotenoid content in the root [50]. According to the InterPro database [51], the trans-isoprenyl diphosphate synthases active domain (IPR033904) between 112–379 amino acids in the carrot PSY1 has two conserved sites at 229–244 aa and 265–290 aa. In PSY2, this domain (146–413 aa) has the conserved sites at 263–278 aa and 299–324 aa. Thus, in this work, the alterations generated in the amino acid sequence at about 17 aa and 250 aa in PSY1, and, at about 39 aa and 135 aa in PSY2 occurred either upstream or within the conserved domains, which would considerably affect the structures of PSY proteins. In particular,

the presence of premature stop codons most likely led to the synthesis of truncated, non-functional proteins. Additionally, the mutants resulted in decreased expression of *psy*1 or *psy2* genes by 50−80%, with the mean reduction by 71% in comparison to WT, independent on the target gene. In consequence, the carotenoid contents were at low or only hardly detectable levels, which unambiguously indicates functional mutations, except for two *psy1* lines (o186 and o196).

The lack of carotenoids in the *psy2* mutants did not correspond with 30% transcription level, but this phenomenon can be explained by a feedback regulation. Changes in the expression levels of genes downstream the carotenoid pathway could affect *psy* expression [52]. The PSY enzyme levels may also change even when the *psy* transcript levels are not altered, indicating that the protein level is modulated by carotenoid metabolites and their precursors [53,54]. In Arabidopsis grown in the dark and in tomato, an increased PSY activity promoted post-transcriptional accumulation and activity of 1-deoxy-D-xylulose 5-phosphate synthase (DXS), the main rate-determining enzyme controlling the MEP pathway flux [53,55]. Hence, PSY activity regulates the availability of MEP pathway-derived precursors. On the other hand, it was shown that overexpression of DXS upregulates *psy1* and *psy2* expressions in carrot leaves and increases carotenoid levels in the roots of dark-grown plants [56]. Hence, the decreased *psy* transcription found in the carrot mutants in this work might be regulated by a lowered DXS level or activity. In the *psy2* mutants, the *psy2* expression decreased, so did the *psy1*, despite that psy2-gRNAs did not target the *psy1* gene. Thus, the knockout of *psy2* reduced the expression of the other paralog, which could be realised by the feedback regulation indicated above. This mechanism is, however, not equally efficient for both paralogs as in some *psy1* mutants the carotenoid level remained unaffected. Moreover, regardless of which gene was targeted, the carotenoids content correlated with the *psy2* transcript level and all *psy2* mutants did not accumulate carotenoids. Hence, *psy1* did not compensate for the absence of functional PSY2. In contrast, *psy1* mutants showed variation in carotenoid contents and only those which had high *psy2* expression were able to accumulate carotenoids in high amounts. All these suggest that the role of PSY1 can be only accessory. These results show that PSY2, but not PSY1, is critical for carotenoid biosynthesis in this callus system. Analogous relationships were shown in pepper fruits where *psy2* compensated for the absence of *psy1*, which is fruit specific in pepper [57]. The lack of carotenoids in the *psy2* mutants may also suggest that either all PSY were non-functional or post-transcriptional regulation was affected that is congruent with previous observations showing similar *psy* transcript levels in both orange and white carrot roots [29]. This can be also related to the development of chromoplasts triggered by the PSY and Orange (OR) protein interaction, also in callus [30,58,59]. A strong post-transcriptional co-regulation between PSY and OR exists in Arabidopsis as PSY overexpression increases OR level while PSY suppression decreases OR level. Additionally, OR overexpression results in higher level of active PSY protein and carotenoid content but not *psy* transcript level [60].

Carotenoid accumulation is interdependent on plastid biogenesis [5] and in the carrot storage root these compounds are synthesised and sequestered in chromoplasts. Mainly crystalloid chromoplasts were found in carrot [61,62] but small number of globular chromoplasts containing numerous plastoglobuli, with usually lipid-dissolved carotenoids, were also identified [63]. Chromoplasts develop as the result of initial proplastids differentiation to leucoplasts and amyloplasts. The latter is indicated as chromoplasts precursors [64] and, at early stages, such amylochromoplasts still contain small starch grains accompanied by globular and crystalline structures containing carotenoids [65]. In the carrots developing white roots and in young roots of orange carrots large amyloplasts were abundant while in fully developed storage orange roots amyloplasts were not observed [61]. Carrot callus which usually is poor in carotenoids also contains many amyloplasts. In this work, the dark-orange callus with enhanced carotenoid biosynthesis was used, which has additional amylochromoplasts and crystaloid chromoplasts that are the dominating plastid type [34]. Hence, a transition of amyloplast to chromoplasts has been proposed as a hypothetical route during storage root development. The ultrastructure analysis of WT and the *psy2*

mutant callus lines in this work provides further evidence supporting this hypothesis as the disturbance in the carotenoid metabolic pathway induced ultrastructural changes of chromoplasts. In WT callus, the chromoplasts were abundant and were represented mostly by the crystalline type as described earlier for this callus line [34] and their ultrastructure had typical organisation, like the one described for carrot root [22,66]. In contrast, in the *psy2* mutant cells the starch-filled plastids were found instead of chromoplasts. Therefore, these cells contained large amyloplasts similar to the cells in the white carrot root [61]. Only some cells had plastids with fragmented internal membranes and a few plastoglobuli coexisting with starch grains. Such organisation indicates an early stage of chromoplast differentiation. The *psy2* mutant cells had no visible pigmentation but the *psy* gene expression occurred at a low level and small amounts of carotenoids were found. The observations of the ongoing transition of amyloplasts to amylochromoplasts in some cells additionally supports the expected plastid differentiation route as the requirement for carotenoids biosynthesis and further sequestration. However, the lack of later stages of chromoplast development indicates that the amounts of carotenoids were insufficient to complete amylochromoplast transition. The presence of plastoglobuli may indicate that at first carotenoids are bound to lipids, and crystals are sequestered only when there is an excess of carotenoids. Such interpretation is in accordance with results presented earlier [34]. It is worth noting that the ultrastructure of plastids in the carotenoid-rich WT dark orange callus resembles the ultrastructure of plastids in orange carrot roots [34] while the ultrastructure of plastids in the carotenoid-free (carotenoid-poor) *psy2* mutant callus resembles the ultrastructure of plastids in white carrot roots [61] where carotenoid biosynthesis pathway is non-functional. Therefore, developed callus seems a valuable model system for further elucidation of carotenogenesis and plastid biogenesis, and their regulation, and their effects on other biochemical processes.

The biosynthesis of carotenoids and polysaccharides depends on the same carbon source but their interrelations are more complex. Changes in the *psy* activity may induce modifications in the cell metabolism. In tobacco, the silencing of *psy1* and *psy2* genes not only markedly decreased the carotenoid biosynthesis but also affected pathways that are involved mainly in the biosynthesis of cell wall components, and the expression of glucan, cellulose, pectin, and galacturonan genes [11]. Suppression of carotenoid metabolism in tomato led to downregulation of genes encoding major cell wall catabolic enzymes and increased fruit firmness [67]. Overexpression of the *SlNAC1* transcription factor in tomato lowered lycopene and total carotenoid contents and influenced cell wall enzymes leading to the increased fruit softening during their ripening. Hence, it was postulated that cell wall components were metabolised via an ABA-dependent pathway [68]. Additionally, the overexpression of *LCYb* gene in tomato resulted in the enhanced metabolism of lycopene to β-carotene and in the increase of ABA content what was linked with extended fruit shelf life [9]. Gene ontology analysis revealed that several genes involved in cell wall organisation and hydrolase activity of *O*-glycosyl compounds were upregulated also in soybean containing the insertion of *psy* overexpressing construct [10]. The *yellow-fruited tomato 1* (*yft1*) mutant, which fruit contained only 6% of the total carotenoids of that of the wild type cultivar, had delayed chromoplast development and a modified cell wall composition [69,70]. Such co-occurring changes in *yft1* resulted from a mutation in an ethylene-insensitive 2 protein, a core factor for the ethylene signal transduction connecting these processes and carotenoid accumulation [71] but there was no evidence for a direct link between carotenoid biosynthesis and wall composition. A negative correlation was noted between the cell wall thickness and total carotenoid content in segment membranes and sac membranes in grapefruit [72]. Additionally, the fungal cell wall was modified when exposed to carrot extract, in particular lutein induced α-1,3-glucan accumulation [73]. These reports collectively indicate that regulation of carotenoid biosynthesis may affect structural changes in the cell wall although the spatial distribution of wall components in relation to the carotenoid biosynthesis has not been shown so far. In this work, immunohistological data show alterations in the wall composition. Apparently, the

differences in the presence of chosen pectic, AGPs, and extensin epitopes occurred between the carotenoid-rich control and the carotenoid-free *psy2* knockout mutant. Among analysed pectic epitopes, low-esterified pectins were less represented in the walls of the *psy2* mutant cells in comparison to WT, but the presence of highly esterified pectins was not affected by the *psy2* gene knockout. This may mean that the changes in carotenoids synthesis affect the degree of pectin de-esterification; however, the signalling pathway between the carotenoid synthesis and pectin modifying enzymes is not yet known. Pectins are the major group of primary wall polymers [74,75] responsible for wall porosity, adhesion, binding of ions, and mechanical properties of cell walls, including elasticity [75]. Pectin methylesterase activity can increase or decrease the degree of calcium-cross linking of homogalacturonan molecules, thus modifying the wall stiffness in different degree [76,77]. Since the inhibition of carotenoid biosynthesis restricts pectin de-esterification, it can be concluded that the lower degree of highly esterified pectins may indicate the reduced cell wall stiffness as described for various plant organs [77,78]. Moreover, the increased level of pectins with a low degree of methylation was detected in *LCYb*-overexpressing tomato fruits, indicating that their increased level was associated with enhanced carotene biosynthesis [9]. The presented results, showing the relationship between carotenoid synthesis and the pectins modifications, are in agreement with the widely accepted opinion that changes in the methylesterification status of pectins are related to the cell wall remodelling that occurs during diverse plant developmental processes and in reaction to biotic and abiotic factors [79,80].

Arabinogalactan proteins (AGPs) belong to subfamily of hydroxyproline-rich glycoproteins (HRGPs; [81,82]). They are believed to be present in each plant cell including cellular compartments such as wall, plasma membrane, and membranes inside of the cell [83,84]. Involvement of AGPs in many developmental processes, such as signal transduction pathways, cell growth and differentiation, programmed cell death, and hormone responses are well documented [85–87]. Moreover, AGPs are believed to be involved in the plant response to a wide range of biotic and abiotic stresses [88,89]. Spatial distribution of analysed AGPs epitopes in this work suggests that knocking out the *psy2* gene considerably affected the presence of LM2 and JIM13 epitopes. Such results are in accordance with the literature data indicating that changes in AGP presence are the manifestation of reaction of cells to changes in cell metabolism. The LM2 antibody detects the AGPs epitope that contains glucuronic acid (GlcA) residues [90]. Our research shows that the LM2 epitope is less represented in the walls of cells from the *psy2* mutant. Analogous occurrence was detected for the JIM13 epitope (which contains β-D-GlcpA-(1→3)-α-D-GalpA-(1→2)-L-Rha residues). This indicates that, at least for these two AGP epitopes, the blocking of carotenoid biosynthesis results in the decrease of AGPs synthesis. Undoubtedly, impaired biosynthesis of carotenoids is a stress factor for the cell. Considering that changes in AGPs contents are the cell response to biotic and abiotic factors [83], the obtained results here are not surprising. However, we showed for the first time that alterations in carotenoid biosynthesis are related to cell wall remodelling, which was visualised directly in the cell walls with the use of immunohistochemistry method. Furthermore, some changes in gene expression and protein synthesis in soybean that were connected to carotenoid biosynthesis were detected for fascilin-like AGP [10]. Our study presents another data that indicate a correlation between AGPs presence and carotene biosynthesis.

Extensins are another group of hydroxyproline-rich glycoproteins, which are structural cell wall proteins characterised by the presence of Ser-Pro2–n repeats (for review see [91]). These proteins are common in different species (for review see [92]), including carrot [93,94]. Extensins can occur not only in the cell wall matrix, but also in intercellular spaces [92]. Recently, they have been found in extracellular layer covering callus cells [95]. In the present work, the JIM20 extensin epitope was found in callus cells of both, the control and the *psy2* mutant, but only in a few cells. The only difference between the control and mutant was the spatial JIM20 distribution. In the control the extensin epitopes were detected in the walls, and in the mutant the epitopes were present in the extracellular matrix that covered

cell aggregates. Callus of the control and the *psy2* mutants differed not only in terms of cell types but also in deposition of extracellular material on the outer walls of peripheral callus cells, which was more pronounced in mutant. The occurrence of extensins in extracellular material may point to different callus competence, what was found for *Actinidia arguta* [96]. Moreover, the involvement of extensins in the development of carrot protoplast-derived cells was also described [97].

4. Materials and Methods

4.1. Plant Material

Callus obtained from roots of the DH1 plants described earlier and characterised by a dark-orange colour due to high accumulation of carotenoids was used [34]. Callus was maintained in Petri dishes on the BI medium (Gamborg B5 mineral medium with vitamins, supplemented with 1 mg/L 2,4-dichlorophenoxyacetic acid, 0.0215 mg/L kinetin and 30 g/L sucrose; pH 5.8; solidified with 2.7% Phytagel) at 26 °C in the dark and was subcultured every 3 weeks to a fresh medium.

4.2. Vector Construction

Two pairs of gRNAs were designed to target the *psy1* (GeneBank Gene ID: 108227339) and *psy2* (GeneBank Gene ID: 108214656) genes based on a reference ASM162521v1 primary assembly of the DH1 carrot genome. Each gRNA was verified not to target another *psy* paralog and other genes in the DH1 carrot genome using the Cas-OFFinder online tool [98]) with default settings. Two plasmid vectors (psy1-g1g2 and psy2-g1g2) were created (Figure 1A,B); each of them contained in the T-DNA region a pair of gRNAs under the control of AtU3 (gRNA1) and AtU6 (gRNA2) promoters, the *Cas9* gene driven by the double 35S CaMV promoter, and the *aph* hygromycin resistance gene also driven by the double 35S promoter. The psy1-g1g2 vector contained gRNA1 (psy1-g1: TATTATCCCAAAGAGATTCATG) complementary to exon 1 in the carrot *psy1* gene and gRNA2 (psy1-g2: GTGGTGGCCTTTGATTCCG) complementary to exon 4 (Figure 1A). The psy2-g1g2 vector contained two gRNAs complementary to exon 1 of the *psy2* gene, gRNA1 (psy2-g1: ATCCATCTAGGTTGGGTTCCC) and gRNA2 (psy2-g2: GCCAGAAATGATTCTTCCG) (Figure 1B). All gRNAs were designed to target sites adjacent to GGG-PAM located either upstream (gRNA1) or within (gRNA2) the region coding for the protein active domain (Figure 1C). Vectors were assembled according to [99] and introduced into *Agrobacterium tumefaciens* LBA4404 strain by electroporation [100].

4.3. Agrobacterium-Mediated Callus Transformation

Agrobacterium-mediated transformation of carrot callus was done as described previously [43]. Briefly, callus clumps of about 5 mm in diameter were immersed for 20 min in *A. tumefaciens* inoculum composed of the BI medium supplemented with 100 µM acetosyringone with OD_{600} adjusted to 0.5. After three days of co-cultivation, callus was rinsed with 800 mg/L cefotaxime and 400 mg/L timentin mixture and cultured on the BI medium supplemented with these antibiotics at concentrations lowered to a half. Putative transformants were selected after three-month culture on the BI medium supplemented with 25 mg/L hygromycin.

4.4. Molecular Identification of Mutants

Genomic DNA extraction, PCR, digestion of amplified fragments with restriction enzymes, cloning and sequencing were performed essentially as described previously [43]. To confirm the presence of T-DNA in putatively transgenic callus, PCR primers matching *aph* and *Cas9* genes were used while the amplification of *psy* gene fragments was obtained using primer pairs flanking either single gRNA targets in the *psy1* gene or both gRNA target sites in the *psy2* gene (Supplementary Materials, Table S2). To detect mutations at 1−4 nucleotides upstream PAM within gRNA targets, the amplified *psy* gene fragments were digested using specific endonucleases recognising restriction sites at these

sites (Figure 1A,B). Additionally, the T7 endonuclease I (T7EI) assay was performed to detect mutations that might occur outside restriction sites recognised by the above said enzymes. For this purpose, 4 µL of PCR reaction obtained using Phusion™ High–Fidelity DNA Polymerase (ThermoScientific, Waltham, MA, USA) were incubated with 0.3 µl T7 endonuclease I (New Englands BioLabs, Ipswich, MA, USA) at 37 °C for 25 min, following hybridization according to manufacturer's instruction. The reaction was stopped by the addition of 1.5 µl of 0.25 M EDTA. Products of PCR and cleavage were visualised after electrophoresis in a 2% agarose gel containing MidoriGreen Advance (Nippon Genetics, Tokyo, Japan). Undigested fragments by specific endonucleases were purified and cloned (5−7 clones per callus line) before Sanger sequencing, for which the Sp6 standard primer was used. Reads were manually aligned to the reference gene sequences.

4.5. Determination of Carotenoids Content

The whole plate of freshly grown callus was lyophilized and ground in a mortar. Extraction was done using ethanol:*n*-hexane (1:1, *v:v*). Extracts were filtered through a sintered glass funnel (G4) before analysis. A high-performance liquid chromatography (HPLC) was performed using the Shimadzu LC–20AD chromatograph equipped with a C18 RP (5 µm) column and the Shimadzu SPDM–20A–DAD photodiode–array detector. The signal detection was set in the wavelengths range of 300–700 nm. The separation was carried out at 25 ± 1 °C using the solvents: (A) 5% water in methanol, (B) methanol, (C) 10% *n*-hexane in acetonitrile). All solvents were ultra pure (Sigma–Aldrich, St. Louis, MO, USA). The identification of β-carotene was based on the retention time of the standard (Sigma–Aldrich, St. Louis, MO, USA) and confirmed by analysis of absorption spectra. The identification of α-carotene and xanthophylls was based on the analysis of the absorption spectra. Quantification of β-carotene was done using a standard curve, while α-carotene and xanthophylls were quantified in relation to β-carotene. The analysis was performed in three biological replicates for each callus line.

4.6. Gene Expression Analysis

RNA isolation and gene expression analysis was performed using a real-time quantitative PCR as described previously [34]. Primers were designed to amplify fragments of exon 5 and exon 4 in *psy1* and *psy2* genes, respectively (Supplementary Materials, Table S2). Normalization was done to the expression of the actin gene. Gene expression analysis was performed for the control and each of ten selected mutant lines, using mixed samples from five callus clumps.

4.7. Light Microscopy

For the histochemical analyses, the samples were fixed in a solution of 3% (*w/v*) paraformaldehyde (PFA), 1% (*v/v*) glutaraldehyde (GA) and 1% sucrose (*w/v*) in phosphate buffered saline (PBS) at pH 7.0, embedded in Steedman's wax [95]. The sections (7-µm thick) were cut using a HYRAX M40 rotary microtome (Zeiss, Oberkochen, Germany) and collected on microscopic slides. Sections were stained with 0.1% toluidine blue O (TBO; Sigma-Aldrich, St. Louis, MO, USA) in PBS and examined under the Olympus BX45 microscope equipped with the Olympus XC50 digital camera.

4.8. Fluorescence Microscopy

For immunohistochemistry, samples were proceeded as described earlier [101]. Briefly, samples were fixed in a mixture of 4% formaldehyde and 1% glutaraldehyde (pH 7.2) at 4 °C for 24 h, then washed in PBS (pH 7.2), dehydrated in a graded ethanol series, infiltrated in LR White resin (medium grade, Polysciences, Eppelheim, Germany). Finally, they were embedded in gelatine capsules with fresh LR White resin and polymerized at 50 °C for 8 h. Semi-thin sections (0.5–1 µm) were cut using the Leica EM UC6 ultramicrotome (Leica Microsystems, Wetzlar, Germany) and mounted on poly-L-lysine coated microscope slides

(Menzel-Glaser, Braunschweig, Germany). Primary antibodies used in the study are listed in Table 1.

Table 1. Primary antibodies used for the detection of cell wall components.

Wall Constituents	Antibody	Epitope	References
Pectins	JIM5	Low methyl-esterified HG	[102]
	JIM7	Highly methyl-esterified HG	[102]
AGPs	LM2	β-D-GlcpA	[90] [103]
	JIM13	β-D-GlcpA-(1→3)-α-D-GalpA-(1→2)-L-Rha	[104] [103]
Extensins	JIM20	Extensin/HRGP glycoprotein	[105]

Abbreviations: HG—homogalacturonan, GlcA—glucuronic acid, GalA—galacturonic acid, Rha—rhamnose, HRGP—hydroxyproline-rich.

4.9. Transmission Electron Microscopy (TEM)

Samples were fixed in 3% glutaraldehyde in a 50 mM cacodylate buffer (Serva, Heidelberg, Germany; pH 7.0) at 4 °C for 24 h. Then, samples were washed three times in cacodylate buffer and post-fixed with 1:1 (*v*/*v*) mixture of 3% potassium ferrocyanide in cacodylate buffer and 4% solution of osmium tetroxide (Serva, Heidelberg, Germany) for 1 h. Samples were washed three times in dH_2O and incubated in 1% solution of thiocarbohydrazide (Sigma-Aldrich, St. Louis, MO, USA) at 60 °C for 20 min. Next, samples were post-fixated in 1% aqueous osmium tetraoxide at room temperature for 30 min, rinsed three times in dH_2O, and incubated overnight in 1% aqueous uranyl acetate at 4 °C. The samples were then rinsed three times (each 5 min) in dH_2O and put into a freshly prepared Walton's lead aspartate for 30 min at 60 °C, washed five times (each 3 min) in dH_2O, dehydrated in graded ethanol series, and in the mixture of 99.8% ethanol and propylene oxide (1:1 *v*/*v*, 15 min), and propylene oxide (2 × 15 min) and gradually embedded in Epon resin (Poly/Bed 812; Polysciences, Eppelheim, Germany). Ultrathin sections of 70 nm thick were cut with the use of the Leica EM UC6 ultramicrotome and collected onto carbon-coated copper grids (200 mesh, Electron Microscopy Science, Hatfield, PA, USA). Samples were analysed in the Jeol JEM-3010 HRTEM (300 kV) equipped with an EDS (Energy Dispersive Spectrometry, IXRF Systems Inc., Austin, TX, USA) spectrometer and a 2 k × 2 k Orius 833 SC200D CCD camera (Gatan, Pleasanton, CA, USA).

4.10. Statistical Analysis

The effect of *psy1* and *psy2* gene mutations on carotenoid content in callus was verified by applying one-way analysis of variance followed by the multiple comparison Tukey's test at the significance level $p = 0.05$. Person linear correlation was calculated to reveal relationship between gene expression and carotenoids content. Data were analysed using the Statistica v13 software (TIBCO; Palo Alto, CA, USA). Relative gene expression was calculated using the REST 2009 (Qiagen, Hilden, Germany) software.

5. Conclusions

In this work, we have successfully knocked out two carrot *psy* genes using CRISPR/Cas9 system and studied the effect of the induced mutations on carotenoids accumulation, plastid ultrastructure, and the cell wall composition. We used callus as a model system that is characterised by high carotenoid content and gene expression levels resembling those observed in the carrot root. The results indicate differential roles and regulation of *psy* paralogs, with *psy2* being critical for carotenoid biosynthesis in this model. Moreover, *psy2* knockout reduced the expression of the *psy1* paralog, which could be explained by the metabolite feedback regulation. Whether, or to what extent, *psy1* contributes to carotenogenesis in callus remains unclear as there was no correlation between its expression level and carotenoid content when *psy2* was active. To the best of our knowledge, it was also demonstrated for the first time

that the impaired biosynthesis of carotenoids interrelates with cell wall remodelling, which is manifested by changes in the composition of pectins and AGPs within the wall. Thus, this work presents that a relationship exists between the cell wall and carotenoid metabolisms, and that the dark orange callus may serve as a usable model for basic genomic studies as well as cell metabolism related to carotenogenesis. Further research should be commenced to reveal these relationships in fully developed plants.

Supplementary Materials: The following are available online at https://www.mdpi.com/article/10.3390/ijms22126516/s1, Figure S1: Amino acid sequences of PSY in the wild type and mutant lines, Figure S2: Morphology and structure of the wild type and *psy2* mutant callus, Table S1: Primers used for PCR and qPCR, Table S2: Cellular epitopes localization and degree of their occurrence within the callus of different lines.

Author Contributions: Conceptualization, T.O., M.K.-C., E.K. and R.B.; methodology, T.O., M.K.-C., K.G.-J., K.S., A.M.-H., Y.Q. and R.B.; formal analysis, T.O., E.K. and R.B.; investigation, T.O., M.K.-C., M.K., K.G.-J., K.S., A.M.-H. and R.B.; resources, T.O. and R.B.; data curation, T.O. and R.B.; writing—original draft preparation, T.O., K.S., E.K. and R.B.; writing—review and editing, E.K. and R.B.; visualization, T.O., M.Z., K.S., A.M.-H. and K.G.-J.; supervision, E.K. and R.B.; project administration, R.B.; funding acquisition, M.K.-C. and R.B. All authors have read and agreed to the published version of the manuscript.

Funding: This research was funded by the National Science Centre in Poland (grant No. 2013/09/B/NZ9/02379).

Institutional Review Board Statement: Not applicable.

Informed Consent Statement: Not applicable.

Data Availability Statement: Not applicable.

Acknowledgments: Tomasz Oleszkiewicz received financial support as part of a doctoral scholarship granted by the National Science Centre in Poland (Etiuda No. 2019/32/T/NZ9/00463).

Conflicts of Interest: The authors declare no conflict of interest.

References

1. Rosas-Saavedra, C.; Stange, C. Biosynthesis of carotenoids in plants: Enzymes and color. In *Carotenoids in Nature: Biosynthesis, Regulation and Function*; Stange, C., Ed.; Springer International Publishing: Cham, Switzerland, 2016; pp. 35–69. [CrossRef]
2. Eggersdorfer, M.; Wyss, A. Carotenoids in human nutrition and health. *Arch. Biochem. Biophys.* **2018**, *652*, 18–28. [CrossRef]
3. Nisar, N.; Li, L.; Lu, S.; Khin, N.C.; Pogson, B.J. Carotenoid metabolism in plants. *Mol. Plant* **2015**, *8*, 68–82. [CrossRef] [PubMed]
4. Sun, T.; Yuan, H.; Cao, H.; Yazdani, M.; Tadmor, Y.; Li, L. Carotenoid metabolism in plants: The role of plastids. *Mol. Plant* **2018**, *11*, 58–74. [CrossRef] [PubMed]
5. Egea, I.; Barsan, C.; Bian, W.; Purgatto, E.; Latché, A.; Chervin, C.; Bouzayen, M.; Pech, J.-C. Chromoplast differentiation: Current status and perspectives. *Plant Cell Physiol.* **2010**, *51*, 1601–1611. [CrossRef] [PubMed]
6. Schweiggert, R.M.; Carle, R. Carotenoid deposition in plant and animal foods and its impact on bioavailability. *Crit. Rev. Food Sci.* **2017**, *57*, 1807–1830. [CrossRef] [PubMed]
7. Chen, K.; Li, G.-J.; Bressan, R.A.; Song, C.-P.; Zhu, J.-K.; Zhao, Y. Abscisic acid dynamics, signaling, and functions in plants. *J. Integr. Plant Biol.* **2020**, *62*, 25–54. [CrossRef]
8. Faizan, M.; Faraz, A.; Sami, F.; Siddiqui, H.; Yusuf, M.; Gruszka, D.; Hayat, S. Role of strigolactones: Signalling and crosstalk with other phytohormones. *Open Life Sci.* **2020**, *15*, 217–228. [CrossRef] [PubMed]
9. Diretto, G.; Frusciante, S.; Fabbri, C.; Schauer, N.; Busta, L.; Wang, Z.; Matas, A.J.; Fiore, A.; Rose, J.K.C.; Fernie, A.R.; et al. Manipulation of β-carotene levels in tomato fruits results in increased ABA content and extended shelf life. *Plant Biotechnol. J.* **2020**, *18*, 1185–1199. [CrossRef]
10. Qin, Y.; Woo, H.-J.; Shin, K.-S.; Lim, M.-H.; Lee, S.-K. Comparative transcriptome profiling of different tissues from beta-carotene-enhanced transgenic soybean and its non-transgenic counterpart. *Plant Cell Tiss. Organ. Cult.* **2020**, *140*, 341–356. [CrossRef]
11. Wang, Z.; Zhang, L.; Dong, C.; Guo, J.; Jin, L.; Wei, P.; Li, F.; Zhang, X.; Wang, R. Characterization and functional analysis of phytoene synthase gene family in tobacco. *BMC Plant Biol.* **2021**, *21*, 32. [CrossRef]
12. Ramirez, V.; Xiong, G.; Mashiguchi, K.; Yamaguchi, S.; Pauly, M. Growth-and stress-related defects associated with wall hypoacetylation are strigolactone-dependent. *Plant Direct* **2018**, *2*, 1–11. [CrossRef] [PubMed]
13. Ruiz-Sola, M.A.; Rodriguez-Concepcion, M. Carotenoid biosynthesis in Arabidopsis: A colorful pathway. *Arabidopsis Book* **2012**, *10*, e0158. [CrossRef] [PubMed]

14. Liang, M.-H.; Zhu, J.; Jiang, J.-G. Carotenoids biosynthesis and cleavage related genes from bacteria to plants. *Crit. Rev. Food Sci.* **2018**, *58*, 2314–2333. [CrossRef] [PubMed]
15. Giuliano, G. Plant carotenoids: Genomics meets multi-gene engineering. *Curr. Opin. Plant Biol.* **2014**, *19*, 111–117. [CrossRef] [PubMed]
16. Goo, Y.-M.; Kim, T.-W.; Ha, S.-H.; Back, K.-W.; Bae, J.-M.; Shin, Y.-W.; Lee, C.-H.; Ahn, M.-J.; Lee, S.-W. Expression profiles of genes involved in the carotenoid biosynthetic pathway in yellow-fleshed potato cultivars (*Solanum tuberosum* L.) from South Korea. *J. Plant Biol.* **2009**, *52*, 49–55. [CrossRef]
17. Bartley, G.E.; Viitanen, P.V.; Bacot, K.O.; Scolnik, P.A. A tomato gene expressed during fruit ripening encodes an enzyme of the carotenoid biosynthesis pathway. *J. Biol. Chem.* **1992**, *267*, 5036–5039. [CrossRef]
18. Bartley, G.E.; Scolnik, P.A. cDNA cloning, expression during development, and genome mapping of PSY2, a second tomato gene encoding phytoene synthase. *J. Biol. Chem.* **1993**, *268*, 25718–25721. [CrossRef]
19. Stauder, R.; Welsch, R.; Camagna, M.; Kohlen, W.; Balcke, G.U.; Tissier, A.; Walter, M.H. Strigolactone levels in dicot roots are determined by an ancestral symbiosis-regulated clade of the PHYTOENE SYNTHASE gene family. *Front. Plant Sci.* **2018**, *9*, 255. [CrossRef]
20. Qin, X.; Coku, A.; Inoue, K. Expression, subcellular localization, and *cis*-regulatory structure of duplicated phytoene synthase genes in melon (*Cucumis melo* L.). *Planta* **2011**, *234*, 737–748. [CrossRef] [PubMed]
21. Llorente, B.; Martinez-Garcia, J.F.; Stange, C.; Rodriguez-Concepcion, M. Illuminating colors: Regulation of carotenoid biosynthesis and accumulation by light. *Curr. Opin. Plant Biol.* **2017**, *37*, 49–55. [CrossRef]
22. Maass, D.; Arango, J.; Wust, F.; Beyer, P.; Welsch, R. Carotenoid crystal formation in Arabidopsis and carrot roots caused by increased phytoene synthase protein levels. *PLoS ONE* **2009**, *4*, e6373. [CrossRef] [PubMed]
23. Iorizzo, M.; Ellison, S.; Senalik, D.; Zeng, P.; Satapoomin, P.; Huang, J.; Bowman, M.; Iovene, M.; Sanseverino, W.; Cavagnaro, P.; et al. A high-quality carrot genome assembly provides new insights into carotenoid accumulation and asterid genome evolution. *Nat. Genet.* **2016**, *48*, 657–666. [CrossRef]
24. Fuentes, P.; Pizarro, L.; Moreno, J.C.; Handford, M.; Rodriguez-Concepcion, M.; Stange, C. Light-dependent changes in plastid differentiation influence carotenoid gene expression and accumulation in carrot roots. *Plant Mol. Biol.* **2012**, *79*, 47–59. [CrossRef]
25. Bowman, M.J.; Willis, D.K.; Simon, P.W. Transcript abundance of phytoene synthase 1 and phytoene synthase 2 is associated with natural variation of storage root carotenoid pigmentation in carrot. *J. Am. Soc. Hortic. Sci.* **2014**, *139*, 63–68. [CrossRef]
26. Wang, H.; Ou, C.-G.; Zhuang, F.-Y.; Ma, Z.-G. The dual role of phytoene synthase genes in carotenogenesis in carrot roots and leaves. *Mol. Breed.* **2014**, *34*, 2065–2079. [CrossRef] [PubMed]
27. Perrin, F.; Hartmann, L.; Dubois-Laurent, C.; Welsch, R.; Huet, S.; Hamama, L.; Briard, M.; Peltier, D.; Gagné, S.; Geoffriau, E. Carotenoid gene expression explains the difference of carotenoid accumulation in carrot root tissues. *Planta* **2017**, *245*, 737–747. [CrossRef]
28. Simpson, K.; Fuentes, P.; Quiroz-Iturra, L.F.; Flores-Ortiz, C.; Contreras, R.; Handford, M.; Stange, C. Unraveling the induction of phytoene synthase 2 expression by salt stress and abscisic acid in *Daucus carota*. *J. Exp. Bot.* **2018**, *69*, 4113–4126. [CrossRef]
29. Clotault, J.; Peltier, D.; Berruyer, R.; Thomas, M.; Briard, M.; Geoffriau, E. Expression of carotenoid biosynthesis genes during carrot root development. *J. Exp. Bot.* **2008**, *59*, 3563–3573. [CrossRef]
30. Kim, S.H.; Ahn, Y.O.; Ahn, M.-J.; Jeong, J.C.; Lee, H.-S.; Kwak, S.-S. Cloning and characterization of an Orange gene that increases carotenoid accumulation and salt stress tolerance in transgenic sweetpotato cultures. *Plant Physiol. Biochem.* **2013**, *70*, 445–454. [CrossRef]
31. Schaub, P.; Rodriguez-Franco, M.; Cazzonelli, C.I.; Álvarez, D.; Wüst, F.; Welsch, R. Establishment of an Arabidopsis callus system to study the interrelations of biosynthesis, degradation and accumulation of carotenoids. *PLoS ONE* **2018**, *13*, e0192158. [CrossRef]
32. Baranska, M.; Baranski, R.; Schulz, H.; Nothnagel, T. Tissue-specific accumulation of carotenoids in carrot roots. *Plant a* **2006**, *224*, 1028–1037. [CrossRef] [PubMed]
33. Baranski, R.; Klocke, E.; Schumann, G. Green fluorescent protein as an efficient selection marker for *Agrobacterium rhizogenes* mediated carrot transformation. *Plant Cell Rep.* **2006**, *25*, 190–197. [CrossRef] [PubMed]
34. Oleszkiewicz, T.; Klimek-Chodacka, M.; Milewska-Hendel, A.; Zubko, M.; Stróż, D.; Kurczyńska, E.; Boba, A.; Szopa, J.; Baranski, R. Unique chromoplast organisation and carotenoid gene expression in carotenoid-rich carrot callus. *Planta* **2018**, *248*, 1455–1471. [CrossRef]
35. Rygula, A.; Oleszkiewicz, T.; Grzebelus, E.; Pacia, M.Z.; Baranska, M.; Baranski, R. Raman, AFM and SNOM high resolution imaging of carotene crystals in a model carrot cell system. *Spectrochim. Acta A* **2018**, *197*, 47–55. [CrossRef]
36. Dudek, M.; Machalska, E.; Oleszkiewicz, T.; Grzebelus, E.; Baranski, R.; Szcześniak, P.; Mlynarski, J.; Zajac, G.; Kaczor, A.; Baranska, M. Chiral amplification in nature: Studying cell-extracted chiral carotenoid microcrystals via the resonance Raman optical activity of model systems. *Angew. Chem. Int. Ed.* **2019**, *58*, 8383–8388. [CrossRef]
37. Zhang, Y.; Malzahn, A.A.; Sretenovic, S.; Qi, Y. The emerging and uncultivated potential of CRISPR technology in plant science. *Nat. Plants* **2019**, *5*, 778–794. [CrossRef]
38. El-Mounadi, K.; Morales-Floriano, M.L.; Garcia-Ruiz, H. Principles, applications, and biosafety of plant genome editing using CRISPR-Cas9. *Front. Plant Sci.* **2020**, *11*, 56. [CrossRef]

39. D'Ambrosio, C.; Stigliani, A.L.; Giorio, G. CRISPR/Cas9 editing of carotenoid genes in tomato. *Transgenic Res.* **2018**, *27*, 367–378. [CrossRef]
40. Dahan-Meir, T.; Filler-Hayut, S.; Melamed-Bessudo, C.; Bocobza, S.; Czosnek, H.; Aharoni, A.; Levy, A.A. Efficient in planta gene targeting in tomato using gemiviral replicons and the CRISPR/Cas9 system. *Plant J.* **2018**, *95*, 5–16. [CrossRef]
41. Zhu, J.; Song, N.; Sun, S.; Yang, W.; Zhao, H.; Song, W.; Lai, J. Efficiency and Inheritance of targeted mutagenesis in maize using CRISPR-Cas9. *J. Genet. Genom.* **2015**, *43*, 25–36. [CrossRef]
42. Klimek-Chodacka, M.; Oleszkiewicz, T.; Qi, Y.; Baranski, R. Carrot genome editing using CRISPR-based systems. *Acta Hortic.* **2019**, *1264*, 53–66. [CrossRef]
43. Klimek-Chodacka, M.; Oleszkiewicz, T.; Lowder, L.G.; Qi, Y.; Baranski, R. Efficient CRISPR/Cas9-based genome editing in carrot cells. *Plant Cell Rep.* **2018**, *37*, 575–586. [CrossRef]
44. Mikami, M.; Toki, S.; Endo, M. Parameters affecting frequency of CRISPR/Cas9 mediated targeted mutagenesis in rice. *Plant Cell Rep.* **2015**, *34*, 1807–1815. [CrossRef]
45. Xu, Z.-S.; Feng, K.; Xiong, A.-S. CRISPR/Cas9-mediated multiply targeted mutagenesis in orange and purple carrot plants. *Mol. Biotechnol.* **2019**, *61*, 191–199. [CrossRef] [PubMed]
46. Zischewski, J.; Fischer, R.; Bortesi, L. Detection of on-target and off-target mutations generated by CRISPR/Cas9 and other sequence-specific nucleases. *Biotechnol. Adv.* **2017**, *35*, 95–104. [CrossRef] [PubMed]
47. Sentmanat, M.F.; Peters, S.T.; Floria, C.P.; Connelly, J.P.; Pruett-Miller, S.M. A survey of validating strategies for CRISPR-Cas9 editing. *Sci. Rep.* **2018**, *8*, 888. [CrossRef]
48. Jang, G.; Lee, S.; Um, T.Y.; Chang, S.H.; Lee, H.Y.; Chung, P.J.; Kim, J.-K.; Choi, Y.D. Genetic chimerism of CRISPR/Cas9-mediated rice mutants. *Plant Biotechnol. Rep.* **2016**, *10*, 425–435. [CrossRef]
49. Huang, H.; Wu, Q. CRISPR double cutting through the labyrinthine architecture of 3D genomes. *J. Genet. Genom.* **2016**, *43*, 273–288. [CrossRef] [PubMed]
50. Welsch, R.; Arango, J.; Bär, C.; Salazar, B.; Al-Babili, S.; Beltrán, J.; Chavarriaga, P.; Ceballos, H.; Tohme, J.; Beyer, P. Provitamin A accumulation in Cassava (*Manihot esculenta*) roots driven by a single nucleotide polymorphism in a phytoene synthase gene. *Plant Cell* **2010**, *22*, 3348–3356. [CrossRef] [PubMed]
51. Blum, M.; Chang, H.-Y.; Chuguransky, S.; Grego, T.; Kandasaamy, S.; Mitchell, A.; Nuka, G.; Paysan-Lafosse, T.; Qureshi, M.; Raj, S.; et al. The InterPro protein families and domains database: 20 years on. *Nucleic Acids Res.* **2021**, *49*, D344–D354. [CrossRef]
52. Moreno, J.C.; Pizarro, L.; Fuentes, P.; Handford, M.; Cifuentes, V.; Stange, C. Levels of lycopene β-cyclase 1 modulate carotenoid gene expression and accumulation in *Daucus carota*. *PLoS ONE* **2013**, *8*, e58144. [CrossRef]
53. Rodríguez-Villalón, A.; Gas, E.; Rodríguez-Concepción, M. Phytoene synthase activity controls the biosynthesis of carotenoids and the supply of their metabolic precursors in dark-grown Arabidopsis seedlings. *Plant J.* **2009**, *60*, 424–435. [CrossRef] [PubMed]
54. Arango, J.; Jourdan, M.; Geoffriau, E.; Beyer, P.; Welsch, R. Carotene hydroxylase activity determines the levels of both α-carotene and total carotenoids in orange carrots. *Plant Cell* **2014**, *26*, 2223–2233. [CrossRef] [PubMed]
55. Fraser, P.D.; Enfissi, E.M.A.; Halket, J.M.; Truesdale, M.R.; Yu, D.; Gerrish, C.; Bramley, P.M. Manipulation of phytoene levels in tomato fruit: Effects on isoprenoids, plastids, and intermediary metabolism. *Plant Cell* **2007**, *19*, 3194–3211. [CrossRef] [PubMed]
56. Simpson, K.; Quiroz, L.F.; Rodríguez-Concepción, M.; Stange, C.R. Differential contribution of the first two enzymes of the MEP pathway to the supply of metabolic precursors for carotenoid and chlorophyll biosynthesis in carrot (*Daucus carota*). *Front. Plant Sci.* **2016**, *7*, 1344. [CrossRef]
57. Jang, S.-J.; Jeong, H.-B.; Jung, A.; Kang, M.-Y.; Kim, S.; Ha, S.-H.; Kwon, J.-K.; Kang, B.-C. Phytoene synthase 2 can compensate for the absence of PSY1 in the control of color in *Capsicum* fruit. *J. Exp. Bot.* **2020**, *71*, 3417–3427. [CrossRef] [PubMed]
58. Li, L.; Paolillo, D.J.; Parthasarathy, M.V.; DiMuzio, E.M.; Garvin, D.F. A novel gene mutation that confers abnormal patterns of β-carotene accumulation in cauliflower (*Brassica oleracea* var. *botrytis*). *Plant J.* **2001**, *26*, 59–67. [CrossRef]
59. Bai, C.; Rivera, S.M.; Medina, V.; Alves, R.; Vilaprinyo, E.; Sorribas, A.; Canela, R.; Capell, T.; Sandmann, G.; Christou, P.; et al. An in vitro system for the rapid functional characterization of genes involved in carotenoid biosynthesis and accumulation. *Plant J.* **2014**, *77*, 464–475. [CrossRef]
60. Zhou, X.; Welsch, R.; Yang, Y.; Álvarez, D.; Riediger, M.; Yuan, H.; Fish, T.; Liu, J.; Thannhauser, T.W.; Li, L. Arabidopsis OR proteins are the major posttranscriptional regulators of phytoene synthase in controlling carotenoid biosynthesis. *Proc. Natl. Acad. Sci. USA* **2015**, *112*, 3558–3563. [CrossRef]
61. Kim, J.E.; Rensing, K.H.; Douglas, C.J.; Cheng, K.M. Chromoplasts ultrastructure and estimated carotene content in root secondary phloem of different carrot varieties. *Plant a* **2010**, *231*, 549–558. [CrossRef]
62. Roman, M.; Marzec, K.M.; Grzebelus, E.; Simon, P.W.; Baranska, M.; Baranski, R. Composition and (in)homogeneity of carotenoid crystals in carrot cells revealed by high resolution Raman imaging. *Spectrochim. Acta A* **2015**, *136*, 1395–1400. [CrossRef] [PubMed]
63. Camara, B.; Hugueney, P.; Bouvier, F.; Kuntz, M.; Monéger, R. Biochemistry and molecular biology of chromoplast development. *Int. Rev. Cytol.* **1995**, *163*, 175–247. [CrossRef] [PubMed]
64. Kumar, A.; Bender, L.; Neumann, K.H. Growth regulation, plastid differentiation and the development of a photosynthetic system in cultured carrot root explants as influenced by exogenous sucrose and various phytohormones. *Plant Cell Tissue Org. Cult.* **1984**, *3*, 11–28. [CrossRef]

65. Hempel, J.; Amrehn, E.; Quesada, S.; Esquivel, P.; Jiménez, V.M.; Heller, A.; Carle, R.; Schweiggert, R.M. Lipid-dissolved γ-carotene, β-carotene, and lycopene in globular chromoplasts of peach palm (*Bactris gasipaes* Kunth) fruits. *Planta* **2014**, *240*, 1037–1050. [CrossRef] [PubMed]
66. Rodriguez-Concepcion, M.; Stange, C. Biosynthesis of carotenoids in carrot: An underground story comes to light. *Arch. Biochem. Biophys.* **2013**, *539*, 110–116. [CrossRef]
67. Sun, L.; Sun, Y.; Zhang, M.; Wang, L.; Ren, J.; Cui, M.; Wang, Y.; Ji, K.; Li, P.; Li, Q.; et al. Suppression of 9-cis-epoxycarotenoid dioxygenase, which encodes a key enzyme in abscisic acid biosynthesis, alters fruit texture in transgenic tomato. *Plant Physiol.* **2012**, *158*, 283–298. [CrossRef] [PubMed]
68. Ma, N.; Feng, H.; Meng, X.; Li, D.; Yang, D.; Wu, C.; Meng, Q. Overexpression of tomato SlNAC1 transcription factor alters fruit pigmentation and softening. *BMC Plant Biol.* **2014**, *14*, 351. [CrossRef]
69. Gao, L.; Zhao, W.; Qu, H.; Wang, Q.; Zhao, L. The *yellow-fruited tomato 1* (*yft1*) mutant has altered fruit carotenoid accumulation and reduced ethylene production as a result of a genetic lesion in *ETHYLENE INSENSITIVE2*. *Theor. Appl. Genet.* **2016**, *129*, 717–728. [CrossRef]
70. Li, L.; Zhao, W.; Feng, X.; Chen, L.; Zhang, L.; Zhao, L. Changes in fruit firmness, cell wall composition, and transcriptional profile in the *yellow fruit tomato 1* (*yft1*) mutant. *J. Agric. Food Chem.* **2019**, *67*, 463–472. [CrossRef]
71. Zhao, W.; Gao, L.; Li, Y.; Wang, M.; Zhang, L.; Zhao, L. Yellow-fruited phenotype is caused by 573 bp insertion at 5′ UTR of YFT1 allele in yft1 mutant tomato. *Plant Sci.* **2020**, *300*, 110637. [CrossRef]
72. Zhang, Y.; Liu, Y.; Liu, F.; Zheng, X.; Xie, Z.; Ye, J.; Cheng, Y.; Deng, X.; Zeng, Y. Investigation of chromoplast ultrastructure and tissue-specific accumulation of carotenoids in citrus flesh. *Sci. Hortic.* **2019**, *256*, 108547. [CrossRef]
73. Otaka, J.; Seo, S.; Nishimura, M. Lutein, a natural carotenoid, induces α-1,3-glucan accumulation on the cell wall surface of fungal plant pathogens. *Molecules* **2016**, *21*, 980. [CrossRef] [PubMed]
74. Tenhaken, R. Cell wall remodeling under abiotic stress. *Front. Plant Sci.* **2015**, *5*, 771. [CrossRef] [PubMed]
75. Cosgrove, D.J.; Anderson, C.T. Plant cell growth: Do pectins drive lobe formation in *Arabidopsis* pavement cells? *Curr. Biol.* **2020**, *30*, R660–R662. [CrossRef]
76. Bidhendi, A.J.; Geitmann, A. Relating the mechanics of the primary plant cell wall to morphogenesis. *J. Exp. Bot.* **2016**, *67*, 449–461. [CrossRef]
77. Brulé, V.; Rafsanjani, A.; Pasini, D.; Western, T.L. Hierarchies of plant stiffness. *Plant Sci.* **2016**, *250*, 79–96. [CrossRef]
78. Braybrook, S.A.; Peaucelle, A. Mechano-Chemical Aspects of Organ Formation in *Arabidopsis thaliana*: The relationship between auxin and pectin. *PLoS ONE* **2013**, *8*, e57813. [CrossRef]
79. Sala, K.; Malarz, K.; Barlow, P.W.; Kurczyńska, E.U. Distribution of some pectic and arabinogalactan protein epitopes during *Solanum lycopersicum* (L.) adventitious root development. *BMC Plant Biol.* **2017**, *17*, 25. [CrossRef]
80. Milewska-Hendel, A.; Zubko, M.; Karcz, J.; Stróż, D.; Kurczyńska, E. Fate of neutral-charged gold nanoparticles in the roots of the *Hordeum vulgare* L. cultivar Karat. *Sci. Rep.* **2017**, *7*, 3014. [CrossRef]
81. Showalter, A.M. Structure and function of plant-cell wall proteins. *Plant Cell* **1993**, *5*, 9–23. [CrossRef]
82. Nothnagel, E.A. Proteoglycans and related components in plant cells. *Int. Rev. Cytol.* **1997**, *174*, 195–291. [CrossRef] [PubMed]
83. Showalter, A.M. Arabinogalactan-proteins: Structure, expression and function. *Cell. Mol. Life Sci.* **2001**, *58*, 1399–1417. [CrossRef] [PubMed]
84. Ellis, M.; Egelund, J.; Schultz, C.J.; Bacic, A. Arabinogalactan-proteins: Key regulators at the cell surface? *Plant Physiol.* **2010**, *153*, 403–419. [CrossRef] [PubMed]
85. Gao, M.; Showalter, A.M. Yariv reagent treatment induces programmed cell death in Arabidopsis cell cultures and implicates arabinogalactan protein involvement. *Plant J.* **1999**, *19*, 321–331. [CrossRef]
86. Mareri, L.; Romi, M.; Cai, G. Arabinogalactan proteins: Actors or spectators during abiotic and biotic stress in plants? *Plant Biosyst.* **2019**, *153*, 173–185. [CrossRef]
87. Park, M.H.; Suzuki, Y.; Chono, M.; Knox, J.P.; Yamaguchi, I. CsAGP1, a gibberellin-responsive gene from cucumber hypocotyls, encodes a classical arabinogalactan protein and is involved in stem elongation. *Plant Physiol.* **2003**, *131*, 1450–1459. [CrossRef] [PubMed]
88. Yang, J.L.; Li, Y.Y.; Zhang, Y.J.; Zhang, S.S.; Wu, Y.R.; Wu, P.; Zheng, S.J. Cell wall polysaccharides are specifically involved in the exclusion of aluminum from the rice root apex. *Plant Physiol.* **2008**, *146*, 602–611. [CrossRef]
89. Mareri, L.; Faleri, C.; Romi, M.; Mariani, C.; Cresti, M.; Cai, G. Heat stress affects the distribution of JIM8-labelled arabinogalactan proteins in pistils of *Solanum lycopersicum* cv Micro-Tom. *Acta Physiol. Plant* **2016**, *38*, 184. [CrossRef]
90. Smallwood, M.; Yates, E.A.; Willats, W.G.T.; Martin, H.; Knox, J.P. Immunochemical comparison of membrane-associated and secreted arabinogalactan-proteins in rice and carrot. *Plant a* **1996**, *198*, 452–459. [CrossRef]
91. Herger, A.; Dünser, K.; Kleine-Vehn, J.; Ringli, C. Leucine-rich repeat extensin proteins and their role in cell wall sensing. *Curr. Biol.* **2019**, *29*, R851–R858. [CrossRef] [PubMed]
92. Lamport, D.T.A.; Kieliszewski, M.J.; Chen, Y.; Cannon, M.C. Role of the extensin superfamily in primary cell wall architecture. *Plant Physiol.* **2011**, *156*, 11–19. [CrossRef]
93. Chen, J.; Varner, J.E. Isolation and characterization of cDNA clones for carrot extensin and a proline-rich 33-kDa protein. *Proc. Natl. Acad. Sci. USA* **1985**, *82*, 4399–4403. [CrossRef]

94. Stafstrom, J.P.; Staehelin, L.A. A second extensin-Like hydroxyproline-rich glycoprotein from carrot cell walls. *Plant Physiol.* **1987**, *84*, 820–825. [CrossRef] [PubMed]
95. Sala, K.; Karcz, J.; Rypień, A.; Kurczyńska, E.U. Unmethyl-esterified homogalacturonan and extensins seal *Arabidopsis* graft union. *BMC Plant Biol.* **2019**, *19*, 151. [CrossRef] [PubMed]
96. Popielarska-Konieczna, M.; Sala, K.; Abdullah, M.; Tuleja, M.; Kurczyńska, E. Extracellular matrix and wall composition are diverse in the organogenic and non-organogenic calli of *Actinidia arguta*. *Plant Cell Rep.* **2020**, *39*, 779–798. [CrossRef] [PubMed]
97. Godel-Jędrychowska, K.; Maćkowska, K.; Kurczyńska, E.; Grzebelus, E. Composition of the reconstituted cell wall in protoplast-derived cells of *Daucus* is affected by phytosulfokine (PSK). *Int. J. Mol. Sci.* **2019**, *20*, 5490. [CrossRef] [PubMed]
98. Bae, S.; Park, J.; Kim, J.-S. Cas-OFFinder: A fast and versatile algorithm that searches for potential off-target sites of Cas9 RNA-guided endonucleases. *Bioinformatics* **2014**, *30*, 1473–1475. [CrossRef]
99. Lowder, L.G.; Zhang, D.; Baltes, N.J.; Paul, J.W.; Tang, X.; Zheng, X.; Voytas, D.F.; Hsieh, T.F.; Zhang, Y.; Qi, Y. A CRISPR/Cas9 toolbox for multiplexed plant genome editing and transcriptional regulation. *Plant Physiol.* **2015**, *169*, 971–985. [CrossRef]
100. Main, G.D.; Reynolds, S.; Gartland, J.S. Electroporation protocols for Agrobacterium. In *Agrobacterium Protocols: Methods in Molecular Biology*; Gartland, K.M.A., Davey, M.R., Eds.; Springer: Totowa, NJ, USA, 1995; Volume 44, pp. 405–412.
101. Potocka, I.; Godel, K.; Dobrowolska, I.; Kurczyńska, E.U. Spatio-temporal localization of selected pectic and arabinogalactan protein epitopes and the ultrastructural characteristics of explant cells that accompany the changes in the cell fate during somatic embryogenesis in *Arabidopsis thaliana*. *Plant Physiol. Biochem.* **2018**, *127*, 573–589. [CrossRef]
102. Clausen, M.H.; Madsen, R. Synthesis of hexasaccharide fragments of pectin. *Chem. Eur. J.* **2003**, *9*, 3821–3832. [CrossRef] [PubMed]
103. Yates, E.A.; Valdor, J.F.; Haslam, S.M.; Morris, H.R.; Dell, A.; Mackie, W.; Knox, J.P. Characterization of carbohydrate structural features recognized by anti-arabinogalactan-protein monoclonal antibodies. *Glycobiology* **1996**, *6*, 131–139. [CrossRef] [PubMed]
104. Knox, J.P.; Linstead, P.J.; Cooper, J.P.C.; Roberts, K. Developmentally regulated epitopes of cell surface arabinogalactan proteins and their relation to root tissue pattern formation. *Plant J.* **1991**, *1*, 317–326. [CrossRef] [PubMed]
105. Smallwood, M.; Beven, A.; Donovan, N.; Neill, S.J.; Peart, J.; Roberts, K.; Knox, J.P. Localization of cell wall proteins in relation to the developmental anatomy of the carrot root apex. *Plant J.* **1994**, *5*, 237–246. [CrossRef]

12. Oświadczenia autorów publikacji wchodzących w skład pracy doktorskiej

UNIWERSYTET ROLNICZY
im. Hugona Kołłątaja w Krakowie

Wydział Biotechnologii i Ogrodnictwa
Katedra Biologii Roślin i Biotechnologii

mgr inż. Tomasz Oleszkiewicz
Katedra Biologii Roślin i Biotechnologii
Wydział Biotechnologii i Ogrodnictwa
Uniwersytet Rolniczy w Krakowie

Kraków, 26.10.2021

Oświadczenie autora publikacji

Oświadczam, że w publikacji:

Oleszkiewicz T., Klimek-Chodacka M., Milewska-Hendel A., Zubko M., Stróż D., Kurczyńska E., Boba A., Szopa J., Baranski R. 2018. Unique chromoplast organization and carotenoid gene expression in carotenoid-rich carrot callus. Planta 248: 1455-1471. https://doi.org/10.1007/s00425-018-2988-5

mój udział polegał na opracowaniu koncepcji badań, uzyskaniu materiału badawczego i jego prowadzeniu w kulturach *in vitro*, wykonaniu charakteryzacji makroskopowej i mikroskopowej, wykonaniu analiz bioinformatycznych i ekspresji genów metodą RT-qPCR, przeprowadzeniu analizy wyników, przygotowaniu pierwszej wersji manuskryptu, w tym dokumentacji graficznej, oraz udziale w tworzeniu ostatecznej wersji publikacji.

Tomasz Oleszkiewicz

mgr inż. Tomasz Oleszkiewicz

PL 31-425 Kraków, Al. 29 Listopada 54
tel. +48 (12) 662 51 87, e-mail: kbrib@urk.edu.pl

UNIWERSYTET ROLNICZY
im. Hugona Kołłątaja w Krakowie

Wydział Biotechnologii i Ogrodnictwa
Katedra Biologii Roślin i Biotechnologii

dr inż. Magdalena Klimek-Chodacka
Katedra Biologii Roślin i Biotechnologii
Wydział Biotechnologii i Ogrodnictwa
Uniwersytet Rolniczy w Krakowie

Kraków, 16.09.2021

Oświadczenie autora publikacji

Oświadczam, że w publikacji:

Oleszkiewicz T., Klimek-Chodacka M., Milewska-Hendel A., Zubko M., Stróż D., Kurczyńska E., Boba A., Szopa J., Baranski R. 2018. Unique chromoplast organization and carotenoid gene expression in carotenoid-rich carrot callus. Planta 248: 1455-1471. https://doi.org/10.1007/s00425-018-2988-5

mój udział był w zakresie planowania badań oraz wykonania części analiz bioinformatycznych i RT-qPCR, a także miałam udział w pisaniu manuskryptu.

dr inż. Magdalena Klimek-Chodacka

PL 31-425 Kraków, Al. 29 Listopada 54
tel. +48 (12) 662 51 87, e-mail: kbrib@urk.edu.pl

dr Anna Milewska-Hendel
Instytut Biologii, Biotechnologii i Ochrony Środowiska
Wydział Nauk Przyrodniczych
Uniwersytet Śląski w Katowicach

Katowice, 09.09.2021

Oświadczenie autora publikacji

Oświadczam, że w publikacji:

Oleszkiewicz T., Klimek-Chodacka M., Milewska-Hendel A., Zubko M., Stróż D., Kurczyńska E., Boba A., Szopa J., Baranski R. 2018. Unique chromoplast organization and carotenoid gene expression in carotenoid-rich carrot callus. Planta 248: 1455-1471. https://doi.org/10.1007/s00425-018-2988-5

mój udział obejmował przygotowanie materiału roślinnego do badań mikroskopowych, obserwacje za pomocą różnych technik mikroskopowych, analizę wyników i pisanie manuskryptu.

Anna Milewska-Hendel

dr Anna Milewska-Hendel

dr Maciej Zubko
Instytut Inżynierii Materiałowej
Wydział Nauk Ścisłych i Technicznych
Uniwersytet Śląski w Katowicach

Katowice, 15.09.2021

Oświadczenie autora publikacji

Oświadczam, że w publikacji:

Oleszkiewicz T., Klimek-Chodacka M., Milewska-Hendel A., Zubko M., Stróż D., Kurczyńska E., Boba A., Szopa J., Baranski R. 2018. Unique chromoplast organization and carotenoid gene expression in carotenoid-rich carrot callus. Planta 248: 1455-1471. https://doi.org/10.1007/s00425-018-2988-5

mój udział polegał na wykonaniu pomiarów i dokumentacji przy użyciu transmisyjnej mikroskopii elektronowej.

dr Maciej Zubko

prof. dr hab. Danuta Stróż
Instytut Inżynierii Materiałowej
Wydział Nauk Ścisłych i Technicznych
Uniwersytet Śląski w Katowicach

Katowice, 10.09.2021

Oświadczenie autora publikacji

Oświadczam, że w publikacji:

Oleszkiewicz T., Klimek-Chodacka M., Milewska-Hendel A., Zubko M., Stróż D., Kurczyńska E., Boba A., Szopa J., Baranski R. 2018. Unique chromoplast organization and carotenoid gene expression in carotenoid-rich carrot callus. Planta 248: 1455-1471. https://doi.org/10.1007/s00425-018-2988-5

mój udział był w zakresie wykonania obserwacji z użyciem transmisyjnej mikroskopii elektronowej.

Signed by / Podpisano przez:

Danuta Stróż
Uniwersytet Śląski w Katowicach

Date / Data: 2021-09-10 10:02

prof. dr hab. Danuta Stróż

prof. dr hab. Ewa Kurczyńska
Instytut Biologii, Biotechnologii i Ochrony Środowiska
Wydział Nauk Przyrodniczych
Uniwersytet Śląski w Katowicach

Katowice, 15.09.2021

Oświadczenie autora publikacji

Oświadczam, że w publikacji:

Oleszkiewicz T., Klimek-Chodacka M., Milewska-Hendel A., Zubko M., Stróż D., Kurczyńska E., Boba A., Szopa J., Baranski R. 2018. Unique chromoplast organization and carotenoid gene expression in carotenoid-rich carrot callus. Planta 248: 1455-1471. https://doi.org/10.1007/s00425-018-2988-5

mój udział polegał na wykonaniu obserwacji mikroskopowych i interpretacji wyników oraz pisaniu manuskryptu.

Ewa Kurczyńska

prof. dr hab. Ewa Kurczyńska

dr Aleksandra Boba
Zakład Biochemii Genetycznej
Wydział Biotechnologii
Uniwersytet Wrocławski

Wrocław, 01.10.2021

Oświadczenie autora publikacji

Oświadczam, że w publikacji:

Oleszkiewicz T., Klimek-Chodacka M., Milewska-Hendel A., Zubko M., Stróż D., Kurczyńska E., Boba A., Szopa J., Baranski R. 2018. Unique chromoplast organization and carotenoid gene expression in carotenoid-rich carrot callus. Planta 248: 1455-1471. https://doi.org/10.1007/s00425-018-2988-5

mój udział polegał na wykonaniu oznaczeń zawartości karotenoidów metodą UPLC.

Aleksandra Boba

dr Aleksandra Boba

prof. dr hab. Jan Szopa
Zakład Biochemii Genetycznej
Wydział Biotechnologii
Uniwersytet Wrocławski

Wrocław, 15.09.2021

Oświadczenie autora publikacji

Oświadczam, że w publikacji:

Oleszkiewicz T., Klimek-Chodacka M., Milewska-Hendel A., Zubko M., Stróż D., Kurczyńska E., Boba A., Szopa J., Baranski R. 2018. Unique chromoplast organization and carotenoid gene expression in carotenoid-rich carrot callus. Planta 248: 1455-1471. https://doi.org/10.1007/s00425-018-2988-5

mój udział był związany z wykonaniem analizy zawartości karotenoidów metodą UPLC.

prof. dr hab. Jan Szopa

UNIWERSYTET ROLNICZY
im. Hugona Kołłątaja w Krakowie

Wydział Biotechnologii i Ogrodnictwa
Katedra Biologii Roślin i Biotechnologii

prof. dr hab. inż. Rafał Barański
Katedra Biologii Roślin i Biotechnologii
Wydział Biotechnologii i Ogrodnictwa
Uniwersytet Rolniczy w Krakowie

Kraków, 28.10.2021

Oświadczenie autora publikacji

Oświadczam, że w publikacji:

Oleszkiewicz T., Klimek-Chodacka M., Milewska-Hendel A., Zubko M., Stróż D., Kurczyńska E., Boba A., Szopa J., Baranski R. 2018. Unique chromoplast organization and carotenoid gene expression in carotenoid-rich carrot callus. Planta 248: 1455-1471. https://doi.org/10.1007/s00425-018-2988-5

mój udział polegał na planowaniu badań, interpretacji wyników, nadzorowaniu badań i tworzeniu manuskryptu oraz pozyskaniu finansowania projektu. Jestem autorem korespondencyjnym.

prof. dr hab. inż. Rafał Barański

PL 31-425 Kraków, Al. 29 Listopada 54
tel. +48 (12) 662 51 87, e-mail: kbrib@urk.edu.pl

UNIWERSYTET ROLNICZY
im. Hugona Kołłątaja w Krakowie

Wydział Biotechnologii i Ogrodnictwa
Katedra Biologii Roślin i Biotechnologii

mgr inż. Tomasz Oleszkiewicz
Katedra Biologii Roślin i Biotechnologii
Wydział Biotechnologii i Ogrodnictwa
Uniwersytet Rolniczy w Krakowie

Kraków, 26.10.2021

Oświadczenie autora publikacji

Oświadczam, że w publikacji:

Oleszkiewicz T., Kruczek M., Baranski R. 2021. Repression of carotenoid accumulation by nitrogen and NH_4^+ supply in carrot callus cells in vitro. Plants 10, 1813, https://doi.org/10.3390/plants10091813

mój udział polegał na opracowaniu koncepcji badań, metodologii, wykonaniu wszystkich doświadczeń w kulturach *in vitro*, analizie karotenoidów metodą spektrofotometryczną, przeprowadzeniu analizy danych, zarządzaniu projektem, pozyskaniu funduszy na realizację projektu, przygotowaniu manuskryptu publikacji w pierwszej i finalnej wersji, w tym dokumentacji graficznej. Jestem autorem korespondencyjnym.

Tomasz Oleszkiewicz

mgr inż. Tomasz Oleszkiewicz

PL 31-425 Kraków, Al. 29 Listopada 54
tel. +48 (12) 662 51 87, e-mail: kbrib@urk.edu.pl

UNIWERSYTET ROLNICZY
im. Hugona Kołłątaja w Krakowie

Wydział Biotechnologii i Ogrodnictwa
Katedra Biologii Roślin i Biotechnologii

mgr inż. Michał Kruczek
Katedra Biologii Roślin i Biotechnologii
Wydział Biotechnologii i Ogrodnictwa
Uniwersytet Rolniczy w Krakowie

Kraków, 06.10.2021

Oświadczenie autora publikacji

Oświadczam, że w publikacji:

Oleszkiewicz T., Kruczek M., Baranski R. 2021. Repression of carotenoid accumulation by nitrogen and NH_4^+ supply in carrot callus cells in vitro. Plants 10, 1813, https://doi.org/10.3390/plants10091813

mój udział polegał na wykonaniu oznaczeń zawartości karotenoidów metodą HPLC.

Michał Kruczek

mgr inż. Michał Kruczek

PL 31-425 Kraków, Al. 29 Listopada 54
tel. +48 (12) 662 51 87, e-mail: kbrib@urk.edu.pl

UNIWERSYTET ROLNICZY
im. Hugona Kołłątaja w Krakowie

Wydział Biotechnologii i Ogrodnictwa
Katedra Biologii Roślin i Biotechnologii

prof. dr hab. inż. Rafał Barański
Katedra Biologii Roślin i Biotechnologii
Wydział Biotechnologii i Ogrodnictwa
Uniwersytet Rolniczy w Krakowie

Kraków, 28.10.2021

Oświadczenie autora publikacji

Oświadczam, że w publikacji:

Oleszkiewicz T., Kruczek M., Baranski R. 2021. Repression of carotenoid accumulation by nitrogen and NH_4^+ supply in carrot callus cells in vitro. Plants 10, 1813, https://doi.org/10.3390/plants10091813

mój udział polegał na nadzorze nad realizacją badań oraz pomocy w analizie statystycznej wyników, interpretacji wyników i tworzeniu manuskryptu.

Rafał Barański

prof. dr hab. inż. Rafał Barański

PL 31-425 Kraków, Al. 29 Listopada 54
tel. +48 (12) 662 51 87, e-mail: kbrib@urk.edu.pl

UNIWERSYTET ROLNICZY
im. Hugona Kołłątaja w Krakowie

Wydział Biotechnologii i Ogrodnictwa
Katedra Biologii Roślin i Biotechnologii

mgr inż. Tomasz Oleszkiewicz
Katedra Biologii Roślin i Biotechnologii
Wydział Biotechnologii i Ogrodnictwa
Uniwersytet Rolniczy w Krakowie

Kraków, 26.10.2021

Oświadczenie autora publikacji

Oświadczam, że w publikacji:

Oleszkiewicz T., Klimek-Chodacka M., Kruczek M., Godel-Jędrychowska K., Sala K., Milewska-Hendel A., Zubko M., Kurczyńska E., Qi Y., Baranski R. 2021. Inhibition of Carotenoid Biosynthesis by CRISPR/Cas9 Triggers Cell Wall Remodelling in Carrot. International Journal of Molecular Sciences 22, 6516. https://doi.org/10.3390/ijms22126516

mój udział polegał na opracowaniu koncepcji badań, stworzeniu wektorów CRISPR/Cas9, wykonaniu transformacji bakterii i kalusa, prowadzeniu kultur *in vitro*, w tym selekcji mutantów, wykonaniu obserwacji makroskopowych i wstępnej oceny mikroskopowej, wykonaniu analiz bioinformatycznych, w tym danych z sekwencjonowania, molekularnej detekcji mutantów, ekspresji genów metodą RT-qPCR, analizy wyników oraz wykonaniu dokumentacji zdjęciowej. Ponadto, wykonałem opracowanie wyników i przygotowałem plansze graficzne do publikacji, przygotowałem pierwszą wersję manuskryptu i brałem udział w tworzeniu ostatecznej wersji publikacji.

Tomasz Oleszkiewicz

mgr inż. Tomasz Oleszkiewicz

PL 31-425 Kraków, Al. 29 Listopada 54
tel. +48 (12) 662 51 87, e-mail: kbrib@urk.edu.pl

UNIWERSYTET ROLNICZY
im. Hugona Kołłątaja w Krakowie

Wydział Biotechnologii i Ogrodnictwa
Katedra Biologii Roślin i Biotechnologii

dr inż. Magdalena Klimek-Chodacka
Katedra Biologii Roślin i Biotechnologii
Wydział Biotechnologii i Ogrodnictwa
Uniwersytet Rolniczy w Krakowie

Kraków, 16.09.2021

Oświadczenie autora publikacji

Oświadczam, że w publikacji:

Oleszkiewicz T., Klimek-Chodacka M., Kruczek M., Godel-Jędrychowska K., Sala K., Milewska-Hendel A., Zubko M., Kurczyńska E., Qi Y., Baranski R. 2021. Inhibition of Carotenoid Biosynthesis by CRISPR/Cas9 Triggers Cell Wall Remodelling in Carrot. International Journal of Molecular Sciences 22, 6516. https://doi.org/10.3390/ijms22126516

mój udział był w zakresie planowania początkowej koncepcji badań, projektowania gRNA, nadzorowałam tworzenie wektorów CRISPR/Cas9 i uczestniczyłam w pozyskaniu funduszy na realizację badań.

dr inż. Magdalena Klimek-Chodacka

PL 31-425 Kraków, Al. 29 Listopada 54
tel. +48 (12) 662 51 87, e-mail: kbrib@urk.edu.pl

UNIWERSYTET ROLNICZY
im. Hugona Kołłątaja w Krakowie

Wydział Biotechnologii i Ogrodnictwa
Katedra Biologii Roślin i Biotechnologii

mgr inż. Michał Kruczek
Katedra Biologii Roślin i Biotechnologii
Wydział Biotechnologii i Ogrodnictwa
Uniwersytet Rolniczy w Krakowie

Kraków, 06.10.2021

Oświadczenie autora publikacji

Oświadczam, że w publikacji:

Oleszkiewicz T., Klimek-Chodacka M., Kruczek M., Godel-Jędrychowska K., Sala K., Milewska-Hendel A., Zubko M., Kurczyńska E., Qi Y., Baranski R. 2021. Inhibition of Carotenoid Biosynthesis by CRISPR/Cas9 Triggers Cell Wall Remodelling in Carrot. International Journal of Molecular Sciences 22, 6516. https://doi.org/10.3390/ijms22126516

mój udział polegał na wykonaniu oznaczeń zawartości karotenoidów metodą HPLC.

mgr inż. Michał Kruczek

PL 31-425 Kraków, Al. 29 Listopada 54
tel. +48 (12) 662 51 87, e-mail: kbrib@urk.edu.pl

mgr Kamila Godel-Jędrychowska
Instytut Biologii, Biotechnologii i Ochrony Środowiska
Wydział Nauk Przyrodniczych
Uniwersytet Śląski w Katowicach

Katowice, 15.09.2021

Oświadczenie autora publikacji

Oświadczam, że w publikacji:

Oleszkiewicz T., Klimek-Chodacka M., Kruczek M., Godel-Jędrychowska K., Sala K., Milewska-Hendel A., Zubko M., Kurczyńska E., Qi Y., Baranski R. 2021. Inhibition of Carotenoid Biosynthesis by CRISPR/Cas9 Triggers Cell Wall Remodelling in Carrot. International Journal of Molecular Sciences 22, 6516. https://doi.org/10.3390/ijms22126516

mój udział był w zakresie wykonania preparatów do analiz histologicznych, immunohistochemicznych i TEM, obserwacji technikami mikroskopowymi, ich analizy i pisania manuskryptu.

Kamila Godel-Jędrychowska

mgr Kamila Godel-Jędrychowska

dr Katarzyna Sala
Instytut Biologii, Biotechnologii i Ochrony Środowiska
Wydział Nauk Przyrodniczych
Uniwersytet Śląski w Katowicach

Katowice, 14.09.2021

Oświadczenie autora publikacji

Oświadczam, że w publikacji:

Oleszkiewicz T., Klimek-Chodacka M., Kruczek M., Godel-Jędrychowska K., Sala K., Milewska-Hendel A., Zubko M., Kurczyńska E., Qi Y., Baranski R. 2021. Inhibition of Carotenoid Biosynthesis by CRISPR/Cas9 Triggers Cell Wall Remodelling in Carrot. International Journal of Molecular Sciences 22, 6516. https://doi.org/10.3390/ijms22126516

mój udział był w zakresie: wykonania preparatów do analiz histologicznych i immunohistochemicznych, obserwacji preparatów z użyciem technik mikroskopowych, ich analizy oraz pisania manuskryptu.

Katarzyna Sala

dr Katarzyna Sala

dr Anna Milewska-Hendel
Instytut Biologii, Biotechnologii i Ochrony Środowiska
Wydział Nauk Przyrodniczych
Uniwersytet Śląski w Katowicach

Katowice, 09.09.2021

Oświadczenie autora publikacji

Oświadczam, że w publikacji:

Oleszkiewicz T., Klimek-Chodacka M., Kruczek M., Godel-Jędrychowska K., Sala K., Milewska-Hendel A., Zubko M., Kurczyńska E., Qi Y., Baranski R. 2021. Inhibition of Carotenoid Biosynthesis by CRISPR/Cas9 Triggers Cell Wall Remodelling in Carrot. International Journal of Molecular Sciences 22, 6516. https://doi.org/10.3390/ijms22126516

mój udział obejmował przygotowanie materiału i obserwacje w wysokorozdzielczym transmisyjnym mikroskopie elektronowym.

Anna Milewska-Hendel

dr Anna Milewska-Hendel

dr Maciej Zubko
Instytut Inżynierii Materiałowej
Wydział Nauk Ścisłych i Technicznych
Uniwersytet Śląski w Katowicach

Katowice, 15.09.2021

Oświadczenie autora publikacji

Oświadczam, że w publikacji:

Oleszkiewicz T., Klimek-Chodacka M., Kruczek M., Godel-Jędrychowska K., Sala K., Milewska-Hendel A., Zubko M., Kurczyńska E., Qi Y., Baranski R. 2021. Inhibition of Carotenoid Biosynthesis by CRISPR/Cas9 Triggers Cell Wall Remodelling in Carrot. International Journal of Molecular Sciences 22, 6516. https://doi.org/10.3390/ijms22126516

mój udział polegał na wykonaniu pomiarów i dokumentacji przy użyciu transmisyjnej mikroskopii elektronowej.

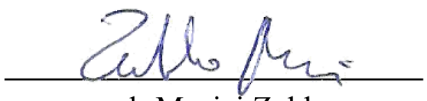

dr Maciej Zubko

prof. dr hab. Ewa Kurczyńska
Instytut Biologii, Biotechnologii i Ochrony Środowiska
Wydział Nauk Przyrodniczych
Uniwersytet Śląski w Katowicach

Katowice, 15.09.2021

Oświadczenie autora publikacji

Oświadczam, że w publikacji:

Oleszkiewicz T., Klimek-Chodacka M., Kruczek M., Godel-Jędrychowska K., Sala K., Milewska-Hendel A., Zubko M., Kurczyńska E., Qi Y., Baranski R. 2021. Inhibition of Carotenoid Biosynthesis by CRISPR/Cas9 Triggers Cell Wall Remodelling in Carrot. International Journal of Molecular Sciences 22, 6516. https://doi.org/10.3390/ijms22126516

mój udział polegał na planowaniu badań w zakresie mikroskopii, wykonaniu obserwacji mikroskopowych i interpretacji uzyskanych wyników, nadzorowaniu tej części badań oraz pisaniu manuskryptu.

Ewa Kurczyńska

prof. dr hab. Ewa Kurczyńska

dr Yiping Qi
Department of Plant Science and Landscape Architecture
University of Maryland

Maryland, 09.09.2021

Authorship declaration

I declare, that in publication:

Oleszkiewicz T., Klimek-Chodacka M., Kruczek M., Godel-Jędrychowska K., Sala K., Milewska-Hendel A., Zubko M., Kurczyńska E., Qi Y., Baranski R. 2021. Inhibition of Carotenoid Biosynthesis by CRISPR/Cas9 Triggers Cell Wall Remodelling in Carrot. International Journal of Molecular Sciences 22, 6516. https://doi.org/10.3390/ijms22126516

my contribution was to provide knowledge and methodology for the construction of CRISPR vectors.

Yiping Qi

dr Yiping Qi

UNIWERSYTET ROLNICZY
im. Hugona Kołłątaja w Krakowie

Wydział Biotechnologii i Ogrodnictwa
Katedra Biologii Roślin i Biotechnologii

prof. dr hab. inż. Rafał Barański
Katedra Biologii Roślin i Biotechnologii
Wydział Biotechnologii i Ogrodnictwa
Uniwersytet Rolniczy w Krakowie

Kraków, 28.10.2021

Oświadczenie autora publikacji

Oświadczam, że w publikacji:

Oleszkiewicz T., Klimek-Chodacka M., Kruczek M., Godel-Jędrychowska K., Sala K., Milewska-Hendel A., Zubko M., Kurczyńska E., Qi Y., Baranski R. 2021. Inhibition of Carotenoid Biosynthesis by CRISPR/Cas9 Triggers Cell Wall Remodelling in Carrot. International Journal of Molecular Sciences 22, 6516. https://doi.org/10.3390/ijms22126516

mój udział polegał na planowaniu badań, interpretacji wyników, nadzorowaniu badań, pozyskaniu finansowania projektu i tworzeniu manuskryptu. Jestem autorem korespondencyjnym.

Rafał Barański

prof. dr hab. inż. Rafał Barański

PL 31-425 Kraków, Al. 29 Listopada 54
tel. +48 (12) 662 51 87, e-mail: kbrib@urk.edu.pl